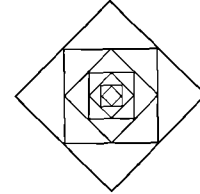


**Bergen  
Environmental  
Sciences &  
Solutions Centre**



**NGU Rapport 93.017**

**A time-variant numerical groundwater flow  
model for the Øvre Romerike aquifer,  
Southern Norway.**

Rapport nr. 93.017		ISSN 0800-3416	Gradering: Åpen	
<b>Tittel:</b> A time-variant numerical groundwater flow model for the Øvre Romerike aquifer, Southern Norway.				
<b>Forfatter:</b> Noelle Odling, David Banks and Arve Misund		<b>Oppdragsgiver:</b> NAVF / NGU / IBM/BSC		
<b>Fylke:</b> Akershus		<b>Kommune:</b> Ullensaker, Nannestad		
<b>Kartbladnavn (M=1:250.000)</b> Hamar		<b>Kartbladnr. og -navn (M=1:50.000)</b> 1915 I,II,III,IV. Eidsvoll, Ullensaker, Nannestad, Hurdal		
<b>Forekomstens navn og koordinater:</b> Øvre Romerike aquifer		<b>Sidetall:</b> 97		<b>Pris:</b> 225,-
<b>Feltarbeid utført:</b> Mai 1992		<b>Rapportdato:</b> 15/3/92	<b>Prosjektnr.:</b> 63.2581.01	<b>Ansvarlig:</b> <i>Tor Esle Frim</i>
<b>Sammendrag:</b> <p>Using a modified version of the USGS MODFLOW code, coupled with a Penman-Grindley type recharge model, it has been possible to produce a transient, 3-dimensional groundwater flow model of the Øvre Romerike aquifer.</p> <p>A steady state model has been calibrated against 183 regional water level observation data from autumn 1975 and against the flows in groundwater-fed springs and streams. The distribution of hydraulic conductivity calibrated using the steady state model was then used to simulate water table variations over a period in excess of 30 years at 3 observation wells. The results show a satisfactory fit with real data, allowing for the limited spatial resolution of the model. A seven-month running average filter has been applied to the recharge data to simulate the damping effects of the unsaturated zone on recharge maxima and minima, resulting in an even better fit.</p> <p>The modelling work has enabled the project's participants to obtain a deeper understanding of the hydraulics of the aquifer, and has also indicated that hydraulic conductivity values obtained from grain size distributions tend to lead to underestimates of aquifer transmissivity. The model provides a framework for further modelling work on contaminant transport at Trandum landfill.</p>				
Emneord: Hydrogeologi		Grunnvann		Kornstørrelse
Miljøgeologi		Modellforsøk		Kornfordeling
Forurensning				Fagrapport

# TABLE OF CONTENTS

1. Introduction . . . . .	6
1.1 Background . . . . .	6
1.2 Pollution threats . . . . .	6
1.3 Geology . . . . .	7
1.4 Hydrology . . . . .	7
1.5 Objective of modelling work . . . . .	7
2. Physical characteristics of the Øvre Romerike aquifer . . . . .	8
2.1 The geological model and surface features . . . . .	8
2.2 Permeability data . . . . .	10
2.3 Storage data . . . . .	11
2.4 Recharge model . . . . .	11
2.4.1 The basic recharge model . . . . .	11
2.4.2 Use of snow data in the recharge model . . . . .	15
2.4.3 Results . . . . .	17
3. Groundwater flow modelling . . . . .	18
3.1 MODFLOW . . . . .	18
3.2 Data preparation and the Graphical User Interface . . . . .	18
3.3 The grid and boundary conditions . . . . .	19
4 The steady state model . . . . .	20
4.1 Calibration of the steady state model . . . . .	20
4.2 The permeability model . . . . .	22
5 The transient model . . . . .	24
5.1 Modifications to MODFLOW . . . . .	24
5.2 Input to the transient model . . . . .	25
5.3 The transient model results and comparison with observations . . . . .	26
6. Conclusion . . . . .	27
7. Acknowledgements . . . . .	28
8. References . . . . .	29

## TABLES

Table 1a - Calculation of recharge from real data from Gardermoen, autumn 1966.. . . .	15
--	----

Table 1b - Calculation of infiltration when SMD is approximately equal to the root constant. Example from Rushton (1983). . . . .	16
Table 2 - Comparison of recharge model with empirical data. Annual averages for period 1968 - 1974. . . . .	17
Table 3 - Outflows from springs; modelled and observed . . . . .	24
Table 4 - Observation wells with time-series data . . . . .	26

## FIGURES

Text Fig. 1. The assumed recharge model . . . . .	12
Text Fig. 2. Actual change in soil moisture deficit, as a function of soil moisture content. . . . .	13
Fig.1(a) Øvre Romerike area showing Hurdalsjøen, Hersjøen, Transjøen, Dagsjøen, airport, Trandum, the rivers Risa, Leira, Vikka and flow gauging stations on the Risa and Vikka. . . . .	33
Fig.1(b) The water table in the Øvre Romerike aquifer, after Østmo (1976) . . . . .	34
Fig.2(a) Photo of coarse layer at Trandum landfill showing fine and coarse intercalated layers . . . . .	35
Fig.2(b) An interpretation of the structure of the Romerike delta, after VIAK (1990) . . . . .	35
Fig.3(a) Contour map of topography . . . . .	36
Fig.3(b) Contour map of top of fine layer . . . . .	37
Fig.3(c) Contour map of base of aquifer . . . . .	38
Fig.4(a) 3D ADVIZE visualisation of topography . . . . .	39
Fig.4(b) 3D ADVIZE visualisation of top of fine layer . . . . .	39
Fig.4(c) 3D ADVIZE visualisation of base of aquifer . . . . .	40
Fig.5(a) Isopach map of the whole aquifer . . . . .	41
Fig.5(b) Isopach map of the coarse layer . . . . .	42
Fig.5(c) Isopach map of the fine layer . . . . .	43
Fig.6 Calibration graph for hydraulic conductivity analysis from grain size samples . . . . .	44
Fig.7 Polynomial curve, fit to calibration curve . . . . .	44

Fig.8 Histogram of all hydraulic conductivity estimates (using the Bayer method - from $d_{10}$ and $d_{60}$ grain sizes) . . . . .	45
Fig.9 Recharge model, (a) monthly data, (b) yearly data . . . . .	46
Fig.10 Rasterised map example (topography) produced by GENAMAP . . . . .	47
Fig.11 Example of the graphical user interface screen . . . . .	48
Fig.12 MODFLOW grid for Øvre Romerike aquifer, with cells defined . . . . .	49
Fig.13 Map of borehole locations for which measurements of head are available from Nov. 1975 (Østmo 1976). . . . .	50
Fig.14 MODFLOW, steady state model: homogeneous layer model - sensitivity of D (average error) to variation in hydraulic conductivity of coarse and fine layers. . . . .	51
Fig.15 Histograms of discrepancies between steady state model and borehole data for: (a) homogeneous layer model, (b) calibrated hydraulic conductivity model . . . . .	52
Fig.16 Resulting hydraulic conductivity field for fine layer after calibration with borehole data. . . . .	53
Fig.17 (a) MODFLOW steady state results for head. . . . .	54
Fig.17 (b) simplification of Østmo's (1976) map for comparison . . . . .	55
Fig.17 (c) 3D ADVIZE picture of modelled water table with base of aquifer . . . . .	56
Fig.18 Transient MODFLOW results, with steady state heads in fig.17(a) (i.e. recharge = $1.27 \cdot 10^{-8}$ m/s) as initial heads: (a) using monthly recharge . . . . .	57
(b) using running averages of monthly recharge over 7 month intervals . . . . .	58
Fig.19 Transient MODFLOW results with steady state heads generated using calibrated hydraulic conductivity field (Fig.16) and recharge of $8.239 \cdot 10^{-9}$ m/sec: (a) using monthly recharge . . . . .	59
(b) using running averages of monthly recharge over 7 month intervals . . . . .	60
 APPENDICES	
APPENDIX 1 - Input files (basic package and block-centred flow package) for MODFLOW, steady state model . . . . .	61

APPENDIX 2 - Input file (block-centred flow package) for MODFLOW, transient model . . . . .	70
APPENDIX 3 - Elevations of drains, rivers and constant head cells. . . . .	79
APPENDIX 4 - Head difference between vertically adjacent cells in the two aquifer layers (steady state) . . . . .	83
APPENDIX 5 - Deviations of modelled head (modelled - observed) in each cell . . . . .	85
APPENDIX 6 - Output files from MODFLOW, flow to drains, rivers and constant head cells . . . . .	90
APPENDIX 7 - Listing of recharge model . . . . .	94

# 1. Introduction

## 1.1 Background

The Øvre Romerike aquifer is the largest discrete aquifer in Norway; in fact, one of the few areally extensive Quaternary aquifers in the country, covering an area of approximately 105 km<sup>2</sup> (Fig. 1a). Due to increasingly stringent requirements as regards the quality of drinking water (SIFF 1987), and the corresponding recognition of the unsatisfactory quality of many surface waters, there is a growing interest in groundwater resources in Norway (Ellingsen & Banks 1992). NGU has recently completed both a nationwide survey of groundwater resources in the country (Ellingsen 1992) and a nationwide survey of landfills and contaminated ground (Misund et al. 1991a,b). The latter survey uncovered several contaminated sites which come into conflict with the groundwater resources of the Øvre Romerike aquifer (Morland et al. 1990). Many of the sites registered in this latter survey have been, or will be, followed up with detailed investigations of their impact on groundwater quality (Storrø & Banks 1992, Sæther et al. 1992, Omejer et al. 1992).

## 1.2 Pollution threats

Situated some 40 km north of Oslo, the proximity of the Øvre Romerike aquifer to Norway's most populated and industrialised region has led to increased interest in the aquifer as a potential source of water. At present, however, the aquifer is utilized to only a few percent of its potential (Bryn 1992), supplying several military bases situated on the aquifer, and some small local communities. Nevertheless, there has already been considerable controversy arising from the conflicting interests of industry/the military and those who wish to preserve groundwater quality. Authorities have placed emphasis on protecting the quality of the groundwater in the aquifer from "potentially polluting activities", as it represents a possible future water resource for municipalities in the Romerike area (Østlandskonsult et al. 1991) with a potential exploitable capacity of up to 570 l/s (Snekkerbakken 1992).

Most of the area is either forest or farmland. A limited degree of "urbanisation" (villages, airport) is concentrated on the southern part of the aquifer. Substantial areas of the aquifer are also occupied by military bases and training grounds.

Known sources of pollution to date on the Øvre Romerike aquifer include various military activities, a military and civil airport at Gardermoen (Davidsen 1991), two known leakages from oil storage tanks (Storrø & Banks 1992) and several landfill sites (Sæther et al. 1992, Omejer et al. 1992). Perhaps the greatest controversy surrounds the proposed removal of Oslo's main international airport (currently situated at Fornebu, west of Oslo) to Gardermoen, on the aquifer (Englund & Moseid 1992, Solnørdal 1992).

### 1.3 Geology

The geology of the area is described in detail by Longva (1987). The Romerike aquifer consists of a ca. 105 km<sup>2</sup> expanse of Quaternary ice-marginal delta sediments built up to, and in some locations above, the marine limit. The upper part of the aquifer consists of dominantly glaciofluvial sand and gravel deposits, with areas of aeolian sand and glaciolacustrine sands and silts. These are underlain by glaciomarine/marine silts and clays. The upper, coarser part of the deposit exceeds 30-40 m thickness in some areas, while the total depth to bedrock (including marine silts and clays) may be as much as 100 m (Østmo 1976, Jørgensen & Østmo 1990).

The aquifer is bounded below by bedrocks of Precambrian age and to the south and west by marine clay sediments which have very low hydraulic conductivities. The delta top is relatively flat, lying at an altitude of around 200m above sea level and is surrounded by hills of outcropping basement rocks, except to the south and south west where the marine sediments form a lower lying plane at an altitude of around 150m. The Romerike deposit is believed to contain 150-200 million m<sup>3</sup> of good quality sand and gravel (Wolden & Erichsen 1990) and a number of pits have been excavated for this purpose throughout the area.

### 1.4 Hydrology

The main surface water drainage of the aquifer consists of the northwards-flowing River Risa and Hersjøen Lake. The river and lake are almost entirely groundwater-fed (Jørgensen & Østmo 1990, Hongve 1992).

There has been intense hydrogeological and hydrochemical investigation of the aquifer due to its selection as a study area for the International Hydrological Decade (Falkenmark 1972, Norwegian National Committee for IHD 1973, 1975). This has resulted in the publication of a hydrogeological map (Østmo 1976), and descriptions of the hydrogeology (Jørgensen & Østmo 1990) and hydrochemistry (Jørgensen et al. 1991). The aquifer is entirely fed by recharge from precipitation. Østmo's (1976) map (Fig. 1b) indicates that the major central part of the aquifer drains towards Hersjøen and the River Risa. The average discharge in the River Risa (in the period 1967-74) was 0.85 m<sup>3</sup>/s (Jørgensen & Østmo 1990). The marginal parts of the aquifer drain outwards towards springs in the periphery of the delta. Hydraulic and hydrochemical balances for the aquifer have been calculated. The permeability within the aquifer is believed to range between 5 m/d for coarse sands to 0.06 m/d for silts on the basis of particle-size distributions (Jørgensen & Østmo 1990).

### 1.5 Objective of modelling work

Groundwater flow modelling provides a quantitative tool that, when sufficient effort is invested in model calibration and verification, can be used to predict the short and long term effects of



varying recharge and groundwater abstraction. It can also provide a basis for further modelling of groundwater pollution incidents and their remediation, and can help in planning preventive action to maintain groundwater quality.

Modelling techniques are in common use in many countries that rely heavily on groundwater to supply domestic and industrial needs (e.g. Netherlands, Denmark, U.S.A.). Until relatively recently, water requirements in Norway were met almost solely from surface supplies, and as a result, competence in the area of groundwater modelling is at a rather low level compared with many other European countries and America.

Part of the aim of the project reported here has therefore been to help build modelling competence at the two participating institutions (Bergen Environmental Sciences and Solutions Centre [IBM/BSC] and the Geological Survey of Norway [NGU]).

The more concrete objective of the project has been to develop a three dimensional (or "2½ dimensional", since vertical discretization is limited to only two layers), time-dependent model of groundwater flow in the Øvre Romerike aquifer. This model has been constructed as a basis for a more detailed modelling study of the impact of a landfill site at Trandum, near the centre of the aquifer, on groundwater quality. The Trandum site lies in relatively close proximity to the Military's abstraction wells, has been investigated in detail by NGU (Misund & Sæther 1991, Sæther et al. 1992) and has produced an excellent set of hydrochemical data which lends itself to a more detailed hydro-chemical/-dynamic modelling attempt. This attempt will form the basis for a project application to the Norwegian Research Council, to be submitted in Spring 1993.

## **2. Physical characteristics of the Øvre Romerike aquifer**

### **2.1 The geological model and surface features**

NGU possesses large amounts of both geological and geophysical data from the Øvre Romerike area which have been used in the study. The main sources of data used to construct the geological model are:

- i) Borehole data collected during the International Hydrological Decade (IHD). These data have been published by Misund & Banks (1993).
- ii) Borehole data from groundwater contamination investigations at Trandum and Sessvollmoen (Storrø 1991, Banks 1991, Misund & Sæther 1991, Storrø & Banks 1992 and Sæther et al. 1992).

iii) Data collected in connection with the proposed Gardermoen main airport (NGI 1991).

iv) Seismic profiles run during the IHD; summarised on Østmo's (1976) map and by Longva (1987).

It is widely accepted that, although complex, the Romerike deposit is a generally fining-downwards glacio-fluvial and glacio-marine sequence (Longva 1987). In some boreholes, and most seismic profiles, it is possible to distinguish at least two distinct subdivisions or "layers"; an upper layer of medium-to-coarse sands and gravels and a lower layer of fine sand and silt grading down into clay. It must be pointed out that this is a considerable oversimplification; in the upper coarse section, wedges of fine sands and silt occur (Fig.2). In the silty layer recent investigations have indicated that several discrete sand horizons can be detected in the Gardermoen area, possibly associated with marginal spring horizons (Sønsterudbråten 1992).

VIAK (1990) have also constructed 3-D block diagrams which, even though they are based on a mixture of "enlightened guesswork" and real data, do illustrate the aquifer's considerable complexity (Fig.2b). However, because of the limited available data and the resolution possible in a numerical model, the aquifer structure chosen for modelling is simplified to two layers; a coarse-grained (high conductivity) upper layer and a finer (lower conductivity) lower layer.

The topography, rivers, roads and other prominent features were derived from 1:50 000 topographical maps of the Romerike area. The topography is taken to represent the top of the upper aquifer layer. Contour maps of the interface between the two layers and the aquifer base (top of bedrock or, where present, very low permeability marine clays/till) have been constructed, primarily from the seismic profiles and some borehole data, and thereafter digitised. Contour maps of the three layer interfaces are presented in Fig.3. Three-dimensional views of the geological model are shown in Fig.4.

The map of the aquifer base (Fig.3c) shows a deep channel lying under Hersjøen and the bed of the Risa river, and a deep basin in the south created by a channel in the bedrocks against which the marine sediments abut. The sediments of the aquifer essentially fill in this topography to produce the flat-lying topography of the delta top (Fig.3(a)). Isopach maps of the aquifer as a whole (Fig.5(a)) show that it is thickest where it fills in the deep basin in the south of the area (150m) and under Hersjøen (100m), and thinnest in the north, near Hurdalsjøen. Fig.5(b) and (c) show that the majority of the aquifer, as modelled, is composed primarily of the finer sediments with a relatively thin layer of coarse sediments laid on top. The coarse sediments

(Fig.5b) are thickest in the region of Hersjøen (up to 50m)<sup>1</sup> and virtually absent in the north-west of the area close to Hurdalsjøen.

## 2.2 Permeability data.

Using samples from the boreholes from sources i) to iii) above, grain size distributions have been analyzed at NGU. These distributions have been used to estimate hydraulic conductivity using the Bayer method (Langguth and Voigt 1980). In this method, the 10% and 60% ( $d_{10}$  and  $d_{60}$ ) grain size fractions are used to estimate hydraulic conductivity, porosity and effective porosity from three calibration graphs (Fig.6a). These graphs can be described very adequately by 5<sup>th</sup>- to 7<sup>th</sup>-order polynomials. For example, for hydraulic conductivity, K:

$$C = a + b \log_{10} U + c (\log_{10} U)^2 + d (\log_{10} U)^3 + e (\log_{10} U)^4 + f (\log_{10} U)^5$$

: where  $U = d_{60}/d_{10}$  and  $K = C \cdot d_{10}^2$  in m/s

A	1	0.120108904410752941E-01
B	2	-0.584932336100109015E-02
C	3	-0.511800227510852306E-03
D	4	0.515919309987529929E-02
E	5	-0.443467400175974902E-02
F	6	0.116482360824580501E-02

The fit of these polynomials to the calibration curves is shown in Fig.7. The polynomials have been entered into a spreadsheet to allow automatic calculation of the hydraulic parameters (Misund & Banks 1993).

In using these estimates of hydraulic conductivity, the limitations of the method and the quality of the data must be considered. The samples from the boreholes are of varying quality. The data from i) above are largely from sediment samples which have been rinsed up with drilling water, or pumped up through a slotted pipe, and are hence likely to be depleted in both fines and the coarsest fraction. Samples from ii) and iii) above are likely to be more representative. Boreholes under investigations ii) were sampled using a "throughflow" sampling device. Many of these considerations indicate that the estimations of hydraulic conductivity using this method are probably incorrect. However, they provide a useful starting point for modelling work, under the expectation that they will need to be adjusted during calibration. All hydraulic conductivity data were plotted on a histogram (Fig.8), and four main maxima were identified corresponding to clay, silt, fine sand and coarse sand/gravel.

---

<sup>1</sup> Due to the relatively sparse input data, the structure contour maps include some smoothing of surfaces, thus excluding local variations. Due to the coarse grid-size used in the numerical model (500 x 500 m), the loss of information this represents is not regarded as problematic. In reality, however, greater thicknesses of coarse aquifer material have been penetrated in narrow zones near Transjøen and Hersjøen (Misund & Banks 1993) than are indicated by the geological model.

## 2.3 Storage data

Very few pumping tests have been carried out in the Øvre Romerike aquifer which have yielded reliable values of storage coefficients. The following values have thus been used, as indicated by Fetter (1988)

Course layer  $S_y = 0.25$ ,  $S_s = 0.0003 \text{ m}^{-1}$

Fine layer  $S_y = 0.20$   $S_s = 0.0003 \text{ m}^{-1}$

## 2.4 Recharge model

### 2.4.1 *The basic recharge model*

There are several methods which can be used to assess recharge to an aquifer from precipitation. Two of the simpler methods which are often used are:

- i) to assume that a fixed percentage (e.g. 30%-50%) of precipitation percolates down to the water table.
- ii) calculation of soil moisture balance

"The soil moisture model" considers the soil zone as a reservoir which contains a certain amount of water (soil moisture). This quantity is typically quoted in mm (i.e.  $\text{m}^3/1000 \text{ m}^2$ ).

The model assumes that percolation of water from the soil down to the water table only occurs if the soil is at "field capacity". If the soil is undersaturated with respect to field capacity, percolation will not occur. The degree of undersaturation with respect to field capacity is called the "soil moisture deficit" (SMD), and is expressed in mm.

In addition the model assumes the following scenario, illustrated in text figure 1.

For any given day:

$$AS = -(P - RO - AE)$$

Where AS = actual change in soil moisture deficit ( $\Delta\text{SMD} - R$ )

P = precipitation

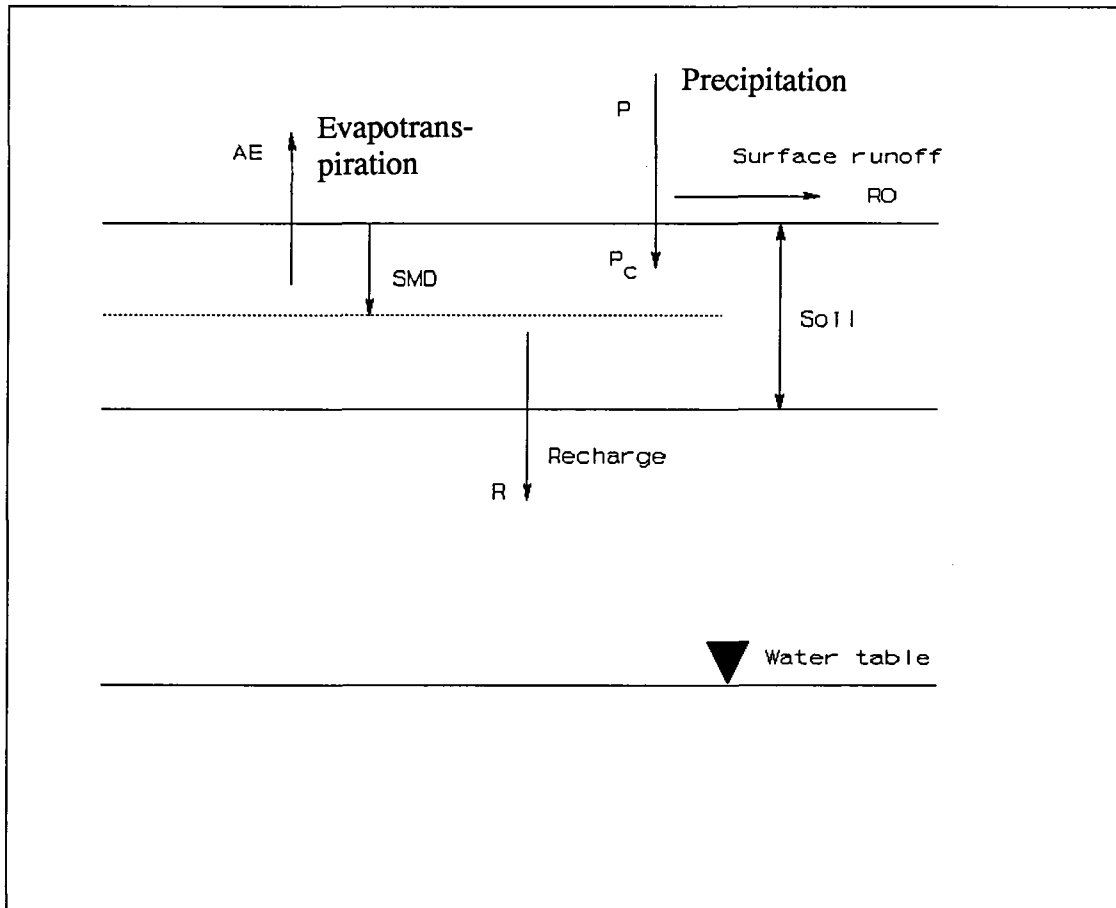
RO = surface run-off

AE = actual evapotranspiration

R = recharge to groundwater

$$R = 0 \text{ if } \text{SMD} > 0.$$

All values are quoted in mm.



*Text Fig. 1. The assumed recharge model*

Surface run-off depends on natural conditions such as e.g. topographical gradient, soil type etc. It is often simply calculated as a fixed percentage of P. In the Øvre Romerike model, surface run-off was assumed to be negligible, due to the porous sediment material, the flat delta surface and the observed lack of surface watercourses on the aquifer.

$$P_c = \text{precipitation corrected for surface run-off} = (P - RO)$$

P is often available from meteorological institutes as daily data, as are values of potential evapotranspiration (PE). PE is the amount of evapotranspiration which can occur under ideal conditions. In reality, AE will often be less than PE, especially if the soil moisture deficit is high. If such is the case, plants cannot suck up as much water as they "want to" because the soil is too dry.

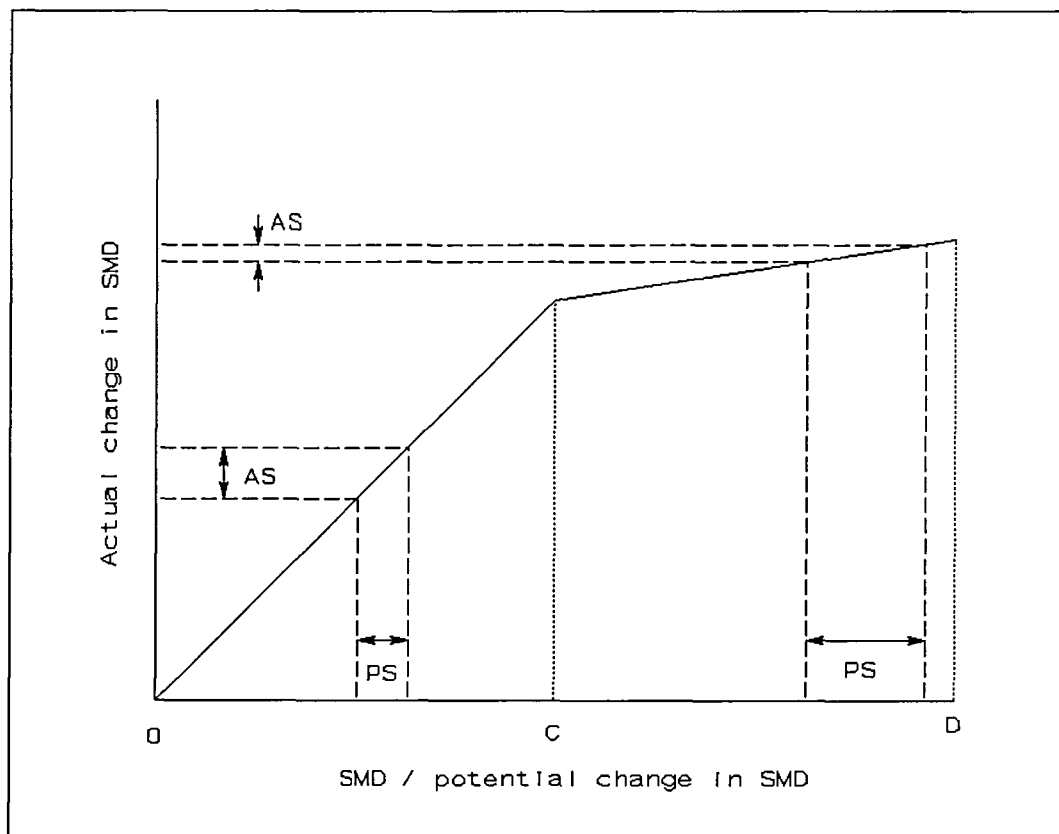
Therefore, in order to solve for recharge, it is necessary to calculate AE and SMD.

The model assumes:

$$PS = -(P - RO - PE) = PE - P_c$$

Where PS = potential change in soil moisture deficit

If the soil is wet, and enough water is available, evapotranspiration occurs at its potential level ( $AE = PE$ ). AS is therefore equal to PS. According to the model, this occurs until the SMD reaches a level called the **root constant** (C). At this point, the soil is so dry that the extent of AE is reduced. The model assumes that if  $SMD > C$ , then  $AS = PS/10$  (Text Fig. 2). If the soil becomes even drier, and SMD reaches **wilting point** (D), the plants die and evapotranspiration ceases. Reality is of course more complex. There is not found a sharp break-point at C or D, only a gradual reduction in AE/PE with increasingly dry soil. The 10 %-factor on exceeding the root constant is also rather arbitrary. Nevertheless, experience has shown that such a model can give sensible results in most situations. It is normally called the "Penman/-Grindley method" (see e.g. Rushton & Redshaw 1979).



Text Fig. 2. Actual change in soil moisture deficit, as a function of soil moisture content.

PS is calculated on a daily basis. Calculations based on periods longer than one day will give misleading results. Every day, one "tests" whether PS is positive or negative. The SMD at the end of the  $n^{\text{th}}$  day is termed  $SMD_n$ .

If PS is negative:

effective precipitation ( $P_c$ ) is greater than PE. There is therefore a lot of available water in the soil for evapotranspiration, and:

$$AE = PE$$

To begin with, one assumes that  $R = 0$ :

$$SMD_n = AS + SMD_{(n-1)} = SMD_{(n-1)} - (P_c - AE)$$

If  $SMD_n > 0$  then  $R = 0$

If  $SMD_n \leq 0$  then  $R = -SMD_n$ , and  $SMD_n$  is reset to 0.

If PS is positive:

there are two possibilities:

i) If  $SMD_{(n-1)} < C$

then  $AS = PS$

$$AE = PE$$

$$SMD_n = AS + SMD_{(n-1)} = SMD_{(n-1)} - (P_c - AE)$$

ii) If  $SMD_{(n-1)} > C$

then  $AS = 10\% \times PS$

$$SMD_n = AS + SMD_{(n-1)} = SMD_{(n-1)} - [0.1 * (P_c - PE)]$$

$$AE = P_c + AS$$

Example

As examples of the use of this model, the following data from Øvre Romerike (Gardermoen meteorological station - Table 1a ) are shown, together with an example from Rushton (1983) (Table 1b).

*Table 1a: Calculation of recharge from real data from Gardermoen, autumn 1966. "Root constant" = 175 mm, and is therefore not reached. Recharge only occurs when SMD = 0. Surface run-off = 0. All values in mm.*

Year	Day	Precipitation	Potential evapotranspiration	Potential change in SMD	Soil moisture deficit	Actual change in SMD	Actual evapotranspiration	Recharge to groundwater
		P	PE	PS	SMD	AS	AE	R
1966	237	0.000E+00	3.200E+00	3.200E+00	1.260E+01	3.200E+00	3.200E+00	0.000E+00
1966	238	0.000E+00	3.100E+00	3.100E+00	1.570E+01	3.100E+00	3.100E+00	0.000E+00
1966	239	0.000E+00	3.200E+00	3.200E+00	1.890E+01	3.200E+00	3.200E+00	0.000E+00
1966	240	0.000E+00	3.000E+00	3.000E+00	2.190E+01	3.000E+00	3.000E+00	0.000E+00
1966	241	0.000E+00	2.600E+00	2.600E+00	2.450E+01	2.600E+00	2.600E+00	0.000E+00
1966	242	0.000E+00	1.800E+00	1.800E+00	2.630E+01	1.800E+00	1.800E+00	0.000E+00
1966	243	0.000E+00	5.000E-01	5.000E-01	2.680E+01	5.000E-01	5.000E-01	0.000E+00
1966	244	1.030E+01	0.000E+00	-1.030E+01	1.650E+01	-1.030E+01	0.000E+00	0.000E+00
1966	245	4.000E-01	1.000E-01	-3.000E-01	1.620E+01	-3.000E-01	1.000E-01	0.000E+00
1966	246	9.400E+00	2.000E-01	-9.200E+00	7.000E+00	-9.200E+00	2.000E-01	0.000E+00
1966	247	5.100E+00	3.000E-01	-4.800E+00	2.200E+00	-4.800E+00	3.000E-01	0.000E+00
1966	248	6.500E+00	2.100E+00	-4.400E+00	0.000E+00	-4.400E+00	2.100E+00	2.200E+00
1966	249	2.000E-01	4.000E-01	2.000E-01	2.000E-01	2.000E-01	4.000E-01	0.000E+00
1966	250	3.400E+00	2.200E+00	-1.200E+00	0.000E+00	-1.200E+00	2.200E+00	1.000E+00
1966	251	0.000E+00	1.500E+00	1.500E+00	1.500E+00	1.500E+00	1.500E+00	0.000E+00
1966	252	0.000E+00	5.000E-01	5.000E-01	2.000E+00	5.000E-01	5.000E-01	0.000E+00
1966	253	0.000E+00	1.000E-01	1.000E-01	2.100E+00	1.000E-01	1.000E-01	0.000E+00
1966	254	6.000E-01	7.000E-01	1.000E-01	2.200E+00	1.000E-01	7.000E-01	0.000E+00
1966	255	1.900E+00	1.000E+00	-9.000E-01	1.300E+00	-9.000E-01	1.000E+00	0.000E+00
1966	256	1.590E+01	1.200E+00	-1.470E+01	0.000E+00	-1.470E+01	1.200E+00	1.340E+01
1966	257	2.600E+00	6.000E-01	-2.000E+00	0.000E+00	-2.000E+00	6.000E-01	2.000E+00
1966	258	7.000E+00	1.000E+00	-6.000E+00	0.000E+00	-6.000E+00	1.000E+00	6.000E+00
1966	259	0.000E+00	1.100E+00	1.100E+00	1.100E+00	1.100E+00	1.100E+00	0.000E+00
1966	260	0.000E+00	1.300E+00	1.300E+00	2.400E+00	1.300E+00	1.300E+00	0.000E+00

#### 2.4.2 Use of snow data in the recharge model

The most common versions of such a model treat snow exactly as rain, i.e. that snow infiltrates directly into the ground. In Scandinavia, this is not satisfactory, as during winter a store of precipitation is built up in a long-lasting snow cover, without significant amounts being recharged to the soil and further to the water table. In Norway, the winter is the period when groundwater levels recede to their lowest levels (Kirkhusmo & Sønsterud 1988, Nordberg 1980), in contrast to e.g. England, where the majority of recharge occurs in winter. Unfortunately there is no simple relationship between the amount of water (in mm) which is stored in the snow cover, and its thickness, as the snow becomes steadily more compacted during winter



*Table 1b: Calculation of infiltration when SMD is approximately equal to the root constant (C 100 mm). All values are in mm. Example from Rushton (1983).*

Day	Precipitation P	Surface run-off RO	Potential evapotranspiration PE	Potential change in SMD PS	Actual change in SMD AS	Soil moisture deficit SMD	Actual evapotranspiration AE	Recharge to groundwater R
179						96,0		
180	0,0	0,0	3,3	3,3	3,3	99,3	3,3	0,0
181	0,0	0,0	3,7	3,7	3,7	103,0	3,7	0,0
182	8,3	1,4	2,7	-4,2	-4,2	98,8	2,7	0,0
183	2,3	0,2	3,2	1,1	1,1	99,9	3,2	0,0
184	0,5	0,1	3,8	3,4	3,4	103,3	3,8	0,0
185	0,0	0,0	3,7	3,7	0,37	103,67	0,37	0,0
186	2,1	0,4	3,4	1,7	0,17	103,84	1,87	0,0
187	15,6	3,6	2,5	-9,5	-9,5	94,34	2,5	0,0
188	0,0	0,0	3,6	3,6	3,6	97,94	3,6	0,0
189	0,0	0,0	3,8	3,8	3,8	101,74	3,8	0,0
190	0,7	0,1	3,6	3,0	0,30	102,04	0,90	0,0

(Nor.Nat.Comm. I.H.D. 1975). One cannot therefore use changes in snow depth to assess whether accumulation or melting of the snow cover is occurring. In NGU/IBM's model it has been chosen to use a simplified model. Data from the Meteorological Institute contain daily measurements of precipitation, snow depth and degree of snow coverage (S) from 0 (no cover) to 4 (100 % cover). The IBM/NGU model considers 3 different modes of treatment of snow data:

i) When  $S \leq 1$ , the model functions as the normal summertime model.

ii) When  $S > 1$ , the model switches to "accumulation mode". No precipitation seeps into the soil layer; it is all stored in the snow layer. Evapotranspiration of existing soil moisture is allowed, such that the SMD steadily increases during this period, and no groundwater recharge occurs.

iii) When the snow cover begins to decrease ( $S_n < S_{n-1}$ ), the model switches again to "melting mode". New precipitation is allowed to enter the soil zone and all precipitation which is stored in the snow layer is allowed to melt and seep into the soil, where it is treated by the model as normal rainfall. The melting occurs as follows:

$$\text{Daily amount of meltwater} = \frac{\text{precipitation stored in snow during accumulation}}{\text{duration of melting period}}$$

During the melting period, relatively large amounts of meltwater seep into the ground, and the SMD is quickly satisfied, allowing recharge to the water table.

The melting period finishes when S reaches 0 again (and the model returns to "normal mode"), or when S begins to rise again (and the model returns to mode ii).

It should be mentioned that the model does not take into account changing run-off due to frozen ground conditions.

### 2.4.3 Results

The recharge model was run for the period 1968-1974 (Fig. 9), using a root constant of 175 mm, and assuming surface run-off = 0, due to the flat and permeable nature of the aquifer surface. The results were found to correspond very well to empirical estimates calculated from the hydrological balance of the aquifer by Jørgensen & Østmo (1990) for the same period (Table 2). The results of the model also give the typical two recharge peaks every year, one at snow melt and one in late summer, a typical pattern for inland Norway (Nordberg 1980).

*Table 2. Comparison of recharge model with empirical data. Annual averages for period 1968 - 1974. (In model run-off = 0, root constant = 175 mm). The recharge models with and without the snow package yield similar average results for the period in question, but the snow package radically improves the distribution of recharge within a given year. In the third column, recharge is not exactly equal to precipitation - evapotranspiration due to end effects of snow storage at the beginning and end of the simulation period)*

	Empirical (Jørgensen & Østmo 1990)	Recharge model with- out snow package (snow treated as rain)	Recharge model (with snow pack- age)
Precipitation mm	794	844	843
Evapotranspiration mm	400	445	447
Recharge mm	394	399	407

## **3. Groundwater flow modelling**

### **3.1 MODFLOW**

To model groundwater flow, the numerical model MODFLOW, written by the USGS, was chosen (McDonald & Harbaugh 1988). This is a finite difference model which is widely used throughout America and Europe and thus has the advantage of being well tested, with clear instructions for its use. MODFLOW can only simulate flow in the saturated zone (below the water table) but this has not been a serious disadvantage for the present project since the data required to model flow in the unsaturated zone are not available for the sediments of the Øvre Romerike area. Both steady state and transient simulations can be performed.

MODFLOW requires a geological model defined on a grid (dimensions and size chosen by the user) as well as arrays defining the cell type, horizontal and vertical hydraulic conductivities, and storage coefficients (for transient simulations) for each grid block in each layer. In addition, files describing the properties and location of rivers, drains, wells and areas of constant head must be provided by the user. In many cases, these files of data must be compatible with each other. Much of the work involved in using MODFLOW lies in the creation of these files. At BSC, time was invested in building a GUI (graphical user interface) to automatically perform as much of this work as possible.

### **3.2 Data preparation and the Graphical User Interface**

The contour maps of the geological model (Fig.3) were automatically digitised using the data capture software developed at IBM/BSC in Bergen. The prepared maps were scanned and the resulting images vectorised to give the contours as a series of points. Each contour was then assigned a height value using the AUTOCAD package. These digitized contour maps were then rasterized using the commercial GIS package GENAMAP (GENYSIS). This procedure results in maps consisting of small square regions (pixels) each of which has a height associated with it. Each pixel represents a region of 50 by 50 m. These rasterized maps provided the basic input for the graphical user interface and an example is shown in Fig.10. The graphical user interface can display the input maps together with information on the location of rivers and roads to help the user define the MODFLOW grid. MODFLOW requires a grid that is uniform and right-angled (i.e. squares or rectangles) when viewed from above. This grid is generated interactively by entering the number of rows and columns in the X-Y grid plane and locating the bottom left hand and top right hand corners of the grid on the map displayed by the GUI using a mouse. The interface then automatically determines the heights of the grid nodes at the top and bottom of each geological layer, using the rasterized maps. Once a satisfactory grid has been generated it may be saved and recalled on later applications of the user interface. The cell type may be altered to "no flow" or "constant head" and properties, such as height of constant

head cells and horizontal hydraulic conductivities may be assigned interactively. Cells containing rivers are automatically detected using the input digitized information on river locations. An example of the interface screen with the windows displayed is shown in Fig.11. The interface then uses this information to create the necessary input files for MODFLOW, checking for internal consistency. At present, files containing information on recharge, drains and output control flags must be created separately. The interface makes possible the rapid generation and modification of the input required for MODFLOW, thus relieving the user of much time-consuming and tedious work. This enables the modeller to run the model many times and allows him/her to concentrate most effort on the generation of a hydrogeologically good model.

### 3.3 The grid and boundary conditions

A grid of 36 by 24 square blocks (Fig.12), covering almost the entire areal extent of the Øvre Romerike aquifer was generated using the user interface. The whole area covered by the grid is 18 by 12 km and each grid block represents an area of 500 by 500 m. Boundary conditions are defined so as to represent external influences on the groundwater system. As much as possible, natural features were used to determine conditions around the model perimeter. The crystalline bedrock underlying the aquifer and the clay-rich marine sediments in the southwest are assumed to be impermeable, and grid cells representing these lithologies are defined as "no-flow" cells. The lakes Hurdalsjøen and Hersjøen were modelled as constant head cells (constant water level throughout the simulation). This seems reasonable since the level of these lakes varies very little with time and they are believed to be in some degree of hydraulic continuity with the aquifer. These no-flow and constant head cells fix conditions on a large proportion of the model's boundary.

The Risa river, the smaller stream from Transjøen to Hersjøen and the small eastern tributary of the Risa were modelled using the river package in MODFLOW. Here rivers are assumed to be continually active and are either influent or effluent with respect to the aquifer depending on the relative heights of the river bottom and the water table. It has been assumed that the river beds represent no significant barrier to water exchange between the aquifer and the river, i.e. that the sediments in the river bed have the same hydraulic conductivity as the aquifer at this level.

Springs which occur along the west and the southwest margins of the aquifer, near the boundary with the underlying marine sediments, are modelled using the drain package of MODFLOW. Here only flow from the aquifer to the spring-fed stream is possible. The springs are only active when the water table is higher than the drain level, and flow is proportional to the water table height above the spring elevation. This allows the simulation of streams or springs which can go dry, and prevents influent (recharge) conditions occurring.

The remaining small portions of the model's outer boundary, which cannot be defined as no-flow cells or drains, are assigned a reasonable value of constant head derived from Østmo's (1976) map. The water level in these cells should strictly be variable, but since there are only a small number of them and they are situated in regions where the aquifer is relatively thin, holding their water levels constant has only minor effects on the rest of the model.

The boundary conditions and allocation of cell types in the model are shown in Fig.12. Recharge is assumed to be constant over the whole region. MODFLOW was used in the mode that adds recharge to the top of the uppermost active cell. No account is therefore taken of the time taken for water to travel through the unsaturated region. Rain falling on bedrock areas is neglected, except in the east where it is, in part, represented by the small eastern tributary of the Risa which rises from a small bedrock outcrop.

The task of modelling the groundwater flow in the Øvre Romerike aquifer was divided into two sections:

- (1) generation and calibration of the hydraulic conductivity model under steady state conditions,
- (2) transient modelling and comparison with the available time series data on water table levels in three observation boreholes.

## 4 The steady state model

### 4.1 Calibration of the steady state model

The aim of the steady state modelling was to generate a hydraulic conductivity model for the two aquifer layers that produces water table levels and water fluxes in rivers and springs in acceptable agreement with observations. A total of 183 water levels measured in boreholes, largely in the period 5-7 November 1975, from Østmo's map (1976) were used in model calibration. They cover most of the region but are especially concentrated in the region surrounding Hersjøen, Fig.13. Two parameters were used to test the fit of the model results to these borehole measurements. To test the fit of the model results to the observations on the scale of the whole model, the average discrepancy,  $D$ , was calculated:

$$D = \frac{\sum (h_m - h_o)}{n}$$

where  $h_m$  and  $h_o$  are the modelled and observed water table levels, respectively, and  $n$  is the number of grid blocks where borehole observations are available. To test the fit of model results to the observations on the scale of one grid block, the root mean square of the discrepancies,  $\text{rms}D$ , was used:

$$rmsD = \sqrt{\frac{\sum (h_m - h_o)^2}{n}}$$

The best fit is obtained when D and rmsD are minimized, although as individual deviations can be positive or negative, more emphasis was laid on minimising rmsD than D itself. Since the borehole observations are point measurements, they reflect a wide range of frequencies of spatial variations in the water table, and several boreholes in a single grid block can exhibit considerably different water levels. In the simulation however, one grid block is allowed a single water level and only variations in water table on the scale of a single grid block or larger can be modelled. Thus, in calibration, an exact fit (i.e. values of rmsD approaching zero) should not be expected.

Other available methods of calibrating the model are to compare the fluxes in rivers and springs. Data are available for the water flux in the Risa river at Risabru (Fig.1a), at the north end of Hersjøen. The flow in the Risa (Jørgensen & Østmo 1990, Norweg. Nat. Comm. IHD 1973, 1975) varies little throughout the year and has an average value of around 0.7 m<sup>3</sup>/sec. In MODFLOW, the flux in rivers is not directly calculated, only the exchange rates between rivers and the aquifer. However, an estimate may be made by considering the upstream influences on flow rates at Risabru (the NVE gauging station on the Risa, at Grid.Ref. 203 801). An estimate of this flow rate from the simulation was obtained by summing the fluxes from the aquifer to:

- 1) constant head cells representing Hersjøen,
- 2) cells representing the stream from Transjøen to Hersjøen,
- 3) the drain cells representing the springs at Dagsjøen
- 4) cells representing the Risa river upstream of Risabru

This sum is likely to overestimate the flow at Risabru as it does not include the effects of evaporation from Herjøen or possible losses to the aquifer between Dagsjøen and Hersjøen.

Water flowing from the springs along the southwest margin of the aquifer provides the main input to the Leira and Vikka rivers which are situated on the marine sediments and flow parallel to the aquifer's margin (Fig.1a). Sporadic data is available on flux in the Vikka river (at UTM 154 722) for the period 1989 to 1991 (NVE 1991), giving an average of 0.089 m<sup>3</sup>/sec. From this a rough estimate can be made of the flux from all the springs along the southwest margin. From the map, approximately one quarter of the southwestern marginal springs feed the Vikka upstream of the measuring station. Assuming that the outflow from each of the springs is roughly comparable along this margin of the aquifer, an estimate of the flux from all springs is therefore given by four times the measured flux in the Vikka. Since the Vikka is partially fed by runoff from the low-permeability marine sediments, this represents an upper boundary. The springs are likely to provide at least half of the influx to the Vikka, so that one half of this

estimated flux provides a lower boundary. The total flux from the springs along the southwestern margin is therefore estimated to lie between 0.36 and 0.18 m<sup>3</sup>/sec.

## 4.2 The permeability model

The major variables still to be determined in the model are grid block hydraulic conductivities (both within and between the two layers) and the recharge rate. For a given recharge rate, there are many possible hydraulic conductivity models that can satisfy the calibration data outlined above. It is therefore not possible to arrive at a unique solution to the hydraulic conductivity field, but by using the available data on hydraulic conductivity and recharge as a guide, a likely solution can be obtained. Time-dependent data indicate that the water table lies at approximately its average level for the year of 1975 during the month of November, although recharge is normally below average in this month. This discrepancy is due to the delaying action of the unsaturated zone on recharge arrival at the water table, and to the fact that November lies on the decaying limb of the previous hydrograph peak of earlier autumn. For the purposes of the steady state model, where the aim is to reproduce the water table levels in November 1975, the average recharge rate for 1975 ( $1.27 \times 10^{-8}$  m/s) was used, rather than the November value for this year (c.  $1 \times 10^{-8}$  m/s). *[All recharges generated using root constant = 175 mm and run-off = 0].*

In reality, both the coarse upper and fine lower layers of the aquifer model are composed of intercalated layers and lenses of coarse and fine sediment, the difference being the relative proportions of sediment grain size fractions. The grain size samples (Misund & Banks 1993) from which hydraulic conductivities are estimated therefore reflect this intermixture of layers and lenses, rather than the overall hydraulic conductivity of the coarse and fine layers. This means that it has not been practical to conclusively identify the boundary between the two modelled layers using the hydraulic conductivity estimates from borehole samples or to assign a grain size sample to a specific layer. However, the histogram of all available hydraulic conductivity estimates (Fig.8), based on  $d_{60}$  and  $d_{10}$  data, shows several peaks which are typical for coarse, fine and clay-rich sediments. This histogram was used as a guide to the likely average hydraulic conductivity values of the two modelled layers, which were thus estimated at  $2.0 \times 10^{-4}$  m/s (coarse layer) and  $7.0 \times 10^{-6}$  m/s (fine layer), corresponding to the "coarse sand" and "fine sand" peaks on the histogram. These conductivities were used as a starting point for model calibration.

To determine the most probable average hydraulic conductivities for each layer, MODFLOW was first run using two spatially homogeneous layers. A hydraulic conductivity of the fine layer of  $7.0 \times 10^{-6}$  m/sec (the value suggested by the histogram in Fig.8) was found to be too low, yielding water table levels which were too high regardless of the hydraulic conductivity assigned to the coarse layer.

In order to develop a strategy for modelling the hydraulic conductivity, the sensitivity of the homogeneous layer model to variations in hydraulic conductivity was tested by holding the hydraulic conductivity of one layer constant, varying the other and recording the change in the average error,  $D$ , as a measure in net change in the water table level. The results, shown in Fig.14, show that the water table level is many times more sensitive to variation in the hydraulic conductivity of the lower fine layer than the coarse upper layer. This is consistent with the observation that the water table tends to be situated close to the interface between the two layers over large areas of the aquifer, indicating that water table levels are largely controlled by properties of the fine layer.

A hydraulic conductivity of  $7.2 \times 10^{-4}$  m/sec was assigned to the coarse layer, a near maximum value. The hydraulic conductivity of the fine layer that minimized the total error,  $D$ , was then found. This resulted in a hydraulic conductivity value of  $3.2 \times 10^{-5}$  m/sec for the fine layer, which is somewhat higher than the initial estimate based on the histogram in Fig.8. The modelled results were discovered to be extremely insensitive to the hydraulic conductivity of the coarse layer.

There are two justifications for the discrepancy between the modelled conductivities for the fine layer and those derived from grain size analysis. Firstly, it is probable that the estimates of hydraulic conductivity from grain size samples are rather inaccurate and contain systematic errors due to the sampling and /or analytical procedure. Secondly, the fine layer is composed of intercalated fine and coarser layers, whereas the 'fine sand' histogram peak probably represents primarily the finer grained portions of the layer and thus leads to an underestimation of the layer's average hydraulic conductivity.

The modelled estimates of the 'average' hydraulic conductivity of each layer (i.e.  $7.2 \times 10^{-4}$  and  $3.2 \times 10^{-5}$  m/s) were considered a satisfactory intermediate point in the development of a hydraulic conductivity model for the Øvre Romerike aquifer. The homogeneous layer model described above, although minimizing the average error,  $D$ , gave a high value of rmsD (5.86m), see Fig.15(a). To improve the fit of modelled to observed water levels, the hydraulic conductivity field within each layer was allowed to vary horizontally. The fit of the modelled to observed data was improved as much as possible by modifying the spatial distribution of hydraulic conductivity within the fine layer, this layer's hydraulic characteristics being the most important for determining the water table level.

Using this approach, rmsD values were improved to 3.4m while maintaining a low value of average error,  $D$  (0.22 m). In most grid cells where observations were available, the discrepancy between the simulated and observed data was 5m or less and frequency histograms of the errors for the homogeneous layer and modified layer models are shown in Fig.15. Although the 5 m error may sound large, it must be remembered (as previously explained) that one is comparing the average water table within a 500 x 500 m grid block, with the observed data



from a single point within the block, often in areas with high water table gradients. The "final" hydraulic conductivity field for the fine layer is shown in Fig.16, and the simulated water table level, compared to Østmo's (1976) map in Fig.17b. A three dimensional view of the aquifer base and the modelled water table are shown in Fig. 17c. Values of flux at Risabru, calculated in the manner described above, and flux from the springs along the southwest margin of the aquifer were acceptably close to the observed values, and are listed in Table 3.

*Table 3 - Outflows from springs; modelled and observed*

Location	Modelled flow m <sup>3</sup> /s	Observed flow m <sup>3</sup> /s
R.Risa at Risabru	0,82	0,7
Springs in SW	0,29	0,18 - 0,36

By comparing the groundwater head values in the upper and lower layers, one can identify vertical head gradients and areas where upward or downward flow is occurring. This has been done, the results being presented in Appendix 4. The 2-layer model is clearly not adequate to satisfactorily model vertical head gradients, but in general downward head differentials are observed in the area corresponding to the main watershed (i.e. recharge area), while upward differentials are observed along the River Risa (discharge area).

## 5 The transient model

### 5.1 Modifications to MODFLOW

The version of MODFLOW received from the USGS is designed to model situations in which the water table is, in general falling, e.g. the development of drawdown cones due to pumping. The model is so written that if a model cell goes dry, it is redefined as a "no flow" cell and remains inactive for the remainder of the simulation. With this code it is therefore not possible to model the behaviour of a water table which is expected to rise over the boundary between two layers. Since, in a significant part of the Øvre Romerike area, the water table is known to lie close to the boundary between the coarse and fine sediment layers, varying recharge is expected to cause the water table to cross this boundary many times in the 31 year period for which time series data is available. Thus, this feature of MODFLOW was a serious drawback for modelling transient behaviour and it was necessary to modify the code.

In order to allow a water table to rise significantly during a single simulation, an additional subroutine was added to MODFLOW to check and, if necessary, modify the conditions at cells which have gone dry at some point during the simulation. When the head in the cell below is

higher than the base of the dry cell (indicating a rising water table), the dry cell is reactivated and its head set to that of the cell below. Cells in the bottom layer and cells underlain by inactive (no flow) cells are reactivated when a minimum of one immediate neighbour has a head greater than the base of the dry cell (indicating potential flow into the dry cell) and their heads set to a value slightly higher (10 cm) than the cell base. Since the subroutine is called between time steps, care must be taken that time steps are small enough to sufficiently resolve upwards movements in the water table, i.e., that changes in head within a single time step are small compared to the average grid height.

## 5.2 Input to the transient model

As a test of MODFLOW in transient mode, a simulation with the average recharge for 1975 ( $1.27 \times 10^{-8}$  m/sec) was run for 16 stress periods of 1 year, with 4 timesteps per stress period and an initial water table at the aquifer top (i.e. topography). The model converged to a solution which lay to within a few centimeters of the steady state model results after some 25 stress periods, confirming the results of steady state modelling.

The transient model was also run with the initial head set below the top of the fine layer. This also converged to the steady state solution, proving that the modifications to MODFLOW, made to allow resaturation of dry cells, function satisfactorily.

For transient simulations using time-dependent recharge data (derived from the recharge model), the length of stress period (i.e. time over which external stress conditions such as recharge are constant) was set to 1 month, the maximum time interval between successive measurements in the observed data. Two time steps of equal length per stress period were found to be sufficient to resolve movements of the water table and no significant difference in the results was obtained by increasing the number of timesteps. Recharge data was calculated for monthly intervals from the meteorological data as described in section 2.4, for the time period from May 1960 to June 1991, giving a total of 374 stress periods.

The hydraulic conductivity field and boundary conditions as determined in the steady state model were used in the transient model. The water table levels in May 1965 (when time-series data for observation wells commences), which should be used as initial levels in the transient modelling, are unknown. The increasing trend in the recharge for the period 1960 to 1965, suggest that the water table was probably at lower than average level in 1960. Two initial water table levels were used in the model to investigate the effect of initial water table levels on the model results at the three observation wells, Hauersetter, Sand and Nordmoen. These two initial conditions were generated by using the calibrated, spatially variable, hydraulic conductivity model and running MODFLOW in steady state mode with recharge values corresponding to:

(1) the average value for 1975 ( $1.27 \times 10^{-8}$  m/sec - as used in the calibration of the hydraulic

conductivity model)

- (2)  $8.293 \times 10^{-9}$  m/sec representing approximately the minimum annual recharge for the time period 1965 to 1990.

### 5.3 The transient model results and comparison with observations.

The model results are compared with observed time series data from the three observation wells at Hauer seter, Sand and Nordmoen (Kirkhusmo & Sønsterud 1988) for the period from May 1967 to September 1991. Information and model input parameters at the locations of the three wells are listed in Table 4 (UTM, height, cell number, thickness of layers, layer hydraulic conductivities).

Table 4 - Observation wells with time-series data (Kirkhusmo & Sønsterud 1988)

Location	UTM coordinates	Elevation, m above sea level	Cell in MODFLOW (col,row)	Elevation of top of fine layer in model	Elevation of base of aquifer in model
Hauer seter	219 745	c.215	(18,25)	196,19	132,63
Sand	191 706	c.200	(13,33)	186,50	123,12
Nordmoen	168 816	c.200	(8,12)	192,96	132,13

The transient model run with the best-fit steady state model heads as initial conditions (i.e. recharge =  $1.27 \times 10^{-8}$  m/s) is shown in Fig.18(a). The model shows similar trends to the real data, but with the absolute elevation of the model results too high for Hauer seter by some 3-4m, and an overall good fit for Nordmoen and Sand. All three model trends show much greater seasonal variations than the observed data. This is due to the 'damping' effect of the unsaturated zone (i.e. the "smearing out" of major recharge peaks) which is not included in the model. It was found that this "smearing" effect could be simulated by taking running averages of the recharge data over 7-monthly periods, and the results are shown in Fig.18(b). This modified model produces results which show very similar variations to the observed data, but with the modelled results lagging some months behind the model data. The magnitude of this lag varies from 1 to 10 months and is roughly correlated with the thickness of the unsaturated zone. This correlation is also seen in the nature of the trends of observed data. The data from Nordmoen, where the thickness of the unsaturated zone is 1 to 3 m, are more jagged, indicating more rapid water-table fluctuations than at Hauer seter and Sand, where the unsaturated zone is between 10 and 20 m thick. This illustrates the "smearing" or "damping" effect of the unsaturated zone, which tends to smooth out the high frequency variations in recharge.

The time lags between observed and modelled data, and the respective unsaturated zone thicknesses, indicate a range of filtration velocities between 1 and 12 cm/day. These results are low compared with estimations from field observations by Jørgensen and Østmo (1990) of around 17 - 20 cm/day during the spring of 1966 at Nordmoen. Filtration velocities are dependent not only on the nature of the sediments, but also on their degree of saturation (hydraulic conductivity decreases markedly with decreasing saturation). Jørgensen and Østmo's observations were made during snow melt when saturation levels were high. In addition, the unsaturated zone was thin (1.35 to 2.65 m) so that high saturation levels throughout the thickness of the unsaturated zone are more easily reached during periods of high recharge.

The modelled trends all show a similar type of deviation from the observed data in that they fall less sharply in the time period from 1967 to 1976 and rise quicker in the time period 1976 to 1991. However the change in discrepancies between modelled and observed water levels in the observation wells over this 26 year period are small (2.5m for Hauerseier, 2.2m for Nordmoen and 1.7m for Sand). These discrepancies are of the same magnitude, or smaller, than the discrepancies between the steady state model and observed water table levels for November 1975.

However, the nature of the water table at the start of transient simulations (May 1960) is unknown and so to test the possible influence of the initial heads on the modelled trends, a further simulation was run with a lower initial water table generated as described above (the steady state solution with a recharge of  $8.293 \times 10^{-9}$  m/sec) and the results are shown in Fig.19.

Comparison of Figures 18(b) and 19(b) show that the lower initial head condition results in a slightly improved fit at Hauerseier. The two trends resulting from the different initial head conditions converge, however, and become indistinguishable after some 160 months. At Sand and Nordmoen, the effect of different initial water tables is less marked and the two trends become indistinguishable after some 90 months. The model trend resulting from the lower initial head condition shows a better fit to the real data trends, with the variations in deviation between the modelled and observed data from 1965 to 1991 reduced to around 1m for all three observation wells.

## 6. Conclusion

Using the U.S.G.S MODFLOW code, coupled with a Penman-Grindley type recharge model, it has been possible to produce a transient, 3-dimensional groundwater flow model of the Øvre Romerike aquifer. It was, however, found necessary to modify the MODFLOW code to allow the water table to rise across the boundary of aquifer layers, and to modify the recharge model to take into account snow effects during winter.

A steady state model has been calibrated against 183 regional water level observation data from autumn 1975 and against the flows in groundwater fed springs and streams. Allowing for the limited resolution attainable using 500 x 500 m grid blocks in areas of high water table gradient, the fit achieved was highly satisfactory. The distribution of hydraulic conductivity calibrated using the steady state model was then used to simulate water table variations over a period in excess of 30 years. Calibration data at 3 observation wells showed satisfactory fits with modelled data, again allowing for the limited spatial resolution of the model, and the uncertain elevations of the real data points. A seven-month running average filter has been applied to the data to simulate the damping effects of the unsaturated zone on recharge maxima and minima, resulting in an even better fit. The seasonal variations in water table level appear to lag the modelled water level data by 1 to 10 months, indicating a considerable delay period in the unsaturated zone. The delay seems to vary with the thickness of the unsaturated zone and indicates filtration velocities between 1 and 12 cm/day. In comparison, Jørgensen & Østmo (1990) calculated an "unsaturated zone delay" of only some 8 - 12 days at Nordmoen, with an unsaturated zone of ca. 2 m.

The modelling work has enabled the project's participants to obtain a deeper understanding of the hydraulics of the aquifer, and has also indicated that hydraulic conductivity values obtained from grain size distributions tend to lead to underestimates of aquifer transmissivity. The model provides a framework for further modelling work on contaminant transport at Trandum landfill. It is debatable, however, whether the model can be used for contaminant modelling in its present form. It is believed that a significantly more detailed geological base model (e.g. more layers) will be needed before attempting contaminant modelling. Experience has shown that, even though a model may yield satisfactory results as regards groundwater flow, it may not be satisfactory for contaminant transport (Guerin & Billaux 1993). Much detailed data is, however, available at the Trandum landfill site, and the prospects appear very hopeful for a fruitful attempt at contaminant and hydrogeochemical modelling at that locality in the future. The present model could, however, be used to estimate the large-scale effects of water abstraction on the Øvre Romerike aquifer.

## **7. Acknowledgements**

At IBM/BSC, Arne Harvorsen did much of the work in programming the interface. Børre Johnson and Brit-Gunn Ersland worked on the automatic digitizing of the geological model and on the design of the graphical user interface.

At NGU, Ola Sæther and Gaute Storrø were of great assistance in processing grain-size data in order to arrive at the permeability histogram.

The modelling work has been financially supported by the Norsk Hydrologisk Komité (a part of Norges Almenvitenskapelige Forskningsråd - NAVF), as well as by the authors' host institutions, IBM/BSC and NGU.

Copies of input files and further results from the model can be obtained by contacting the authors.

## 8. References

- Banks, D. 1991. *Kartlegging av oljeforurensset grunn/grunnvann ved bygning 14, Sessvollmoen militærleir [Mapping of oil-contaminated ground/groundwater at building 14, Sessvollmoen military base - in Norwegian]*. Nor. geol. unders. report 91.190. 148 pp.
- Bjor, K. & Huse, M. 1988. *Variations in groundwater level at the field station Nordmoen, Romerike*. Medd.Nor.Inst.Skogforsk 41.38: 543-554.
- Bryn, K.Ø. 1992. *Gardermoen - grunnvannsressursen som alle vil beskytte, ingen bryr seg om og ingen vil bruke! [Gardermoen - the groundwater resource that everyone wants to protect, nobody cares about and nobody will use! - in Norwegian]*. Vann 27, No. 1c, 144-149.
- Davidsen, F. 1990. *Gardermoen og vannforurensende aktiviteter [Gardermoen and water-polluting activities]*. Vann, No.3, 1990, 216-225.
- Ellingsen, K. 1992: *Grunnvann i Norge (GiN) - Sluttrapport [Groundwater in Norway (GiN) - Final report - in Norwegian]*. Nor. geol. unders. Skrifter 111, 36pp.
- Ellingsen, K. & Banks, D. 1992. *Norway's tonic*. World Water & Environmental Engineer, Nov. 1992, 31-32 (& cover)
- Englund, J.-O. & Moseid, T. (eds.) 1992. *Introductory report; the Gardermoen Project - literature review and project catalogue*. Norwegian National Committee for Hydrology, March 1992. ISBN 82-7216-765-4.
- Ersland, B.G., Johnsen, B., Odling, N., Banks, D. & Misund, A. 1992. *Numerisk modellering av grunnvannsstrømning - en introduksjon [Numerical modelling of groundwater flow - an introduction - in Norwegian]*. Nor. geol. unders. rep. 92.258.
- Falkenmark, M. (ed.) 1972: *Hydrological data - Norden. Representative basins, introductory volume*. National Committees for the International Hydrological Decade in Denmark, Finland, Iceland, Norway & Sweden.

Fetter C.W. 1988. *Applied Hydrogeology*. Publ. Merrill, 592pp.

Guerin, F.P.M. & Billaux, D.M. 1993. *On the relationship between connectivity and the continuum approximation in fracture flow and transport modeling*. In: Banks, S.B. & Banks, D. (eds.) "Hydrogeology of Hard Rocks" Proc. XXIVth Congr. Int. Assoc. Hydrogeol., Ås, Oslo, 1993.

Jørgensen, P. & Østmo, S.R. 1990. *Hydrogeology in the Romerike area, Southern Norway*. Nor. geol. unders. Bull 418, 19-26.

Jørgensen, P., Stuanes, A.O. & Østmo, S.R. 1991: *Aqueous geochemistry of the Romerike area, Southern Norway*. Nor. geol. unders. Bull. 420, 57-67.

Hongve, D. 1992. *Verneverdige innsjøer på Øvre Romerike [Lakes worthy of protection on Øvre Romerike - in Norwegian]*. Vann, 27, No. 1, 21-28.

Kirkhusmo, L.A. & Sønsterud, R. 1988: *Overvåking av grunnvann. Landsomfattende grunnvannsnnett (LGN). [Monitoring of groundwater, the nationwide groundwater network - Norwegian]*. Nor. geol. unders. report 88.046, 72pp.

Langguth, H.R. & Voigt, R.H. 1980: *Hydrogeologische Methoden [Hydrogeological methods - in German]*. Springer Verlag, 486 pp.

Longva, O. 1987: *Ullensaker 1914-II. Beskrivelse til kvartærgeologisk kart - M 1:50.000 Ullensaker mapsheet 1914-II. Description of Quaternary geological map, scale 1:50,000 - in Norwegian]*. Nor. geol. unders. Skrifter 76.

McDonald, M.G. & Harbaugh, A.W. 1988. *A modular three dimensional finite difference groundwater flow model*. Tech.wat. res. planning U.S.G.S. Book 6, Chapter A1.

Misund, A., Banks, D., Morland, G. & Brunstad, H. 1991a: *Norwegian national survey of hazardous waste in landfills and contaminated ground*. Waste Manage. Today (News J.), 4, No.8, Aug.1991, 30-35.

Misund, A., Morland, G., Brunstad, H., Banks, D. 1991b: *Kartlegging av spesialavfall i deponier og forurenset grunn - Sluttrapport [Survey of hazardous waste in landfills and contaminated ground, final report - in Norwegian]*. Statens forurensningstilsyn report 91/01, 53 pp.

Misund, A. & Sæther, O.M. 1991: *Undersøkelser av forurenset grunn og grunnvann ved Trandum militærleir [Investigations of contaminated ground and groundwater at Trandum military base - in Norwegian]. Nor. geol. unders. report 91.228, 137 pp.*

Misund, A. & Banks, D. 1993. *Geologiske og hydrogeologiske bakgrunnsdata fra Øvre Romerike, innsamlet av Norges geologiske undersøkelse i perioden 1966-92 [Geological and hydrogeological background data from Øvre Romerike, collected by the Geological Survey of Norway in the period 1966-92 - in Norwegian]. Nor. geol. unders. rep. 93.017, 234 pp.*

Morland, G., Folkestad, B., Hauge, A., Kolstad, P., & Forsberg, C.F. 1990. *Kartlegging av spesialavfall i deponier og forurenset grunn i Akershus fylke [Survey of hazardous waste in landfills and contaminated ground in Akershus county - in Norwegian]. Nor. geol. unders. report 90.084. 170 pp.*

NGI 1991. *Hovedflyplassprosjekt, Gardermoen - grunnundersøkelser [Main airport project, Gardermoen - site investigations - in Norwegian]. Nor. geotech. inst. report from contract 900086.*

Nordberg, L. 1980 (ed.). *The national groundwater observation networks of the Nordic countries. Nordic International Hydrological Programme, Report No. 3.*

Norwegian National Committee for the IHD 1973. *Hydrological data - Norden. Representative basins; Romerike, Norway. Data 1965-71. Norwegian National Committee for the International Hydrological Decade, Oslo, 1973.*

Norwegian National Committee for the IHD 1975. *Hydrological data - Norden. Representative basins; Romerike, Norway. Data 1972-74. Norwegian National Committee for the International Hydrological Decade, Oslo, 1975.*

NVE 1991. Unpublished hydrological data - hydrological area 102, River Vikka, gauging station 2868-0.

Omejer, N.A., Mørch, T. & Ellefsen, V. 1992. *Investigation of hazardous waste in landfills and in contaminated ground at Norwegian military bases. Proc. Conf. on "Environmentally sound life-cycle planning of military facilities and training areas", Dombås, Norway, 23-25/9/92.*

Rushton, K.R. 1983. *Groundwater hydrology. Lecture notes; M.Sc. course in hydrogeology, Univ. of Birmingham, U.K., 1983-84.*

Rushton, K.R & Redshaw, S.C. 1979. *Seepage and groundwater flow. Wiley & Sons. 339 pp.*



Sæther, O.M., Misund, A., Ødegård, M., Andreassen, B.Th. & Voss, A. 1992. *Groundwater contamination from a landfill at Trandum, Southeastern Norway*. Nor. geol. unders. Bull. 422.

Snekkerbakken, A.M. 1992. *Grunnvannsmagasinet på Gardermoen - bergning av kapasitet [The Gardermoen aquifer - calculation of capacity - in Norwegian]*. Vann 27, No. 1c, 150-157.

Solnørdal, K. 1992. *Hovedflyplass Gardermoen - beskyttelse av vannressursene [Gardermoen main airport - protection of water resources - in Norwegian]*. Vann 27, No. 1c, 141-143.

Storrø, G. 1991. *Kartlegging av oljeforurensset grunn/grunnvann ved bygning 111, Trandum militærleir [Mapping of oil contaminated ground/groundwater at building 111, Trandum military base - in Norwegian]*. Nor. geol. unders. report 91.155, 71 pp.

Storrø, G. & Banks, D. 1992. *Oil leakages on the Øvre Romerike aquifer, Southern Norway*. Nor. geol. unders. Bull. 422, 67-82.

Sønsterudbråten, S. 1992. *Sedimentologiske undersøkelser ved Gardermoen*. Fagmøtet "Miljø i Grunnen", Ås Hotell, 3/12/92.

VIAK AB 1990. *Luftfartsverket, Gardermoen. Jordartsgeologisk modell [Airport authority, Gardermoen. Quaternary geological model - in Norwegian]*. Report no. 12202.662360. VIAK Malmö, Sweden.

Wolden, K. & Erichsen, E. 1990. *Compilation of geological data for use in local planning and administration*. Engineering geol., 29, 333-338.

Østlandskonsult A/S, Geofuturum A/S, Akershus fylkeskommune & Luftfartsverket 1991: *Hovedflyplass Gardermoen; grunnvannet som drikkevannskilde; en utredning av grunnvannet som aktuell drikkevannskilde for Romerike [Gardermoen main airport; an evaluation of groundwater as a drinking water resource for Romerike - in Norwegian]*.

Østmo, S.R. 1976. *Hydrogeologisk kart over Øvre Romerike [Hydrogeological map of Øvre Romerike]*. Scale 1:20000, Nor.geol.unders.

## NORTHERN ROMERIKE QUATERNARY MAP

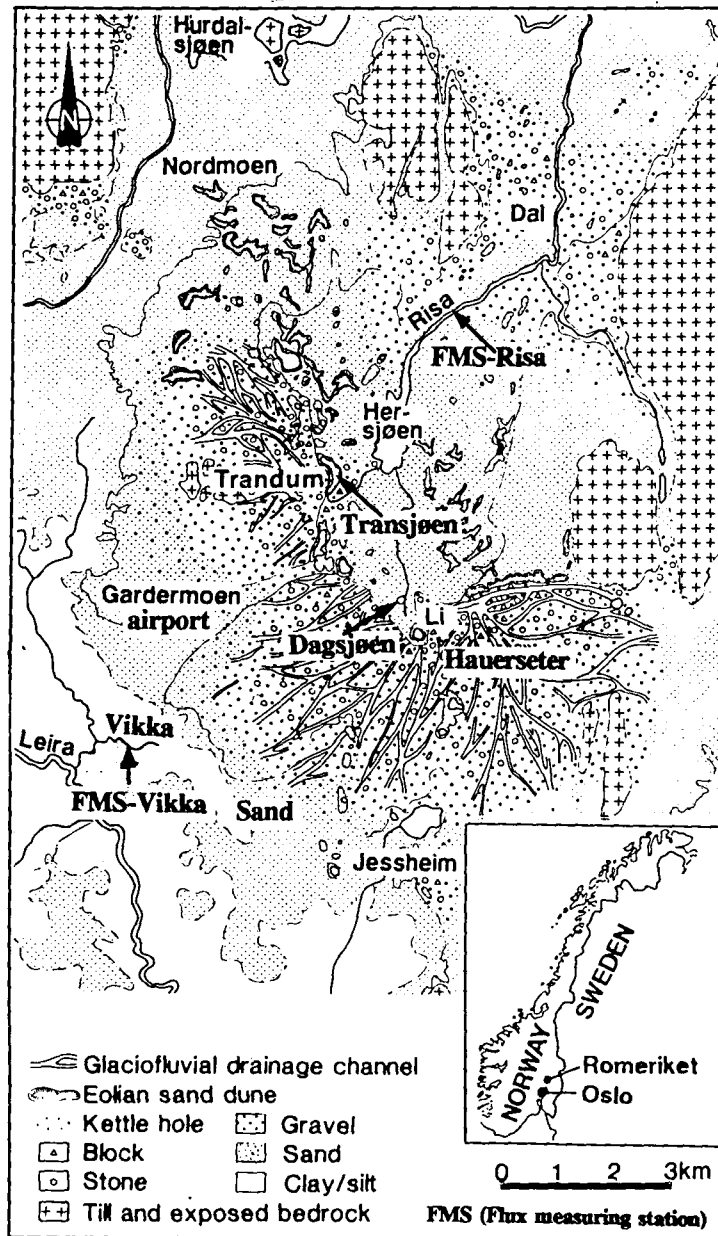


Fig.1(a) Øvre Romerike area showing Hurdalsjøen, Hersjøen, Transjøen, Dagsjøen, airport, Trandum, the rivers Risa, Leira, Vikka and flow gauging stations on the Risa and Vikka.

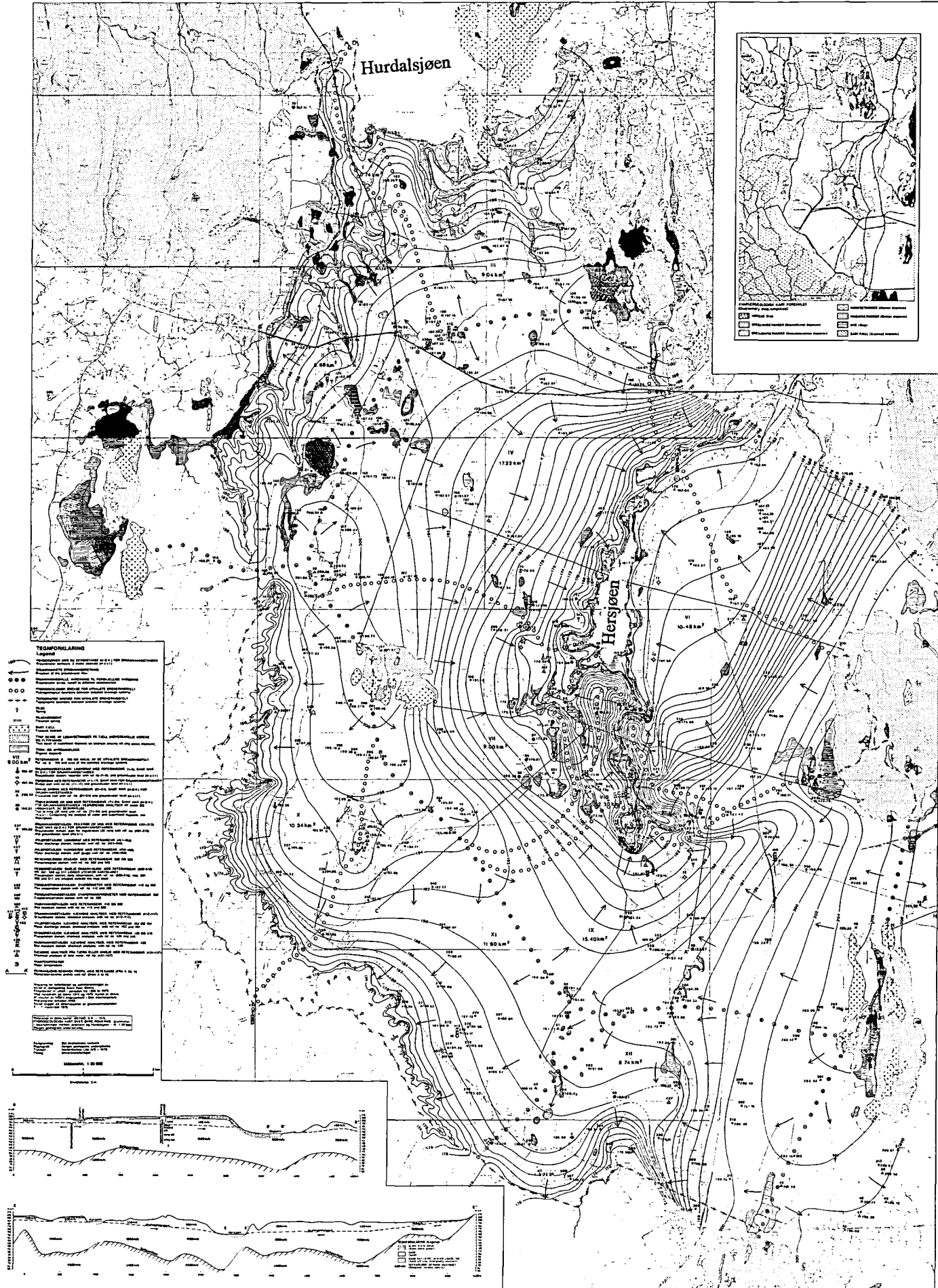


Fig.1(b) The water table in the Øvre Romerike aquifer , Østmo (1976). Contours show water table (2 m intervals). Arrows show groundwater flow.



Fig.2(a) Photo of coarse layer at Trandum landfill showing fine and coarse intercalated layers

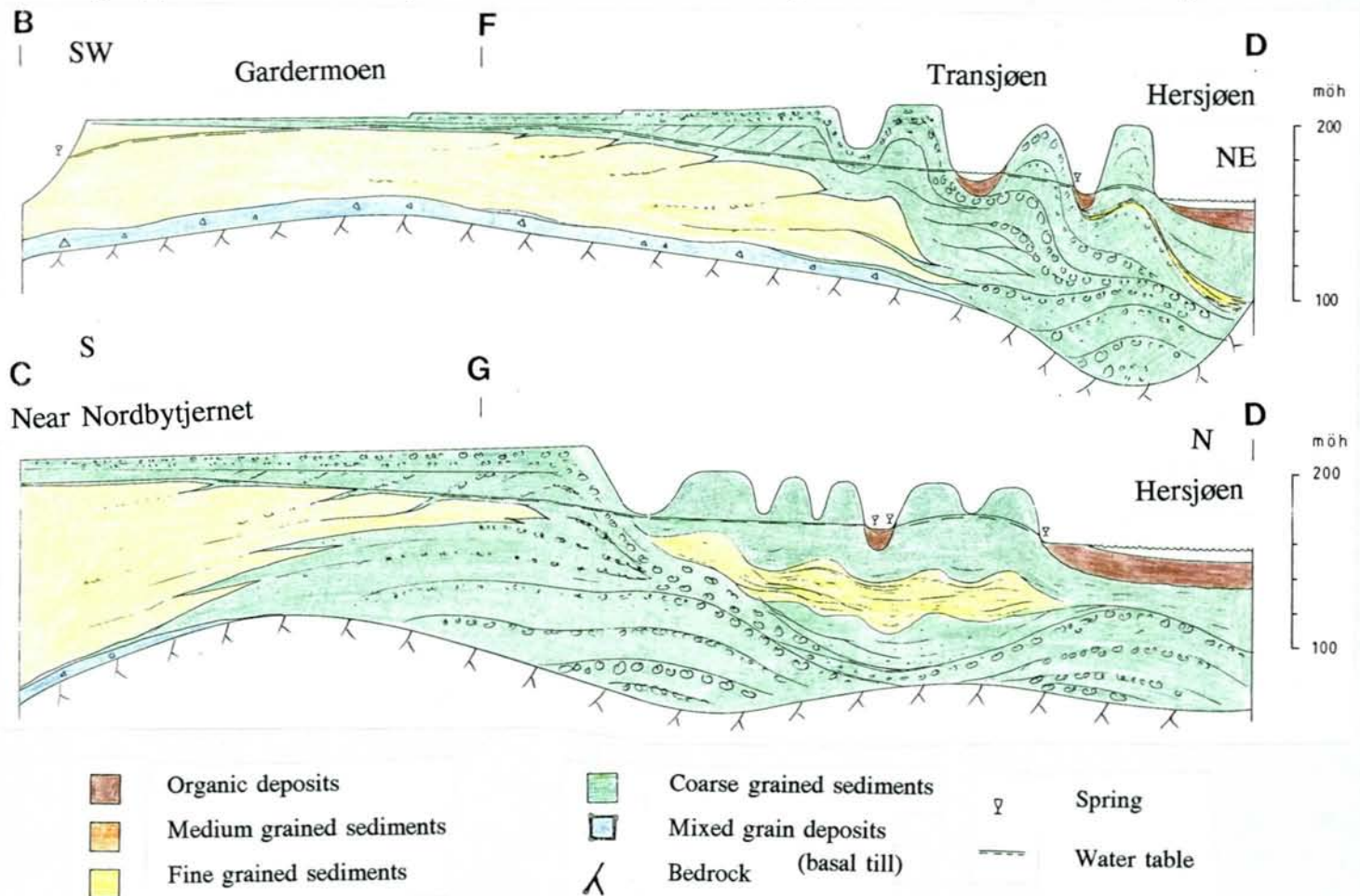


Fig.2(b) An interpretation of the structure of the Romerike delta, after VIAK (1990)

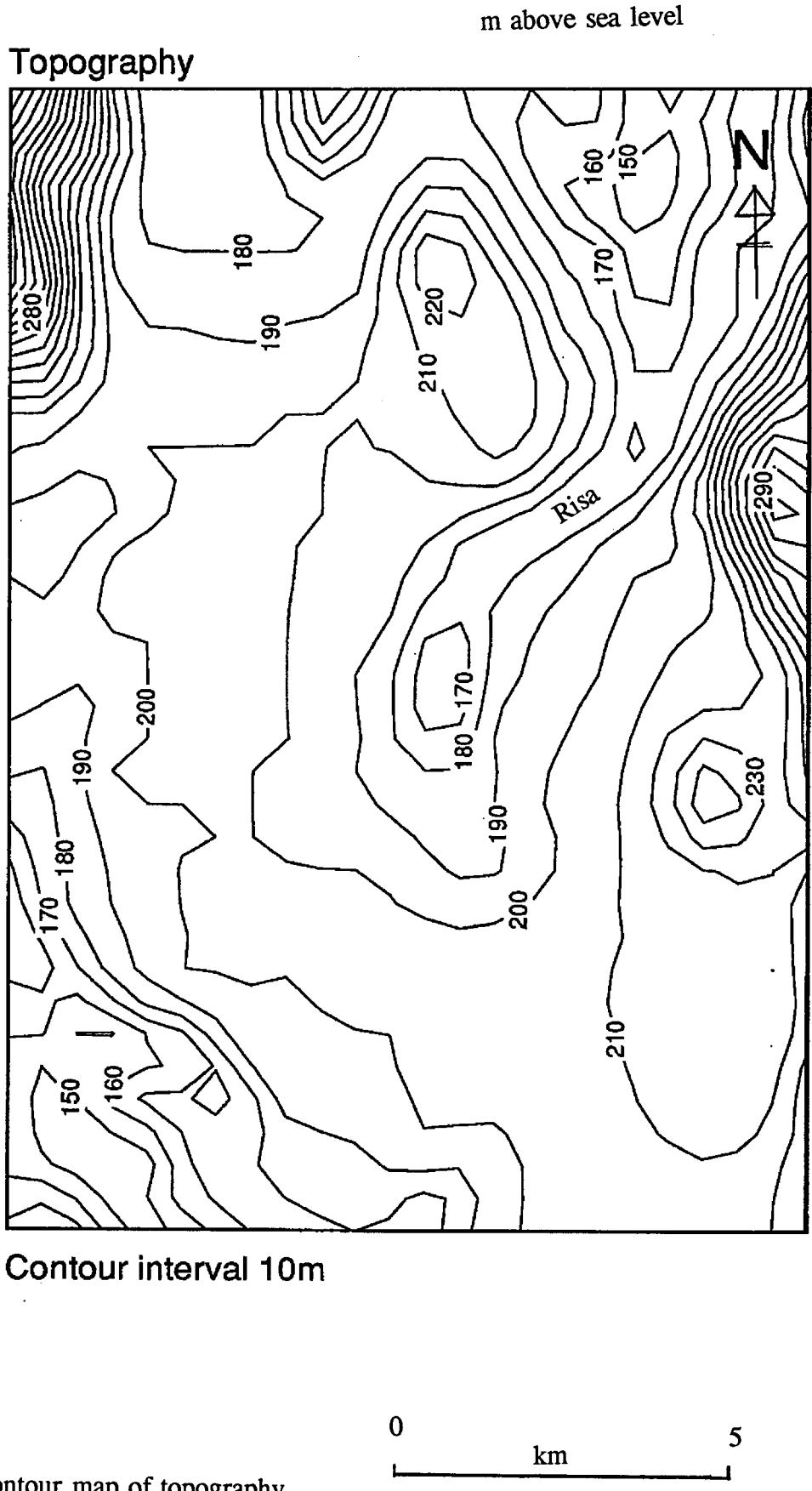
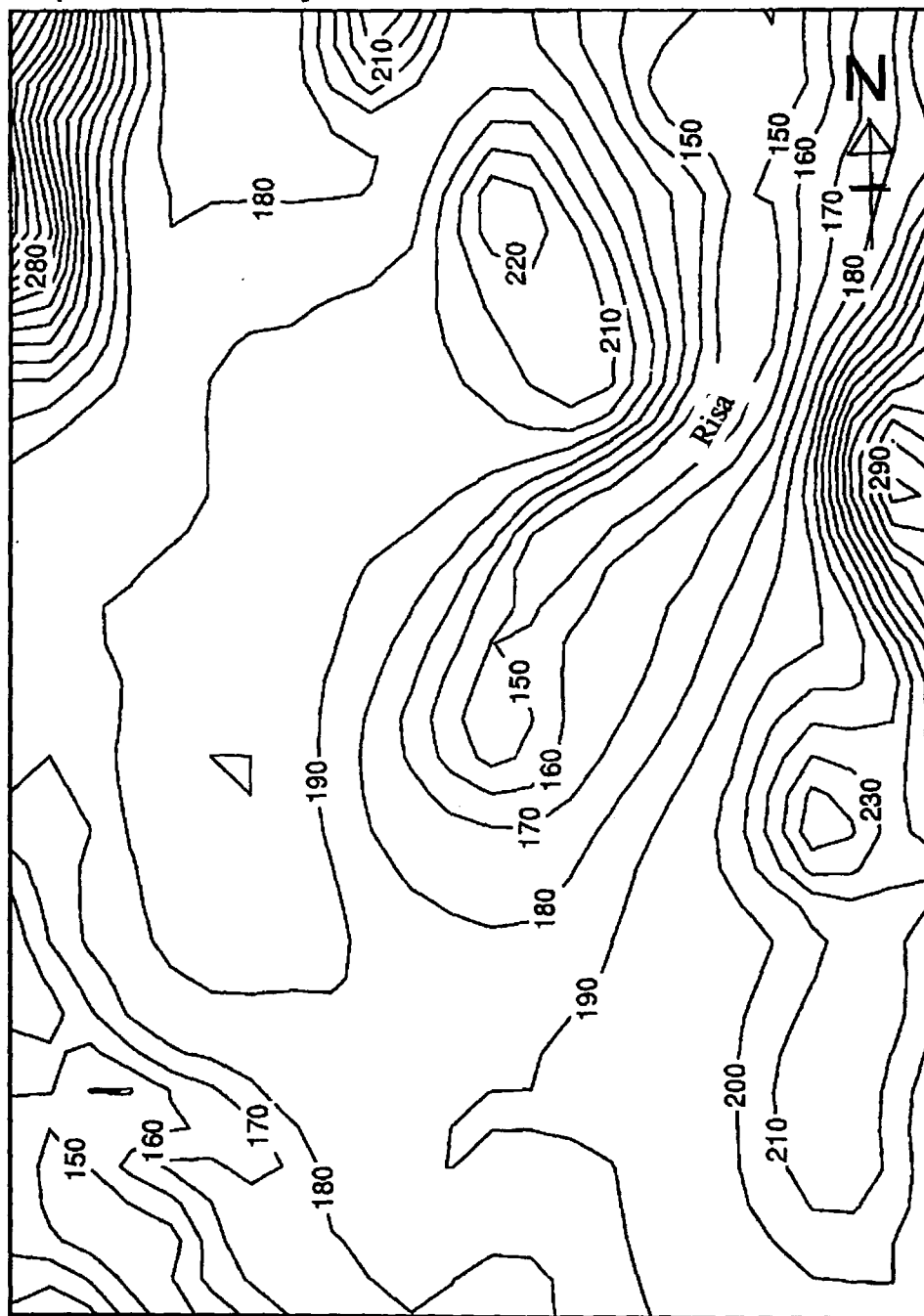


Fig.3(a) Contour map of topography

m above sea level

Top lower fine layer



Contour interval 10m

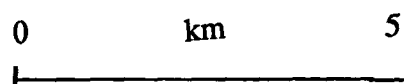
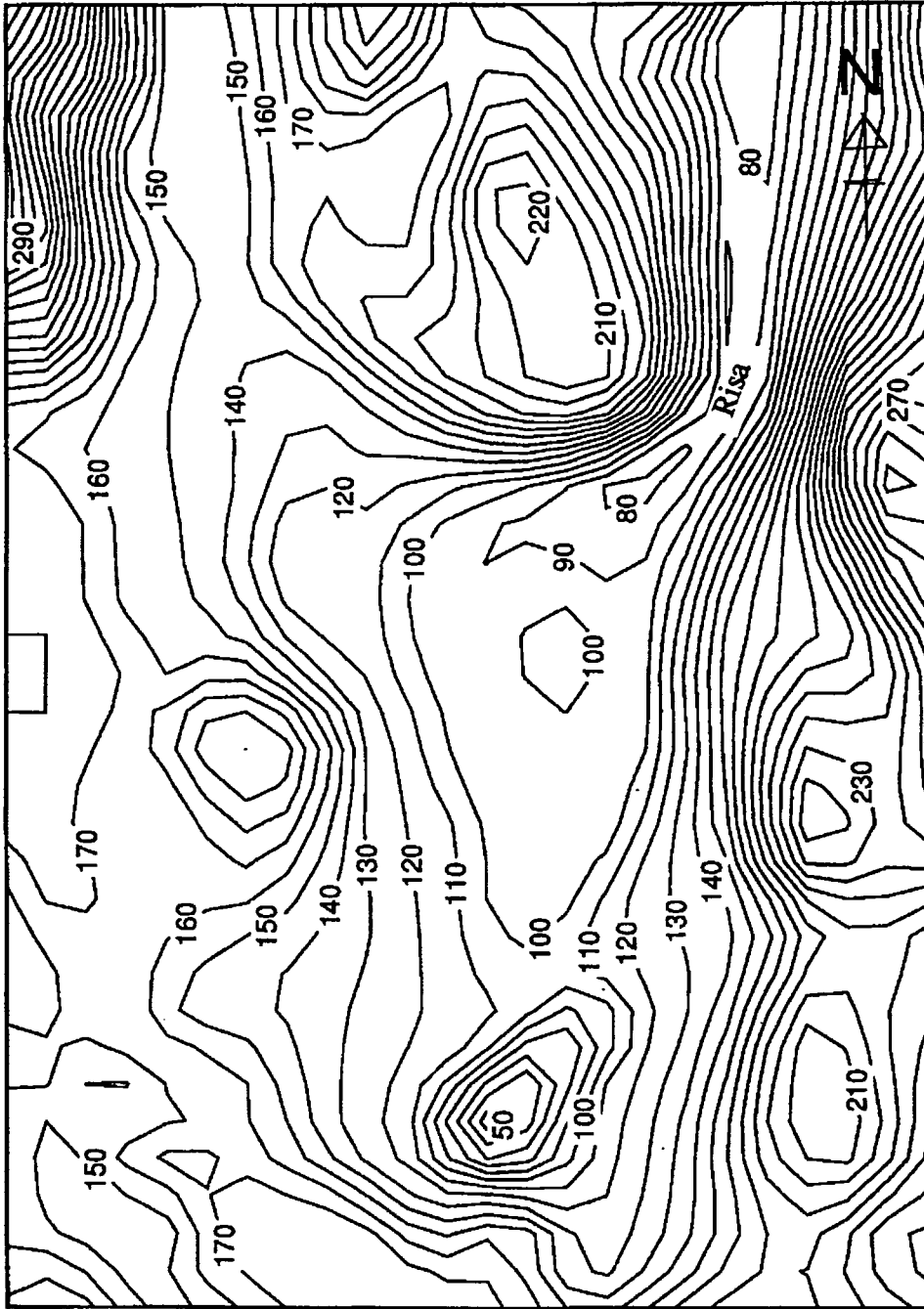


Fig.3(b) Contour map of top of fine layer

m above sea level

Base aquifer



Contour interval 10m

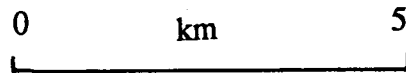


Fig.3(c) Contour map of base of aquifer

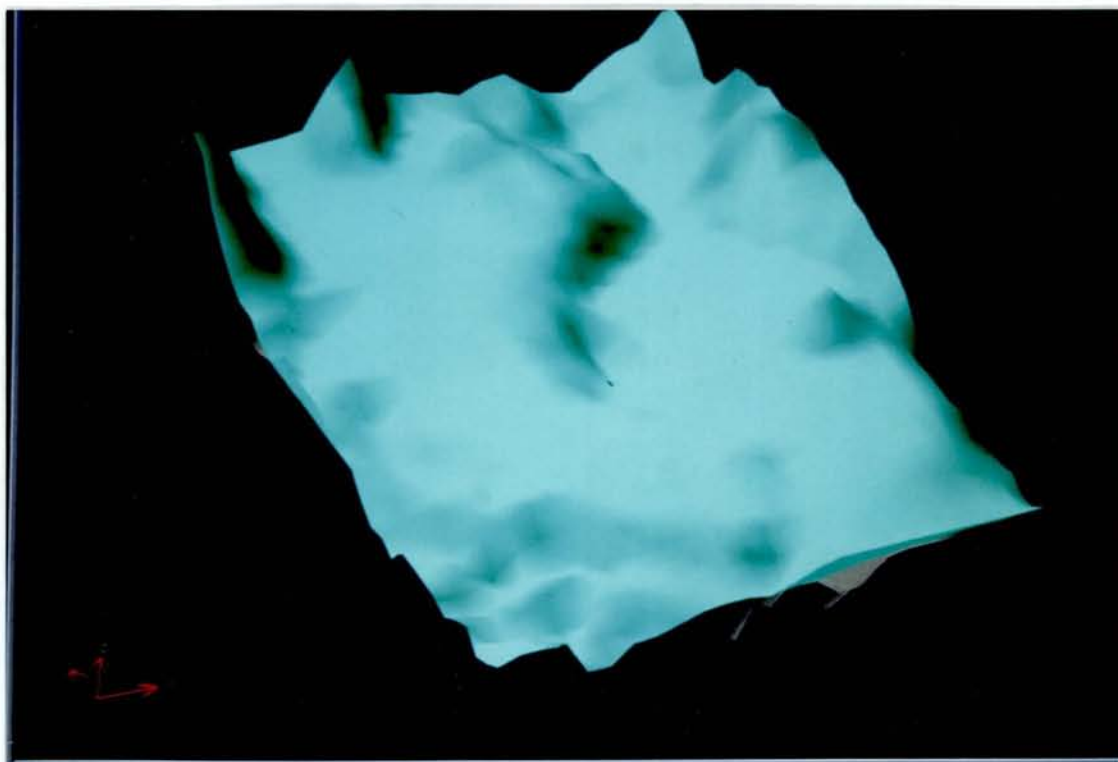


Fig.4(a) 3D ADVIZE visualisation of topography

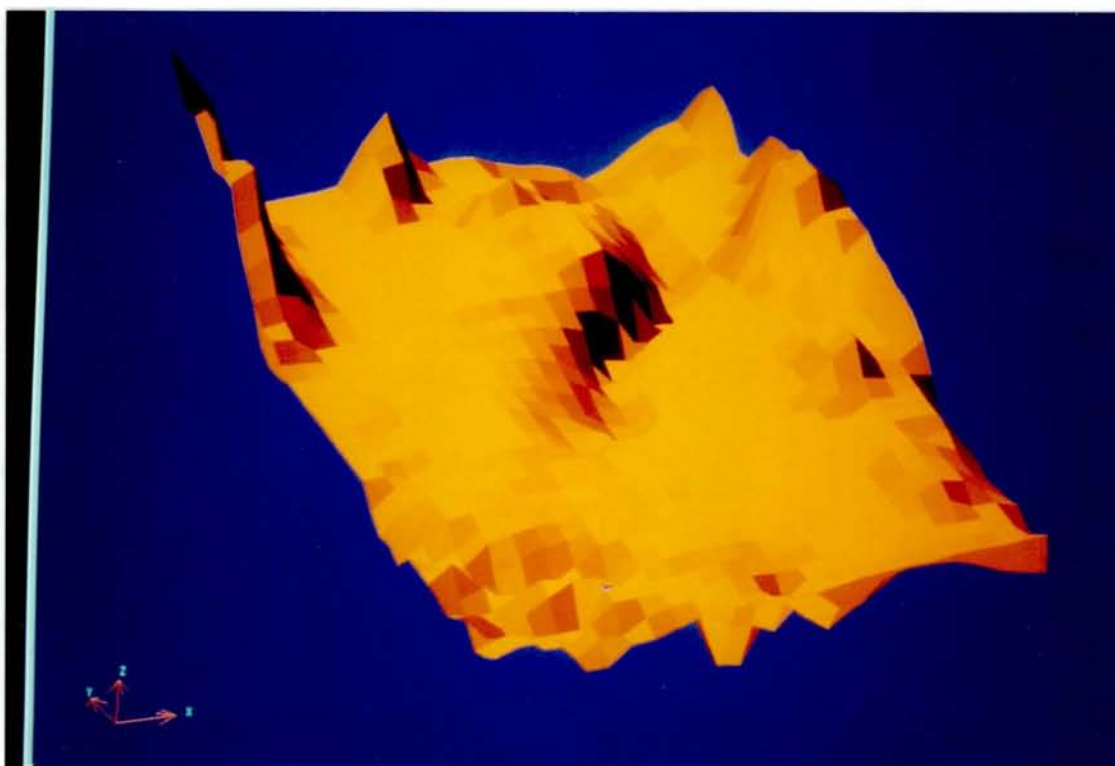


Fig.4(b) 3D ADVIZE visualisation of top of fine layer



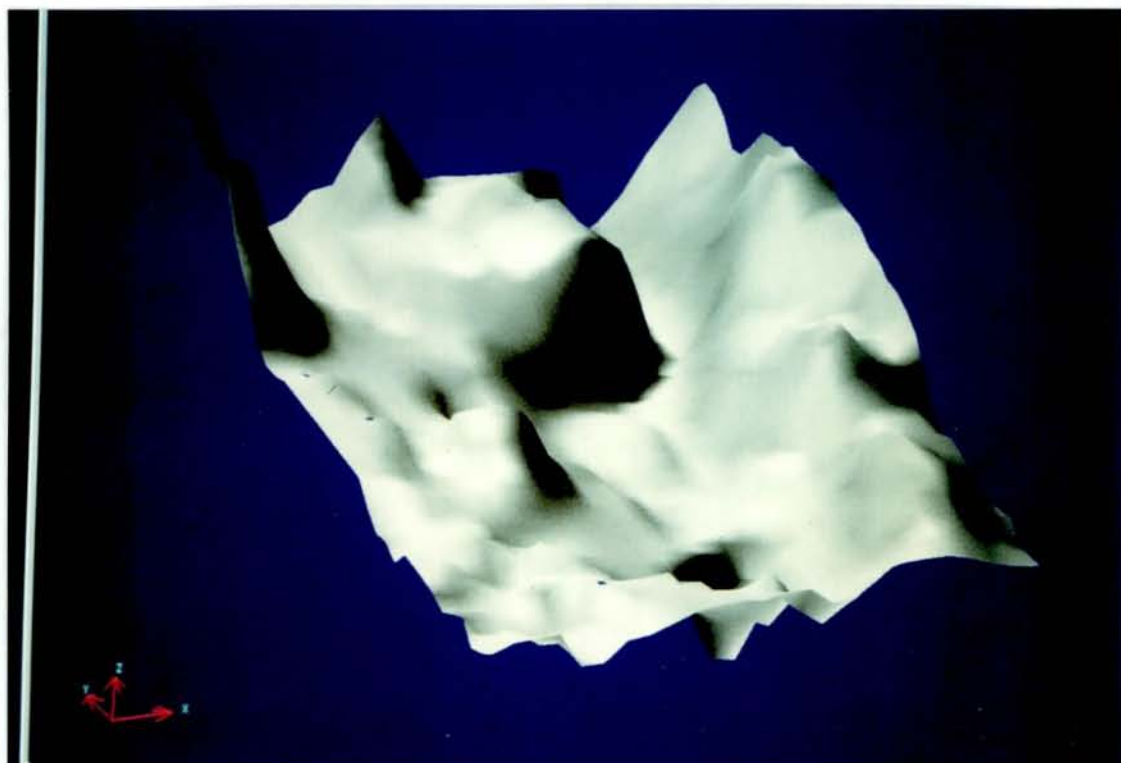
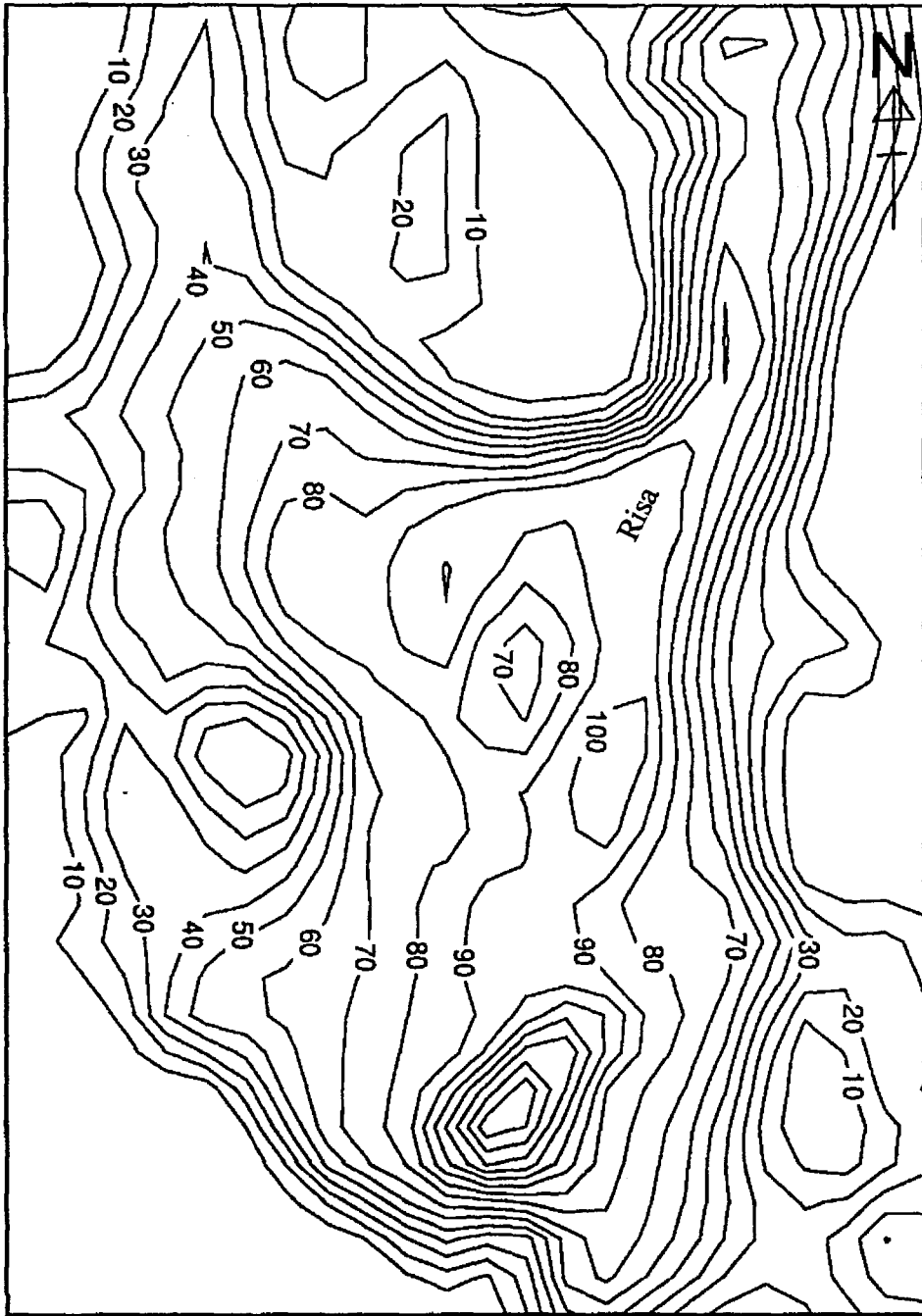


Fig.4(c) 3D ADVIZE visualisation of base of aquifer

Total aquifer thickness



contour interval 5m

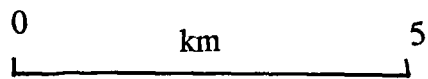
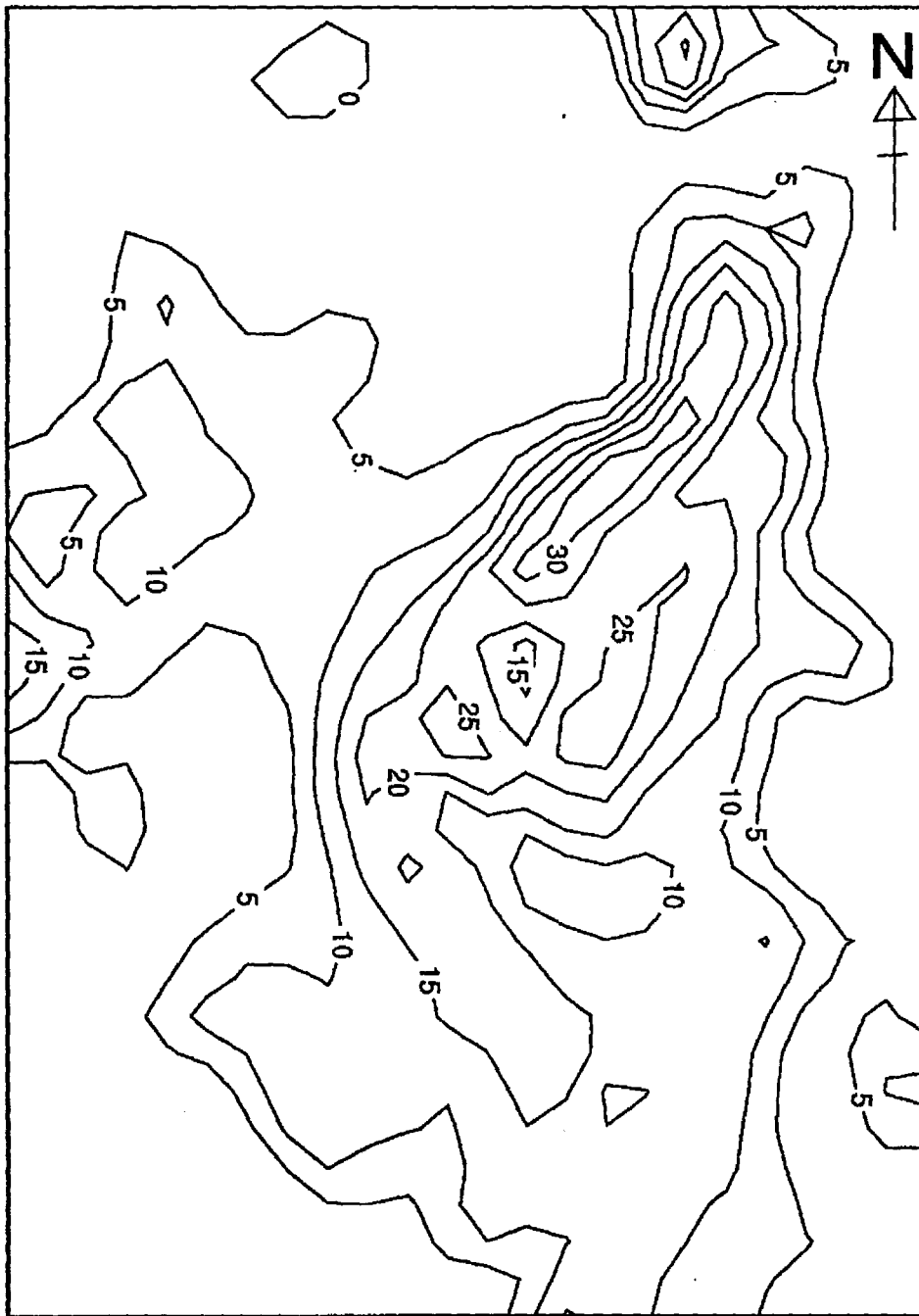


Fig.5(a) Isopach map of the whole aquifer

Upper coarse layer thickness



contour interval 5m

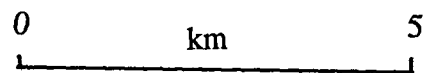
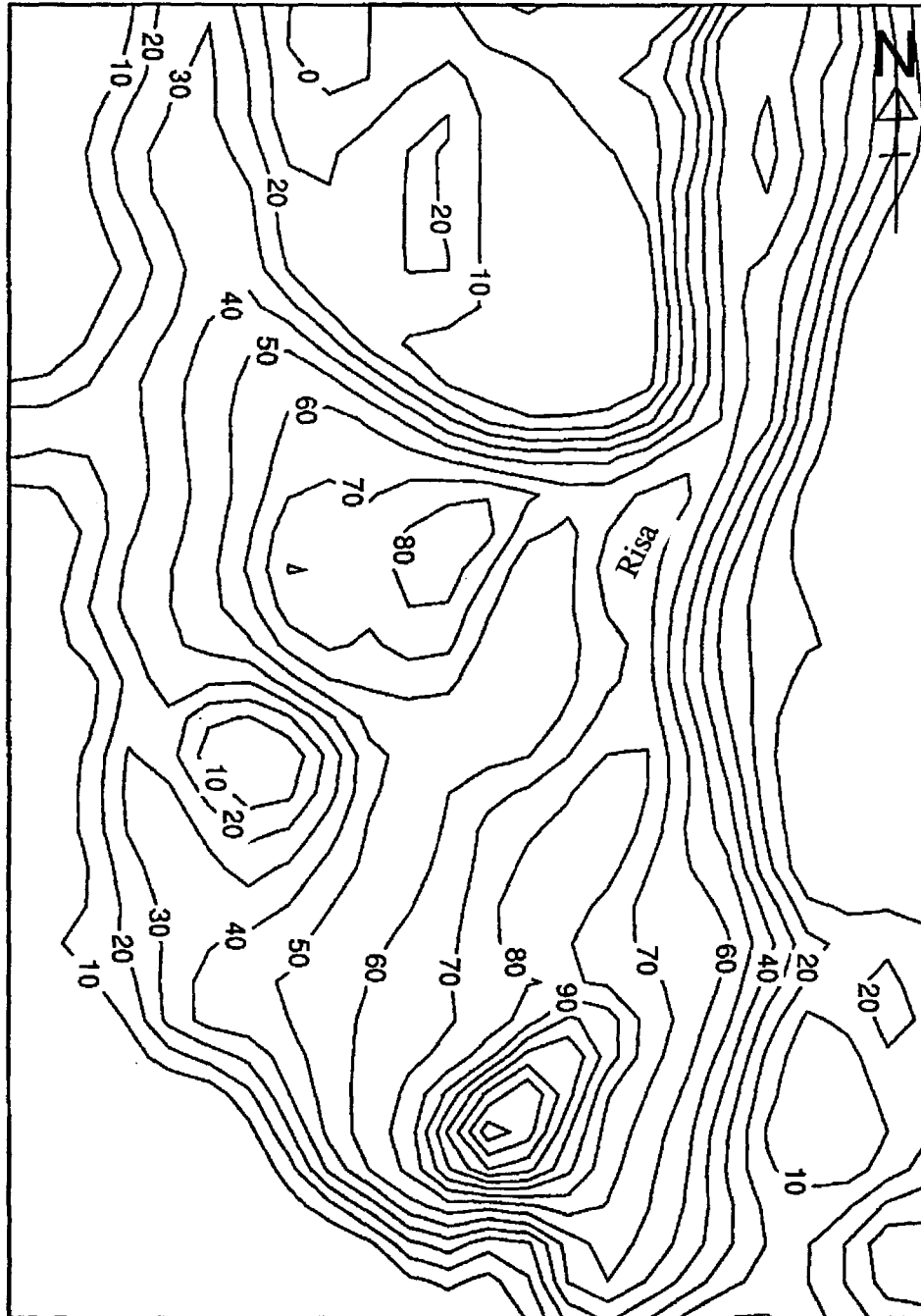


Fig.5(b) Isopach map of the coarse layer

## Lower fine layer thickness



contour interval 5m

0 km 5

Fig.5(c) Isopach map of the fine layer

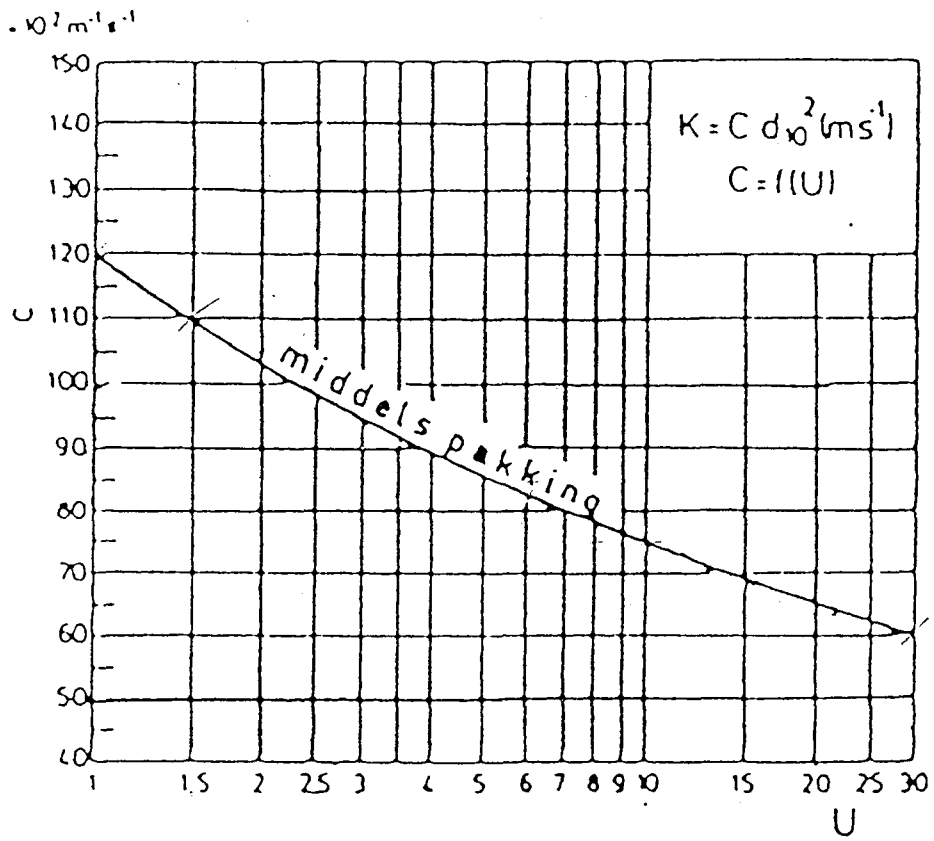


Fig.6 Calibration graph for hydraulic conductivity analysis from grain size samples (Bayer method - after Langguth & Voigt)

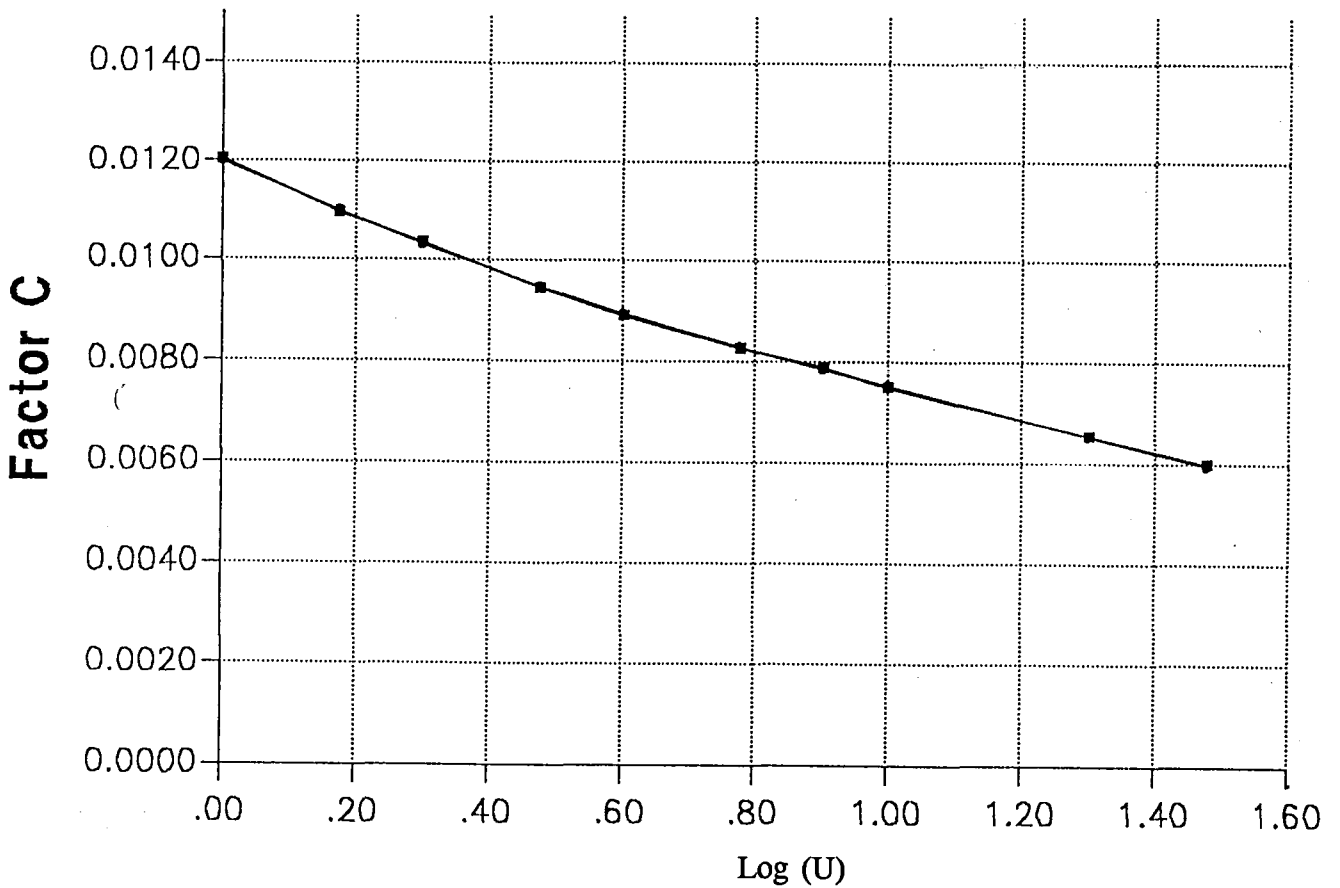


Fig.7 Polynomial curve, fit to calibration curve (the two curves are exactly coincident !)

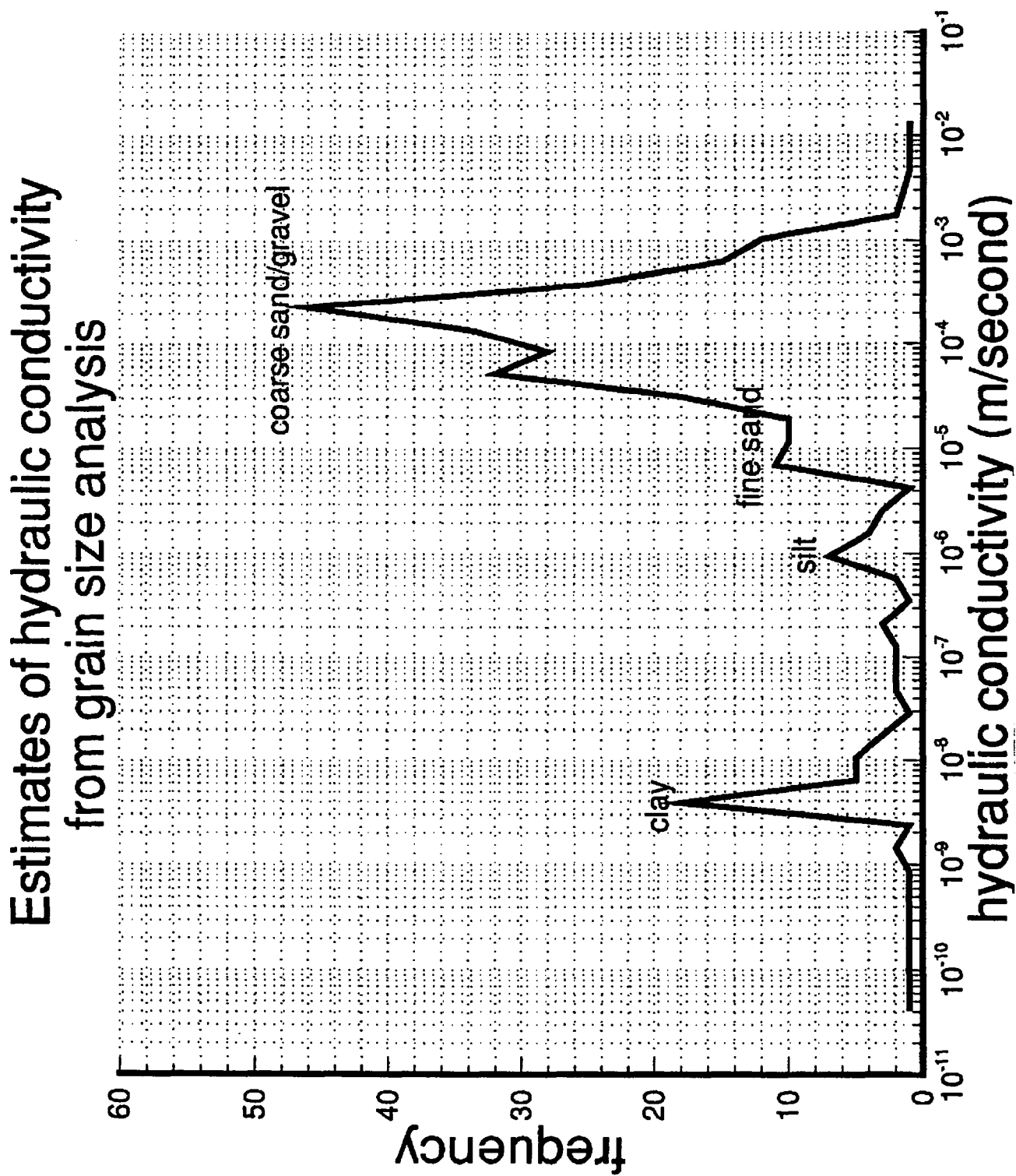
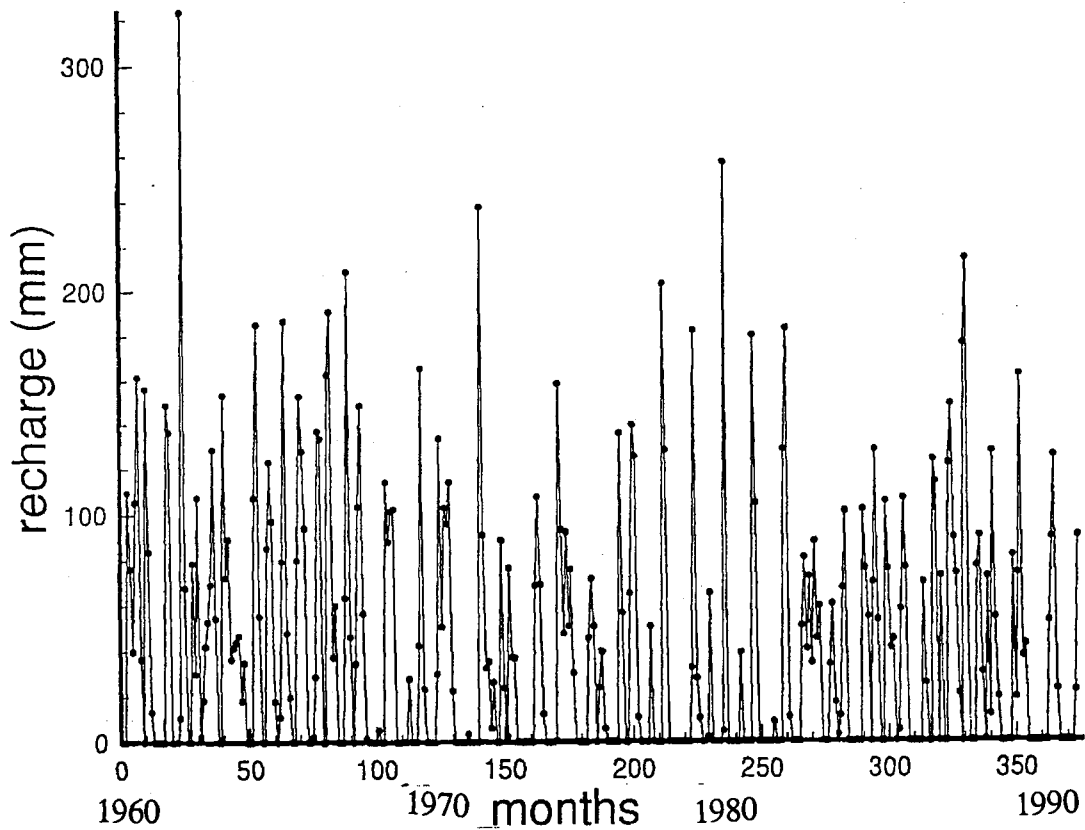


Fig.8 Histogram of all hydraulic conductivity estimates (using the Bayer method - from  $d_{10}$  and  $d_{60}$  grain sizes)

Monthly recharge from May 1960 to July 1991



Aquifer recharge (snow data included)

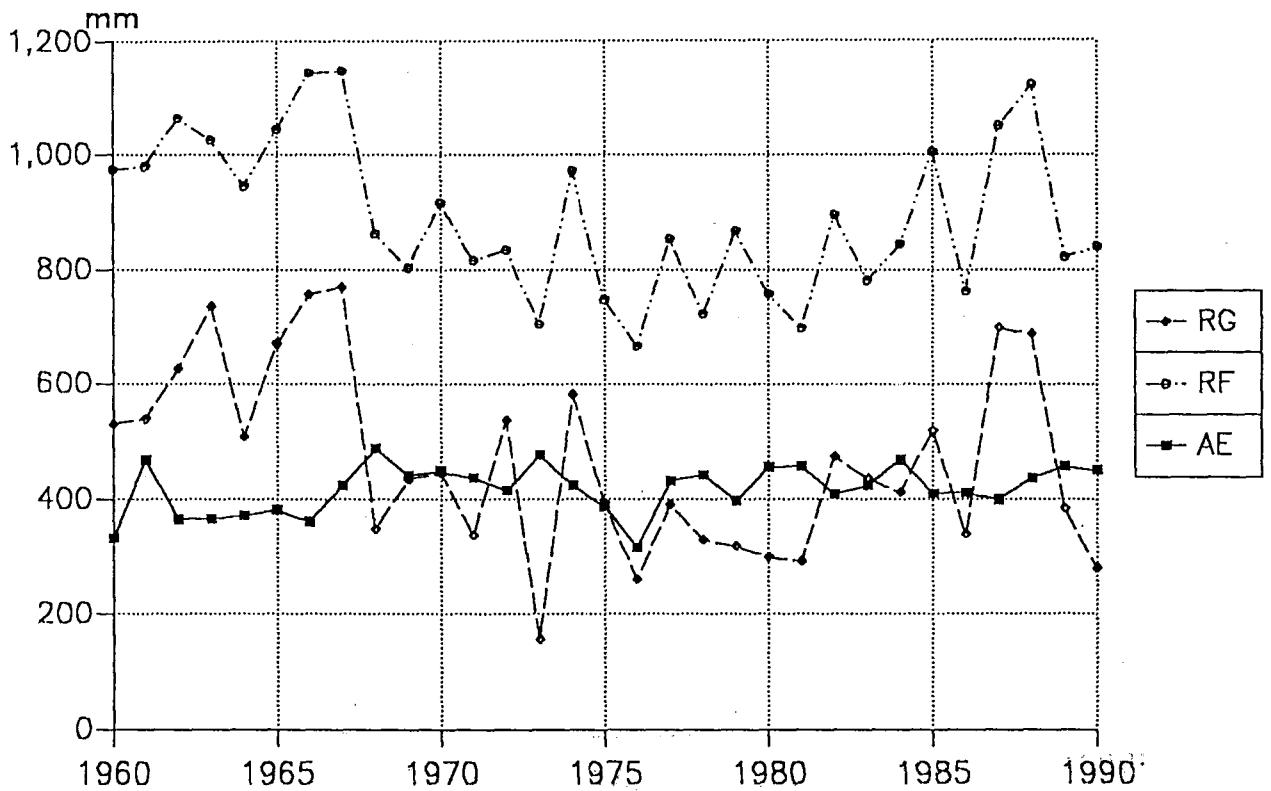


Fig.9 Recharge model, (a) monthly data, (b) yearly data

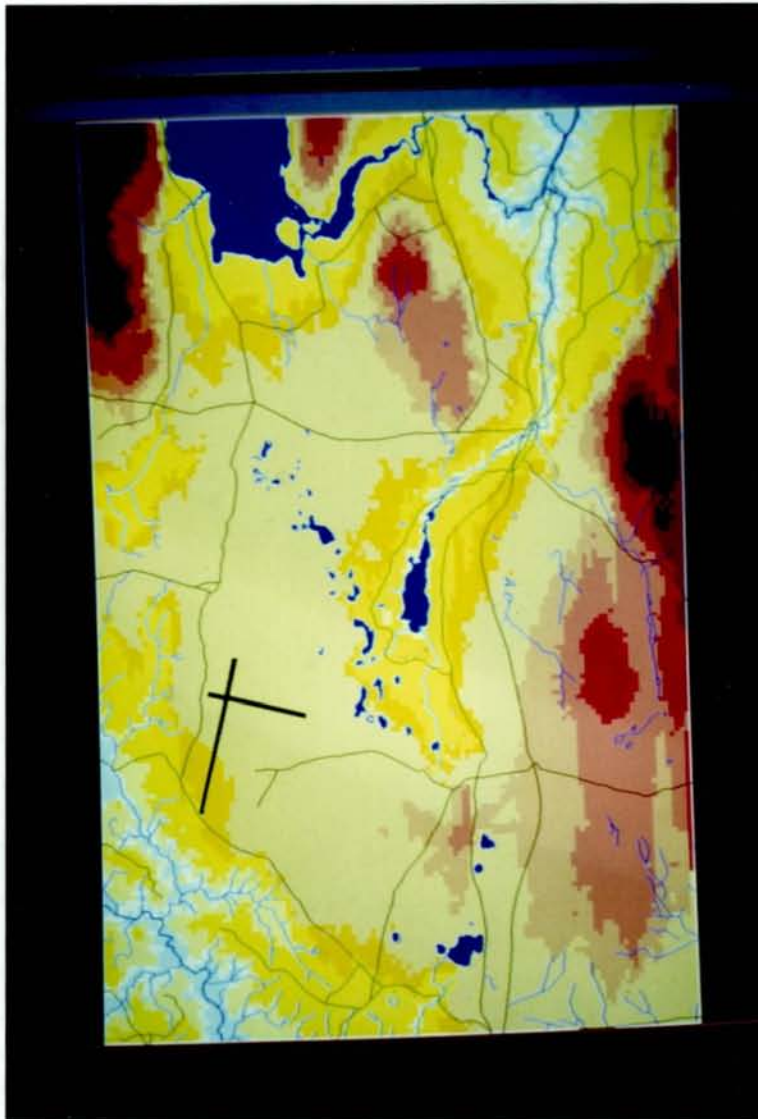


Fig.10 Rasterised map example (topography) produced by GENAMAP





Windows (from top)

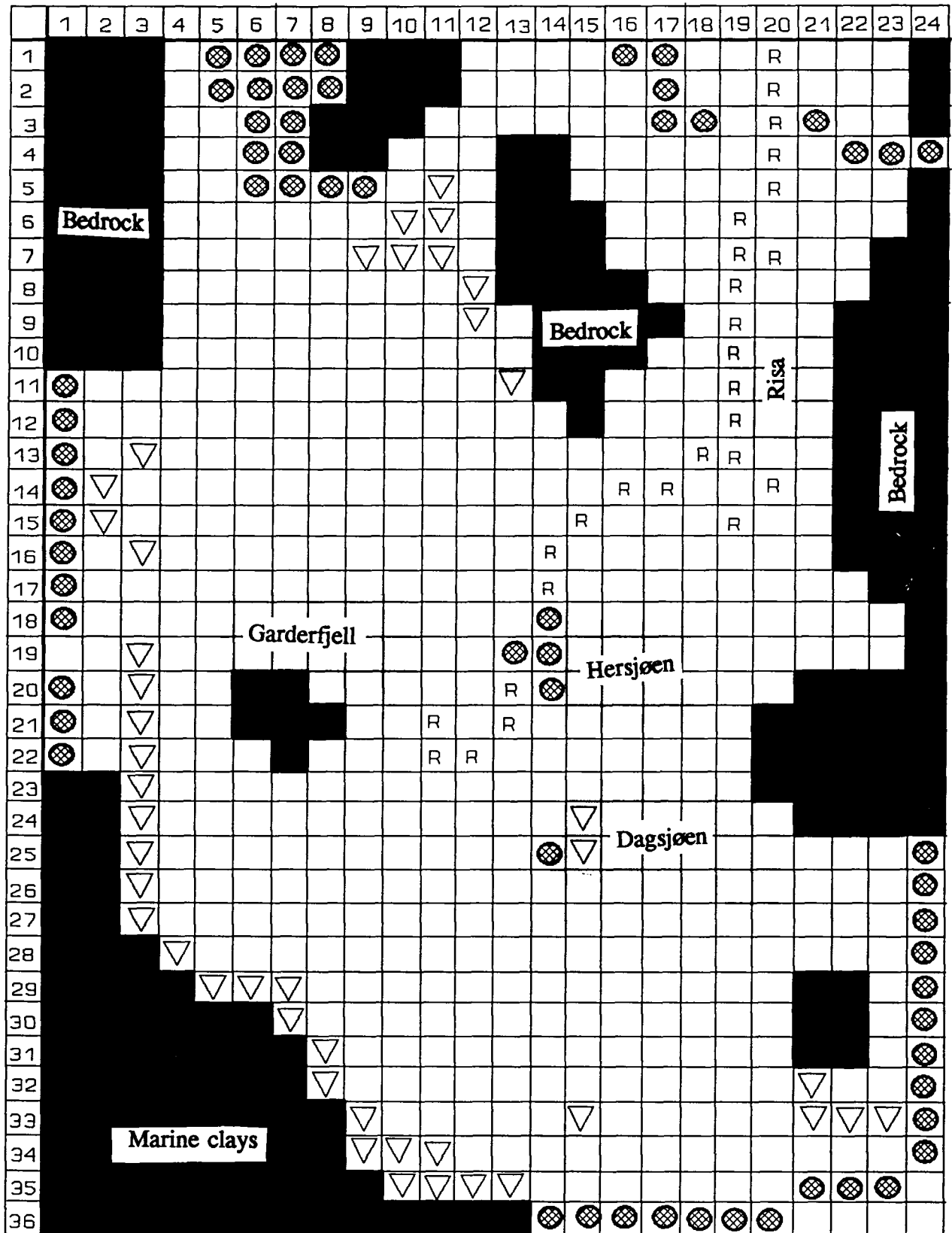
Groundwater Workstation  
GridOprDialog

GIVE HEAD

GIVE TRANS

Fig.11 Example of the graphical user interface to MODFLOW. The grid has been defined and is displayed, together with roads, rivers and topography, in the right hand window. On the left are windows that enable the user to (a) modify the grid (GridOprDialog window), (b) define constant head cells (GIVE\_HEAD window) and (c) define hydraulic conductivity in individual cells (GIVE\_TRANS window).

Hurdalssjøen

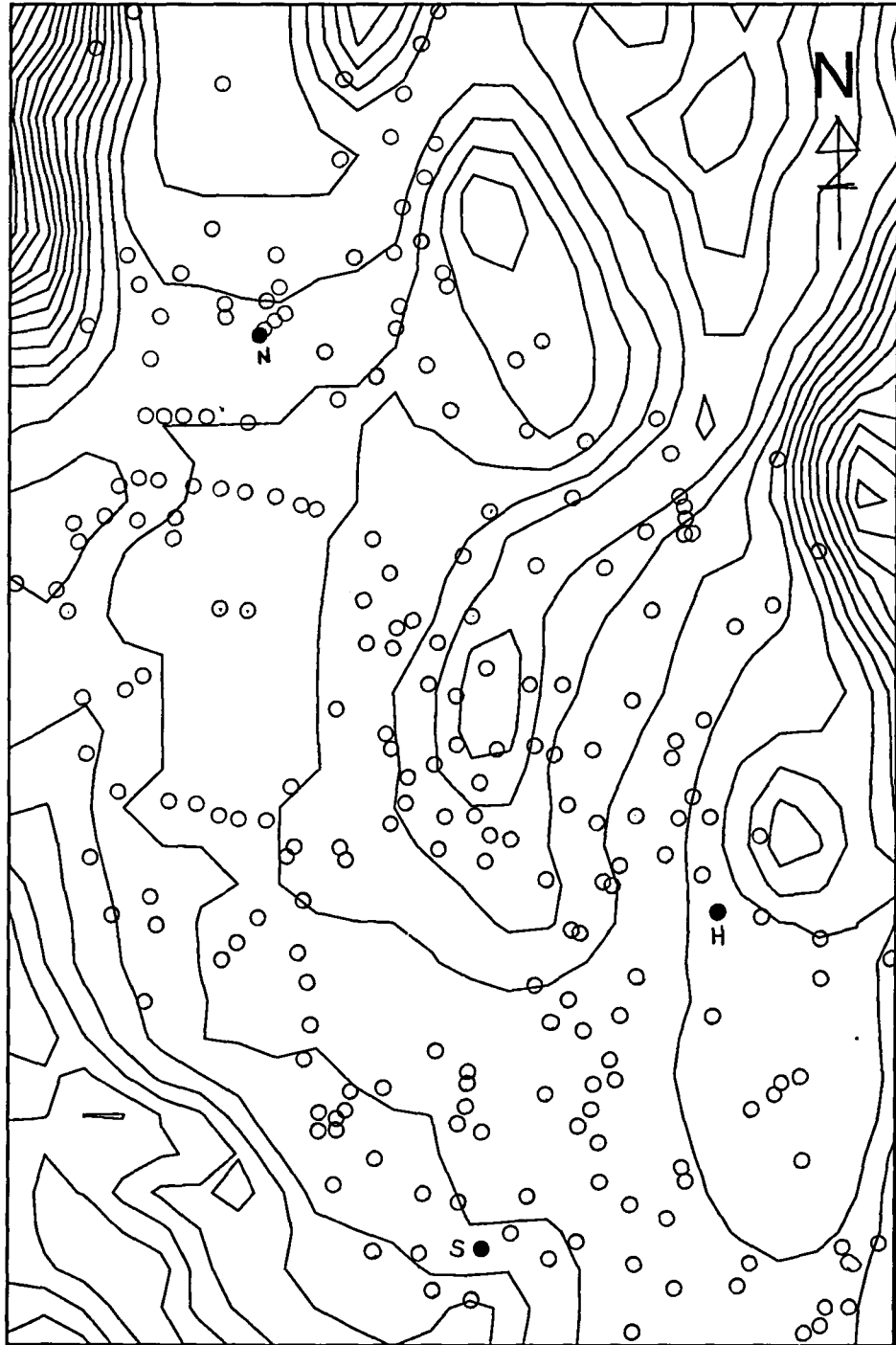


R = river cell    ▽ = drain cell    0 ————— km ————— 5

⊗ = constant head cell    ■ = no flow cell

Fig. 12. MODFLOW grid for Øvre Romerike with cells defined

## Borehole locations



Contour interval 10m

0 km 5

Fig.13 Map of borehole locations for which measurements of head are available from Nov. 1975 (Østmo 1976). S = Sand, H = Hauersetter, N = Nordmoen

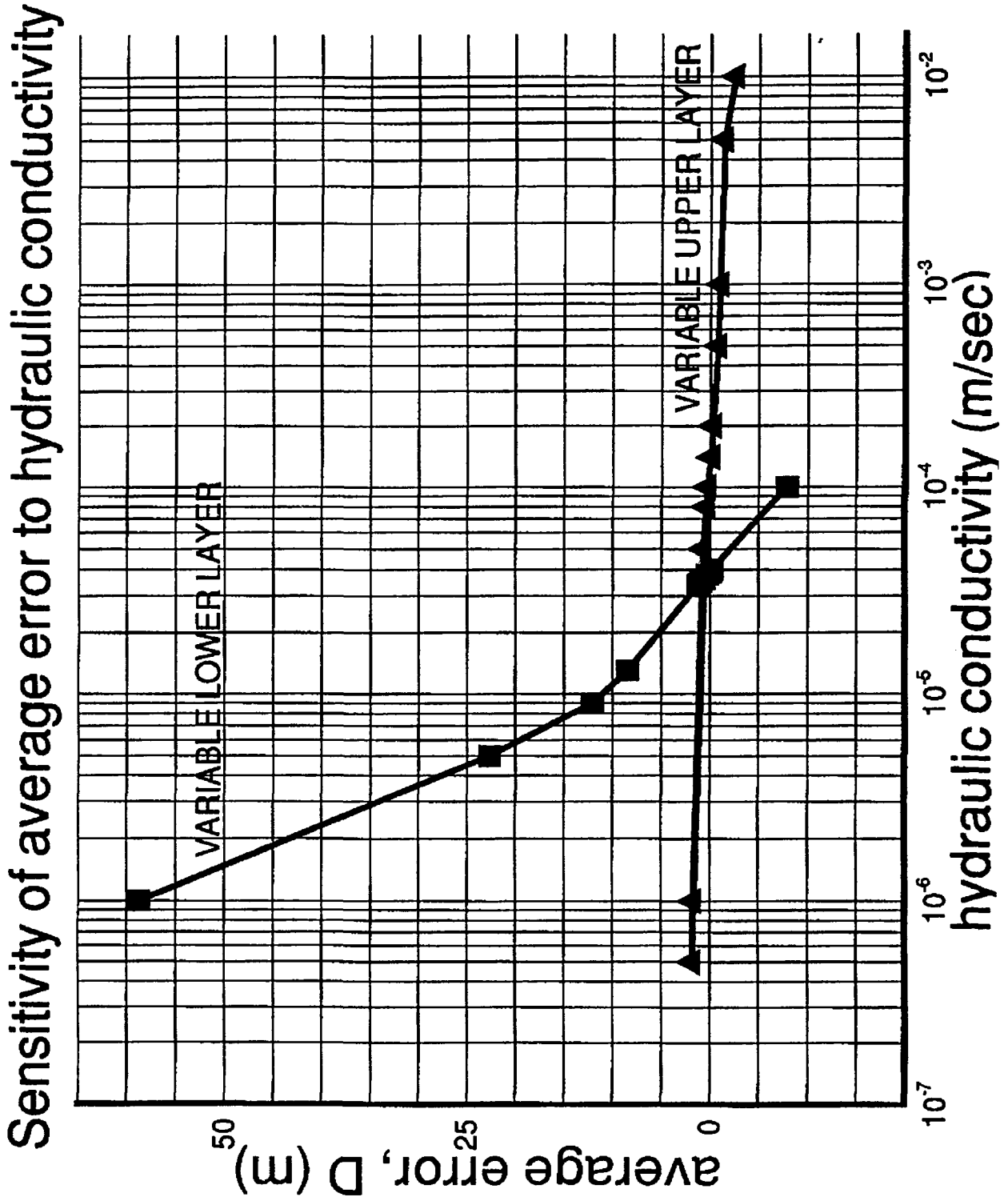
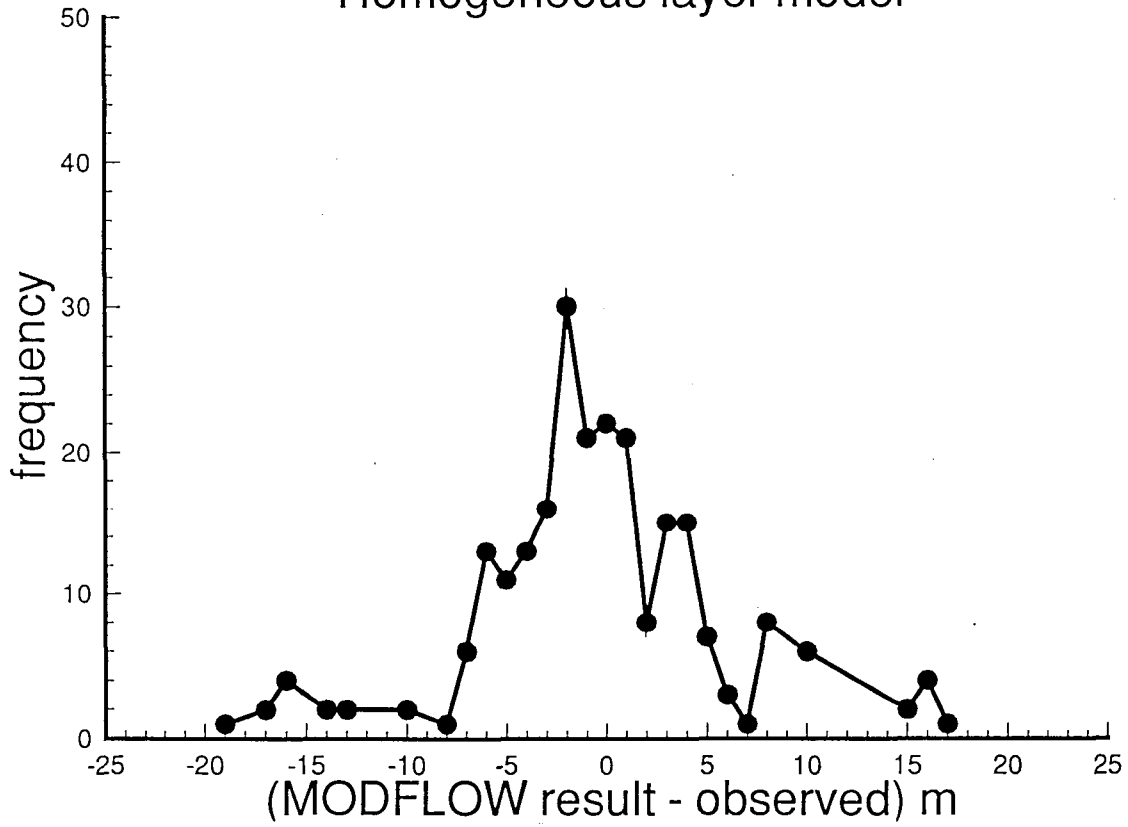


Fig.14 MODFLOW, steady state model: homogeneous layer model - sensitivity of  $D$  (average error) to variation in hydraulic conductivity of coarse and fine layers.



Variable conductivity model

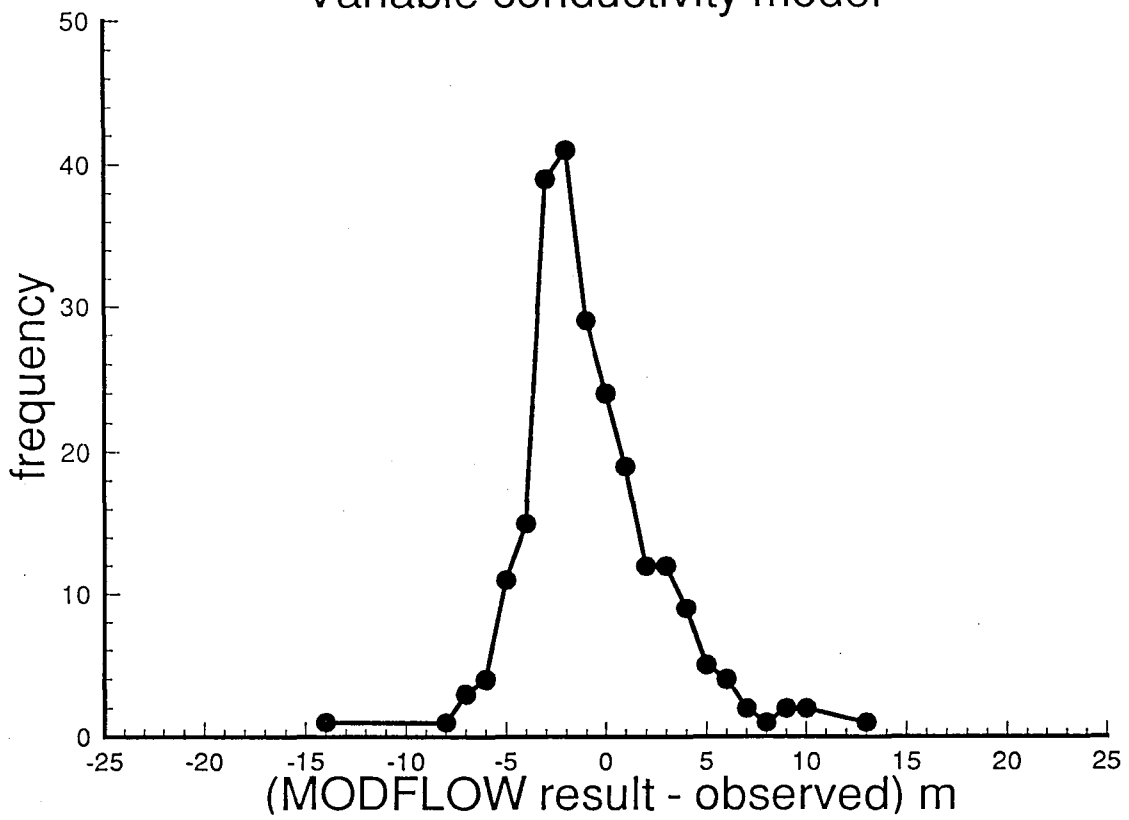


Fig.15 Histograms of discrepancies between steady state model and borehole data for:  
(a) homogeneous layer model  
(b) calibrated hydraulic conductivity model

Model of hydraulic conductivity for fine layer

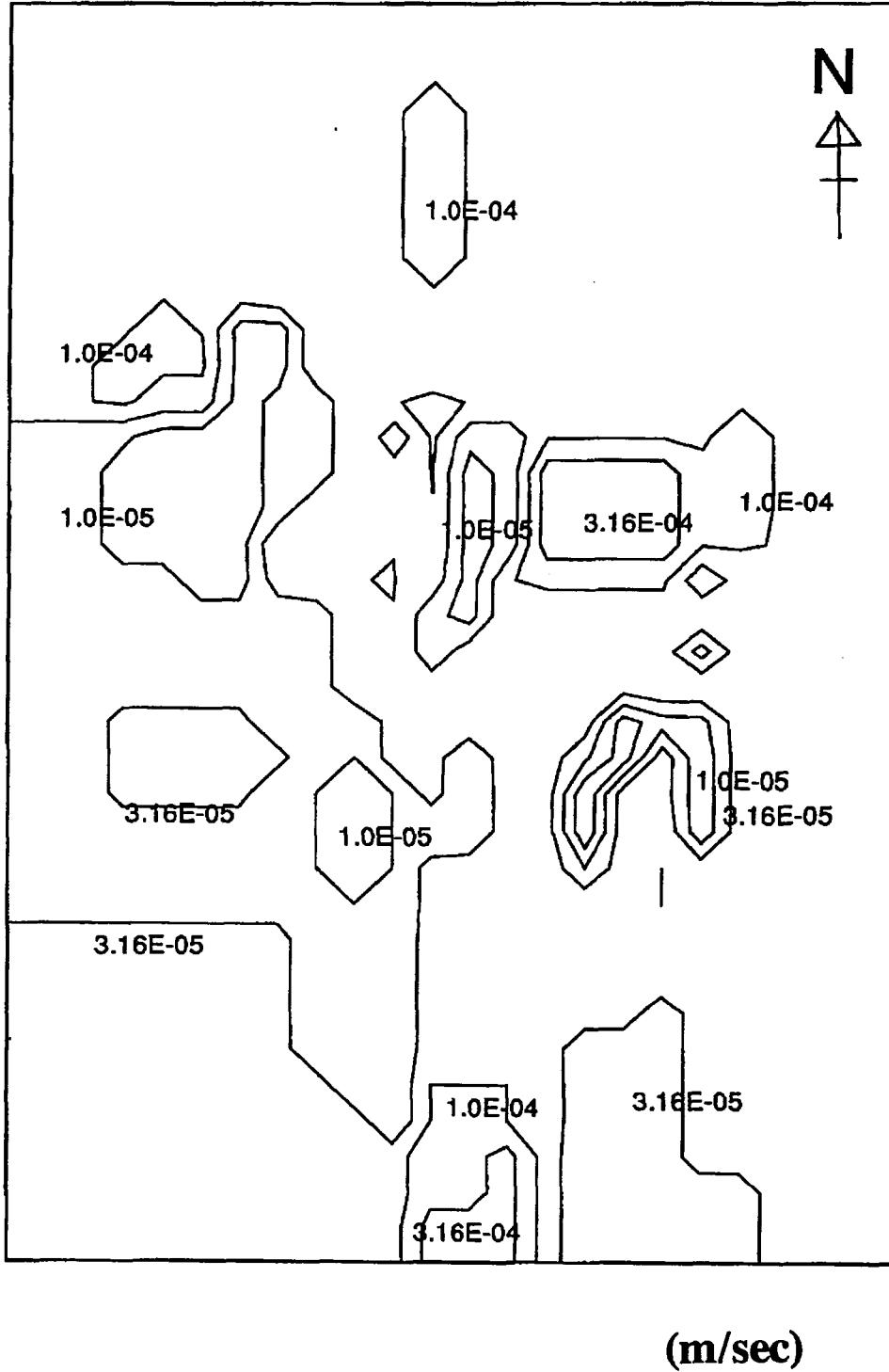
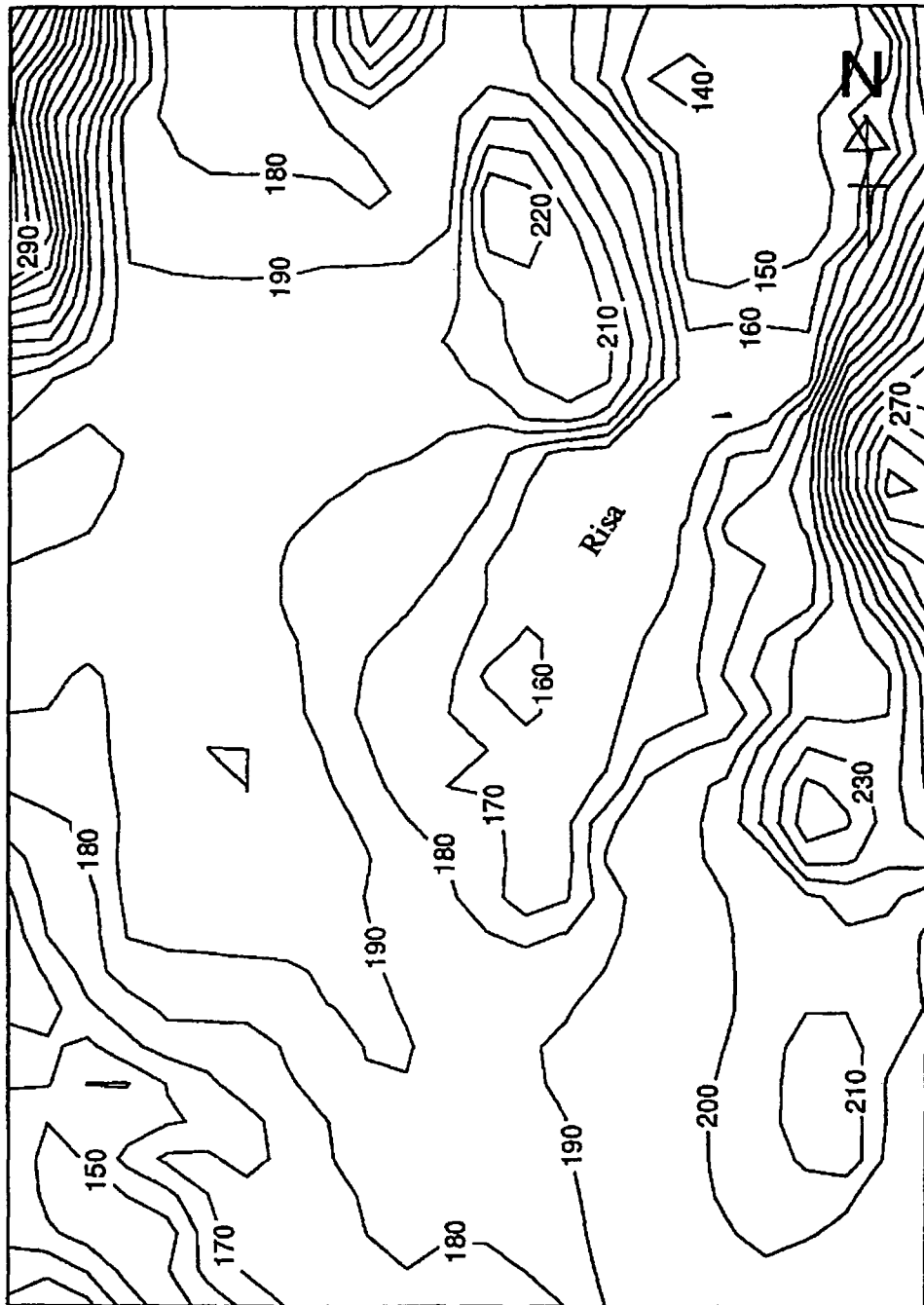


Fig.16 Resulting hydraulic conductivity field for fine layer after calibration with borehole data.

## Head levels, steady state MODFLOW results



Contour interval 10m

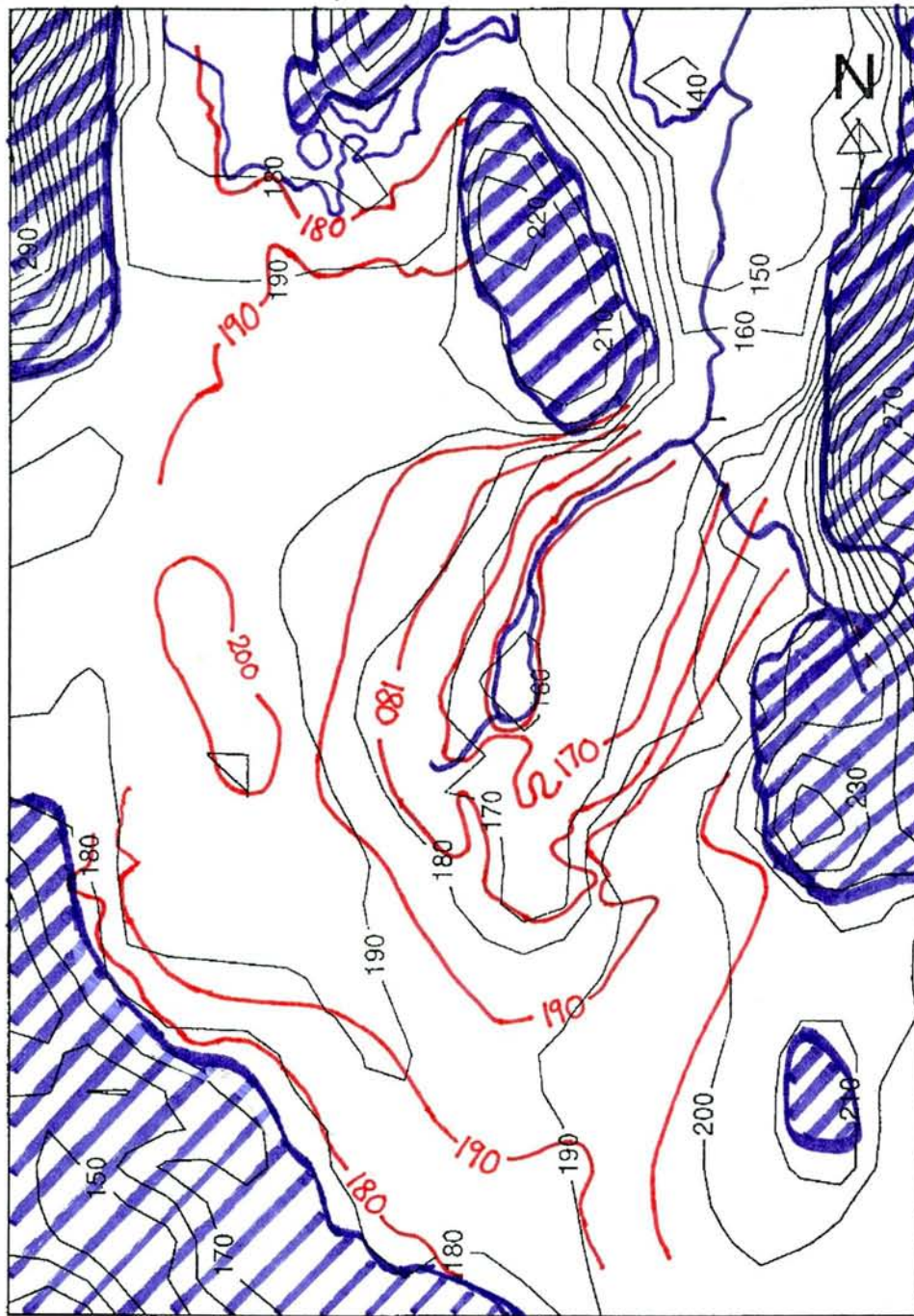
Fig.17 (a) MODFLOW steady state results for head.

m above sea level

0 km 5

m above sea level

## Head levels, steady state MODFLOW results



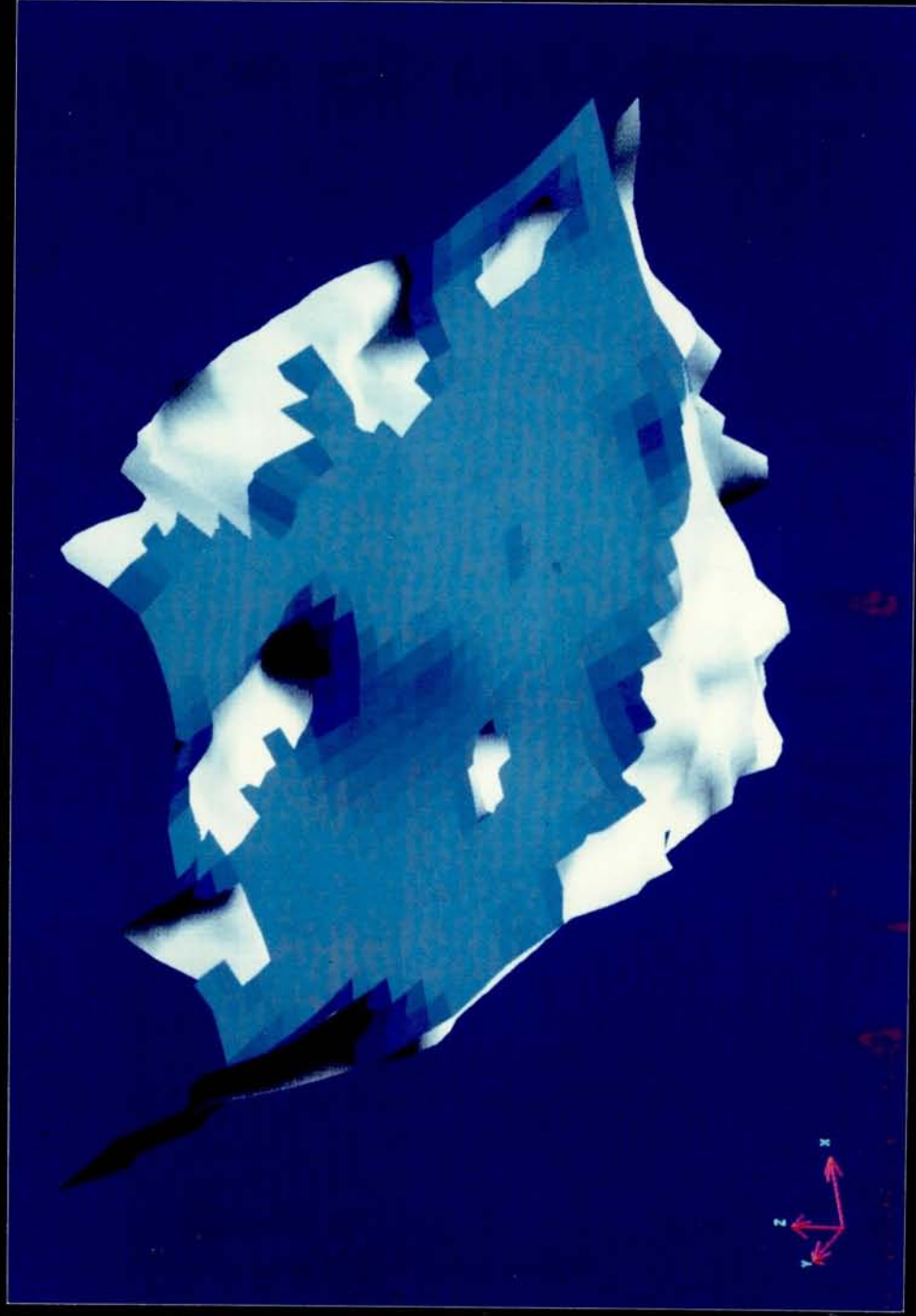
Contour interval 10m

Red = Østmo's (1976) contours, Blue = rivers, lakes, Blue striping = no-flow areas

Fig.17 (b) simplification of Østmo's (1976) map for comparison



# ØVRE ROMERIKE AQUIFER GROUNDWATER FLOW MODELLING



Bergen Environmental Sciences IBM - ADVIZE

Fig.17 (c) 3D ADVIZE picture of modelled water table (blue) with base of aquifer (grey)

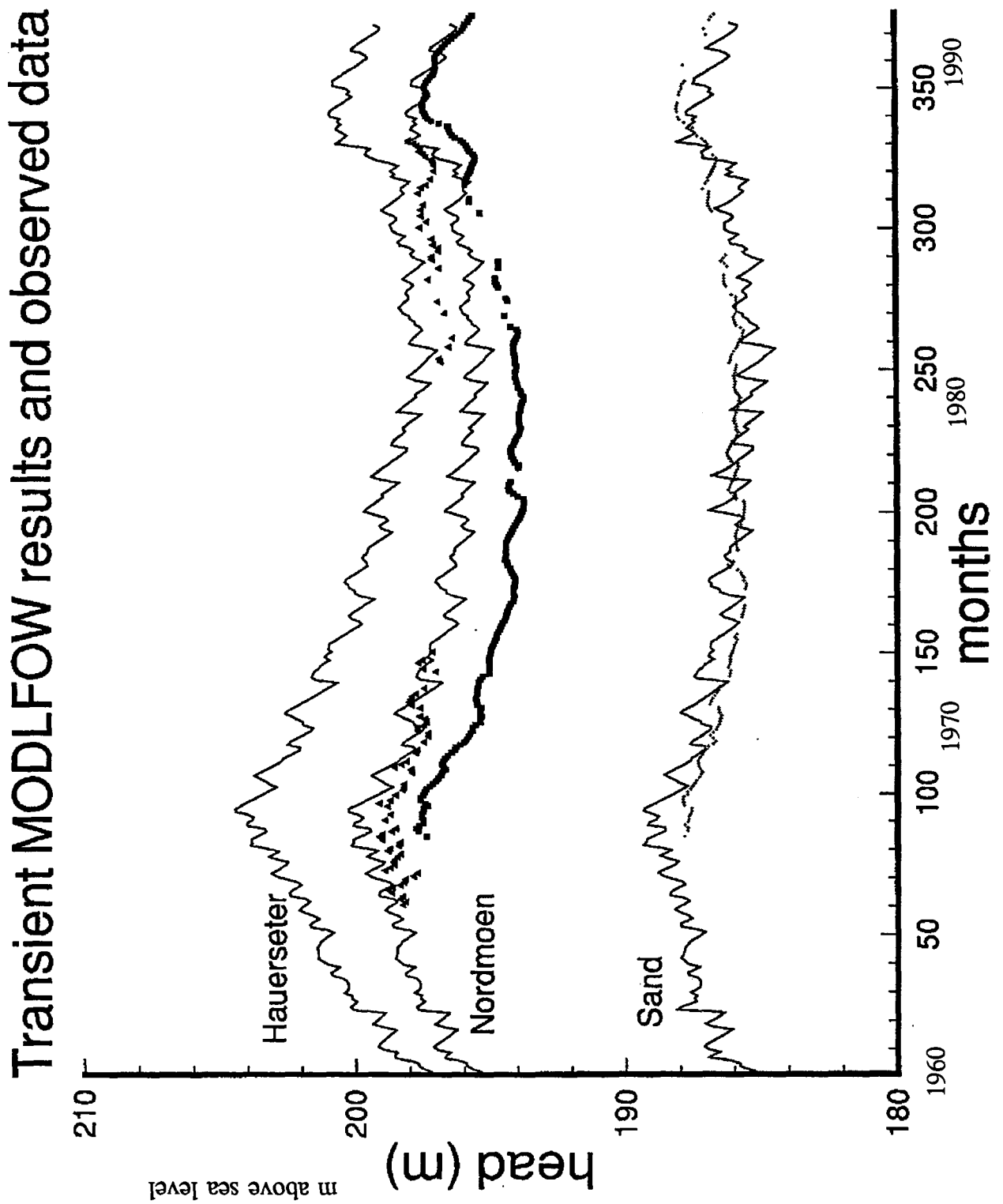


Fig.18 Transient MODFLOW results, with steady state heads in fig.17(a) (i.e. recharge =  $1.27 \times 10^{-8}$  m/s) as initial heads:

(a) using monthly recharge

# Transient MODFLOW results and observed data

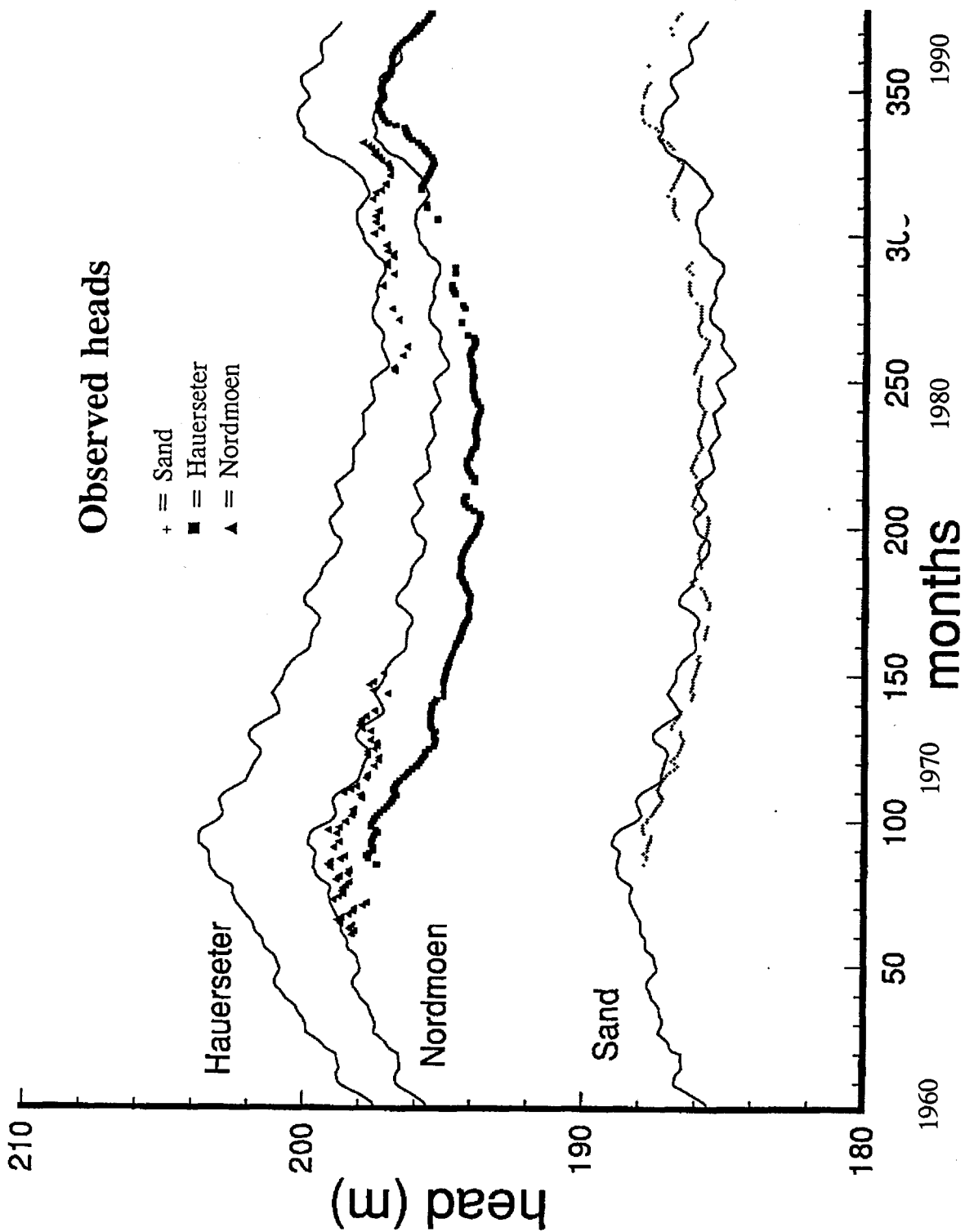


Fig.18 Transient MODFLOW results, with steady state heads in fig.17(a) (i.e. recharge =  $1.27 \times 10^{-8}$  m/s) as initial heads:  
 (b) using running averages of monthly recharge over 7 month intervals

# Transient MODFLOW results and observed data

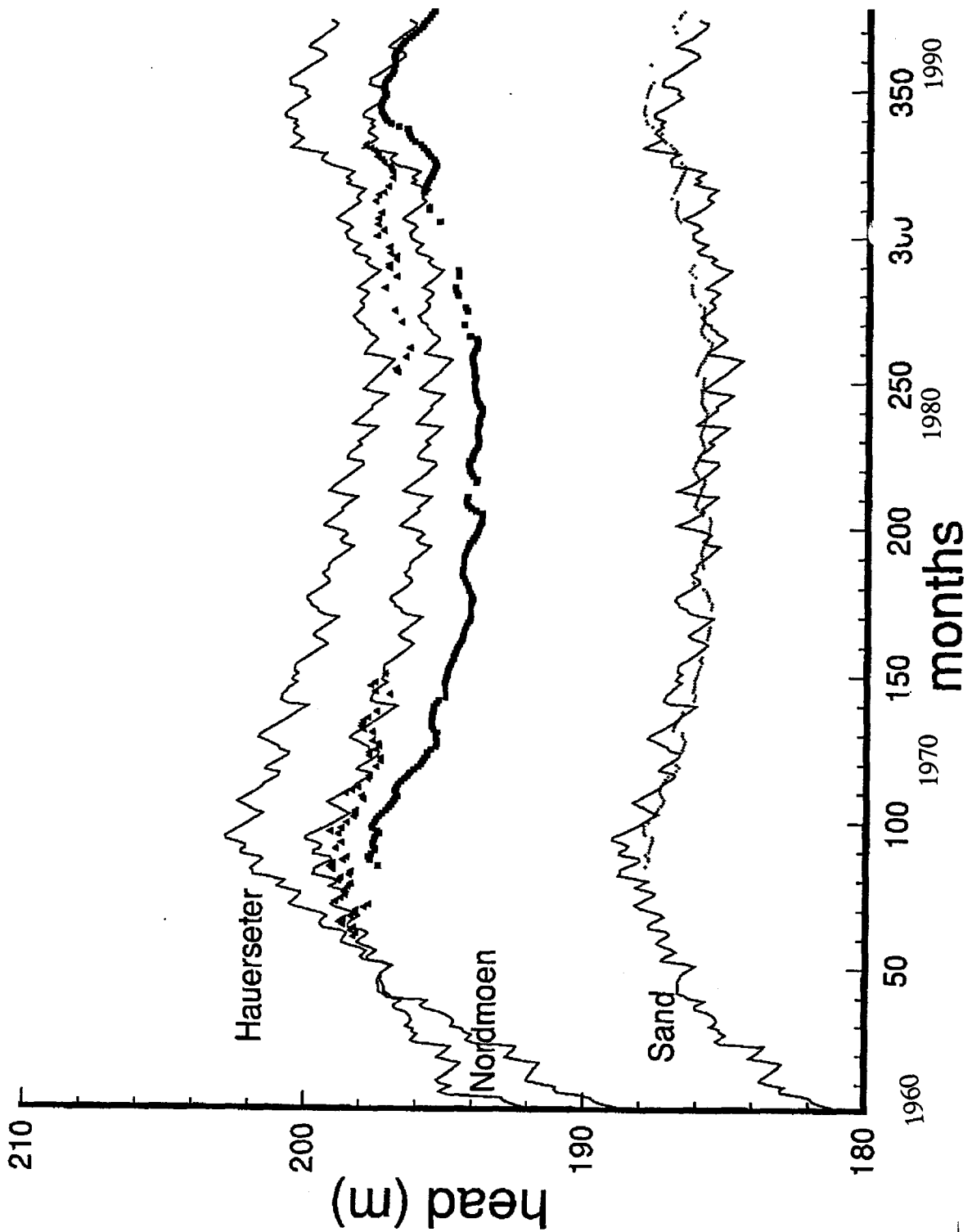


Fig.19 Transient MODFLOW results with steady state heads generated using calibrated hydraulic conductivity field (Fig.16) and minimum recharge of  $8.239E-09$  m/sec:  
 (a) using monthly recharge

# Transient MODFLOW results and observed data

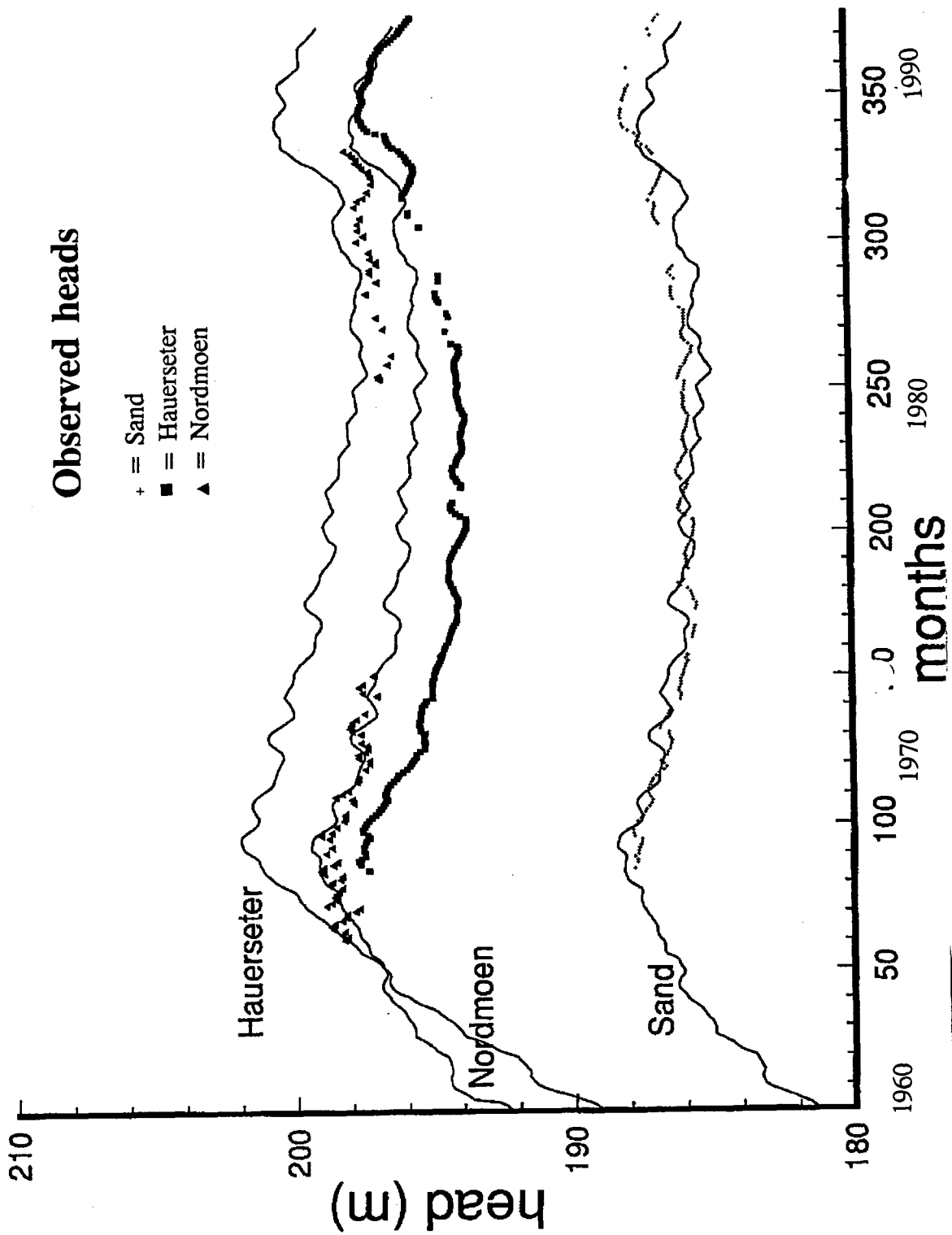


Fig.19 Transient MODFLOW results with steady state heads generated using calibrated hydraulic conductivity field (Fig.16) and minimum recharge of  $8.239E-09$  m/sec:  
(b) using running averages of monthly recharge over 7 month intervals

**APPENDIX 1 - Input files (basic package and block-centred flow package) for  
MODFLOW, steady state model**







999.99 999.99 182.12 187.97 194.28 196.96 195.55 193.43 191.35 186.26 181.38 179.19 177.77 163.00 182.58 188.42 192.92 196.19 198.75 203.48 213.31 218.16 218.03 204.50  
 999.99 999.99 182.13 187.11 192.53 194.51 193.04 191.97 191.16 188.65 185.02 182.15 181.19 181.88 185.29 189.85 193.21 195.72 197.93 199.95 207.83 213.60 214.84 198.50  
 999.99 999.99 175.92 184.55 189.08 191.29 191.00 190.47 190.38 189.30 187.54 185.13 183.08 184.58 187.97 190.74 193.52 195.89 197.88 201.03 209.66 215.33 215.56 198.50  
 999.99 999.99 999.99 181.23 185.68 188.12 188.84 189.06 189.42 188.97 188.40 186.63 185.09 187.56 189.98 191.40 193.66 195.95 198.12 204.24 213.75 215.47 213.88 199.50  
 999.99 999.99 999.99 178.83 182.41 184.59 187.54 188.96 188.48 188.45 188.32 188.42 189.76 190.56 191.62 193.67 195.94 198.29 208.01 999.99 999.99 209.72 197.00  
 999.99 999.99 999.99 999.99 999.99 177.99 185.84 188.07 188.14 188.74 189.77 190.00 190.01 190.56 191.57 193.46 195.93 198.44 209.69 999.99 999.99 207.51 191.50  
 999.99 999.99 999.99 999.99 999.99 999.99 999.99 178.35 186.48 188.31 189.38 190.00 189.98 190.25 191.00 192.87 195.62 198.46 208.84 999.99 999.99 206.82 190.00  
 999.99 999.99 999.99 999.99 999.99 999.99 999.99 171.43 184.36 188.10 189.88 189.36 189.17 189.40 189.84 192.07 195.22 198.46 206.33 216.09 217.42 207.59 191.50  
 999.99 999.99 999.99 999.99 999.99 999.99 999.99 999.99 180.99 184.68 187.91 188.39 186.50 186.66 188.43 189.50 191.62 194.66 197.91 202.79 210.56 211.28 203.76 194.00  
 999.99 999.99 999.99 999.99 999.99 999.99 999.99 999.99 179.57 180.91 183.63 184.35 182.38 182.58 185.66 188.57 191.29 193.87 196.79 199.73 203.40 202.67 200.00 193.00  
 999.99 999.99 999.99 999.99 999.99 999.99 999.99 999.99 999.99 180.00 180.60 180.17 174.95 175.99 183.57 188.07 190.91 193.01 195.43 197.77 197.00 197.00 197.00 190.74  
 999.99  
 2  
 1.5000  
 60.000









Jan 14 1993 17:49:19 fort.11.steadystate

Table with 30 columns and 1000 rows of numerical data. The columns represent various variables and the rows represent time steps. The data shows fluctuations over time, with some values reaching zero or negative values.

**APPENDIX 2 - Input file (block-centred flow package) for MODFLOW,  
transient model**



















**APPENDIX 3 - Elevations of drains, rivers and constant head cells.**



45	41	spring cells modelled as drains		
45	15	1.875E+02	2.600E+00	
2	13	1.720E+02	2.600E+00	South and east sides
2	35	1.720E+02	2.600E+00	
2	35	1.800E+02	2.600E+00	
2	34	1.830E+02	2.600E+00	
2	34	1.800E+02	2.600E+00	
2	34	1.795E+02	2.600E+00	
2	35	1.798E+02	2.600E+00	
2	33	1.730E+02	2.600E+00	
2	33	1.740E+02	2.600E+00	
1	8	1.740E+02	2.600E+00	
2	31	1.740E+02	2.600E+00	
2	30	1.740E+02	2.600E+00	
2	7	1.740E+02	2.600E+00	
2	29	1.740E+02	2.600E+00	
2	29	1.740E+02	2.600E+00	
2	29	1.740E+02	2.600E+00	
2	28	1.740E+02	2.600E+00	
2	27	1.740E+02	2.600E+00	
2	27	1.750E+02	2.600E+00	
2	26	1.760E+02	2.600E+00	
2	25	1.760E+02	2.600E+00	
1	24	1.810E+02	2.600E+00	
1	23	1.820E+02	2.600E+00	
1	22	1.840E+02	2.600E+00	
1	21	1.850E+02	2.600E+00	
1	20	1.870E+02	2.600E+00	
1	19	1.880E+02	2.600E+00	
1	16	1.920E+02	1.400E+00	western boundary
1	15	1.880E+02	1.400E+00	
1	14	1.840E+02	1.400E+00	
1	13	1.820E+02	1.400E+00	
2	5	1.810E+02	2.600E-01	small streams
2	6	1.824E+02	2.600E-01	SE of Hurdalsjoen
2	7	1.829E+02	2.600E-01	
2	8	1.963E+02	2.600E-01	
2	9	2.022E+02	2.600E-01	
2	6	1.778E+02	2.600E-01	
2	7	1.828E+02	2.600E-01	
2	7	1.827E+02	2.600E-01	Deggsjoen
2	25	1.680E+02	7.800E-02	
2	24	1.660E+02	7.800E-02	S of bedrock nr. Rissa bru
2	11	1.990E+02	2.600E-02	
2	9	1.930E+02	2.600E-02	
1	33	2.108E+02	2.600E+00	S of bedrock in SE corner
1	32	2.080E+02	2.600E-01	S of bedrock in SE corner
1	33	2.130E+02	2.600E-01	
1	33	2.060E+02	2.600E-01	
-1				
-1				

Drains

31	1	17	1.638E+02	5.754E+01	1.633E+02
31	1	14	1.654E+02	1.497E+02	1.649E+02
1	15	14	1.636E+02	1.732E+02	1.631E+02
1	14	16	1.647E+02	1.385E+02	1.642E+02
1	14	17	1.636E+02	1.600E+02	1.631E+02
1	13	18	1.603E+02	1.801E+02	1.598E+02
1	12	19	1.596E+02	1.688E+02	1.591E+02
1	11	19	1.671E+02	3.725E+01	1.666E+02
1	10	19	1.639E+02	1.704E+02	1.634E+02
1	9	19	1.553E+02	1.684E+02	1.548E+02
2	8	19	1.426E+02	1.438E+02	1.421E+02
2	7	20	1.435E+02	6.835E+01	1.430E+02
2	7	19	1.406E+02	1.082E+02	1.401E+02
2	6	19	1.420E+02	7.270E+01	1.415E+02
2	5	20	1.449E+02	1.681E+02	1.444E+02
2	4	20	1.420E+02	1.732E+02	1.415E+02
1	3	20	1.420E+02	1.081E+02	1.415E+02
2	2	20	1.413E+02	1.851E+02	1.408E+02
1	1	20	1.424E+02	7.616E+01	1.419E+02
1	1	20	1.645E+02	6.869E+00	1.640E+02
1	21	13	1.700E+02	3.181E+01	1.695E+02
1	22	12	1.700E+02	5.340E+00	1.695E+02
1	22	11	1.700E+02	7.149E+00	1.685E+02
1	21	11	1.700E+02	9.768E+00	1.695E+02
1	13	19	1.795E+02	1.214E+02	1.790E+02
1	14	20	1.929E+02	1.709E+02	1.924E+02
1	15	19	1.930E+02	4.175E+01	1.925E+02
1	15	20	1.965E+02	3.097E+01	1.960E+02
1	15	21	2.086E+02	5.770E+02	2.081E+02
1	17	22	2.186E+02	4.469E+02	2.181E+02
1	19	23	2.186E+02	1.620E+01	2.181E+02

Rivers

		CONSTANT HEAD CELLS		
62	31			
1	11	2.089E+02	2.600E-04	western boundary
1	12	2.009E+02	2.600E-04	
1	13	1.950E+02	2.600E-04	
1	14	1.850E+02	2.600E-04	
1	15	1.850E+02	2.600E-04	
1	16	1.900E+02	2.600E-04	
1	17	1.980E+02	2.600E-04	
1	18	1.980E+02	2.600E-04	
1	20	1.900E+02	2.600E-04	
1	21	1.850E+02	2.600E-04	
1	22	1.810E+02	2.600E-04	
2	24	2.045E+02	2.600E-06	southeastern boundary
2	26	1.985E+02	2.600E-06	
2	27	1.985E+02	2.600E-06	
2	28	1.995E+02	2.600E-06	
2	29	1.970E+02	2.600E-06	
2	30	1.915E+02	2.600E-06	
2	31	1.900E+02	2.600E-06	
2	32	1.915E+02	2.600E-06	
2	33	1.940E+02	2.600E-06	
2	34	1.930E+02	2.600E-06	
2	35	1.970E+02	2.600E-06	
2	35	1.970E+02	2.600E-06	
2	36	1.970E+02	2.600E-06	
1	36	1.970E+02	1.400E-04	
1	19	1.970E+02	1.400E-04	
2	36	1.720E+02	1.400E-04	
2	36	1.800E+02	1.400E-04	
1	36	1.900E+02	1.400E-04	
1	36	1.900E+02	1.400E-04	
1	36	1.970E+02	1.400E-04	
1	1	1.770E+02	2.600E-04	Start Hurdalsjoen
1	1	1.770E+02	2.600E-04	
1	1	1.770E+02	2.600E-04	
1	1	1.770E+02	2.600E-04	
1	2	1.770E+02	2.600E-04	
1	2	1.770E+02	2.600E-04	
1	2	1.770E+02	2.600E-04	
1	3	1.770E+02	2.600E-04	
1	3	1.770E+02	2.600E-04	
1	4	1.770E+02	2.600E-04	
1	4	1.770E+02	2.600E-04	
2	5	1.766E+02	2.600E-04	
2	5	1.766E+02	2.600E-04	
2	5	1.766E+02	2.600E-04	End Hurdalsjoen
2	5	1.766E+02	2.600E-06	
2	1	1.600E+02	2.600E-06	
2	1	1.500E+02	2.600E-06	
2	2	1.450E+02	2.600E-06	
2	3	1.400E+02	2.600E-06	
2	3	1.370E+02	2.600E-06	
2	3	1.400E+02	2.600E-06	
2	4	1.600E+02	2.600E-06	
2	4	1.700E+02	2.600E-06	
2	4	1.800E+02	2.600E-06	
2	4	1.800E+02	2.600E-06	
1	18	1.580E+02	1.400E-04	Herjoen
1	19	1.580E+02	1.400E-04	
1	20	1.580E+02	1.400E-04	
1	20	1.580E+02	1.400E-04	
2	2	1.630E+02	2.600E-06	Dagsjoen
-1	-1			

Constant head cells

**APPENDIX 4 - head difference between vertically adjacent cells in the two aquifer layers (steady state)**



**APPENDIX 5 - deviations of modelled head (modelled - observed) in each cell**

Steady state. Recharge =  $1.27 * 10^{-8}$  m/s



25	198.4600067	209.8000031	2.339996338	12	10
26	198.5899963	197.1000061	-1.489990234	12	11
27	197.2533417	196.3000031	-0.9533386230	8	11
28	197.2533417	196.3000031	-0.9533386230	8	11
29	197.2533417	196.3000031	-0.9533386230	8	11
30	195.7533417	196.5000000	0.7466583252	8	12
31	195.7533417	196.5000000	0.7466583252	8	12
32	195.7533417	196.5000000	0.7466583252	8	12
33	182.6000061	194.6999969	-2.099990845	5	12
34	196.3699951	195.8999939	-0.4700012207	9	12
35	194.2749939	191.8999939	-2.375000000	10	13
36	197.2700043	195.6999969	-1.570007324	11	11
37	196.4499969	193.6000061	-2.849990845	11	12
38	192.9700012	188.6999969	-4.270004272	12	13
39	197.5449982	191.3000031	-6.244995117	14	12
40	197.5449982	191.3000031	-6.244995117	14	12
41	197.2500000	195.6999969	-1.550003052	5	14
42	197.3349915	197.1999969	-0.1349945068	6	14
43	197.3349915	197.1999969	-0.1349945068	6	14
44	197.2700043	197.1999969	-0.7000732422E-01	7	14
45	196.6199951	194.6999969	-1.919998169	8	14
46	194.2749939	191.8999939	-2.375000000	10	13
47	185.5699951	186.1999969	0.8300018311	12	13
48	171.5299988	169.3000031	-2.229995728	14	14
49	158.3000031	164.3999939	6.099990845	15	14
50	154.8699951	163.6000061	8.730010986	17	14
51	162.5500031	166.8000031	4.250000000	17	15
52	178.9900055	193.0000000	14.00999451	20	15
53	164.6450043	167.6999969	3.054992676	17	16
54	164.3349976	170.6000061	5.665008545	18	16
55	164.3349976	170.6000061	5.665008545	18	16
56	164.9349976	170.6000061	5.665008545	18	16
57	164.6450043	167.6999969	3.054992676	17	16
58	162.8399963	164.8999939	2.059997559	15	16
59	172.7599945	169.6000061	-3.159988403	13	16
60	191.2900085	187.1000061	-4.190002441	9	16
61	191.2900085	187.1000061	-4.190002441	9	16
62	182.4700012	186.6999969	-3.770004272	8	16
63	195.3000031	191.0000000	-4.300003052	8	15
64	197.1300049	197.3000031	0.1699981689	7	15
65	197.7200012	198.1999969	0.4799957275	6	15
66	197.5433350	197.0000000	-0.5433349609	5	15
67	197.5433350	197.0000000	-0.5433349609	5	15
68	197.5433350	197.0000000	-0.5433349609	5	15
69	200.3399963	197.8000031	-2.539993286	5	16
70	199.8399963	198.6000061	-1.239990234	6	16
71	200.4400024	198.0000000	-2.440002441	6	17
72	198.2135010	195.3999939	-2.813507080	4	16
73	198.2135010	195.3999939	-2.813507080	4	16
74	198.2100067	195.6000061	-2.610000610	2	18
75	195.9900055	196.1000061	0.1100006104	4	17
76	191.8099976	194.3000031	2.490005493	3	18
77	191.8099976	194.3000031	2.490005493	3	18
78	199.1000061	197.3999939	-1.700012207	7	18
79	197.6100060	191.0000000	-6.610000610	8	18
80	187.8399963	183.1000061	-4.739990234	10	17
81	182.3399963	180.3000031	-2.039993286	10	18
82	178.8999984	180.5000000	1.610000610	11	17
83	182.3399963	180.3000031	-2.039993286	10	18
84	172.3300018	169.6999969	-2.630004883	13	17
85	178.3766632	175.5000000	-2.876663208	11	19
86	165.1799927	165.6000061	0.4200134277	13	18
87	161.2299957	163.8000031	2.570007324	14	17
88	165.3699951	166.3999939	1.029998779	16	17
89	167.3300018	169.5000000	2.169998169	17	18
90	164.3349976	170.6000061	5.665008545	18	16
91	193.0599976	193.1999969	0.1399993896	20	18
92	197.6399994	200.3999939	2.759994507	21	17
93	191.9900055	193.1999969	1.209991455	4	20
94	198.6350098	198.8999939	0.2649841309	5	20
95	198.6350098	198.8999939	0.2649841309	5	20



96	180.2100067	177.8999939	-2.310012817	10	19
97	178.3766632	175.5000000	-2.876663208	11	19
98	178.3766632	175.5000000	-2.876663208	11	19
99	169.0299988	171.8999939	2.869995117	12	19
100	167.5899963	169.8999939	2.309997559	12	20
101	167.5899963	169.8999939	2.309997559	12	20
102	159.8099976	164.5000000	4.690002441	13	20
103	159.0099945	158.0000000	-1.009994507	14	20
104	164.6000061	163.3999939	-1.200006000	15	20
105	169.8999939	167.8999939	-2.000000000	16	20
106	187.5899963	186.0000000	-1.589996338	19	19
107	190.9700012	195.3999939	4.429992676	4	22
108	181.2200012	174.1000061	-7.119995117	10	21
109	174.9049988	170.0000000	-4.904998779	11	21
110	174.9049988	170.0000000	-4.904998779	11	21
111	176.9499969	172.6000061	-4.34999845	11	22
112	173.4100037	170.0000000	-3.410003662	12	22
113	169.1499939	170.1000061	0.950012070	12	21
114	175.7999878	169.6000061	-6.199981689	13	22
115	160.7500000	164.5000000	3.750000000	14	21
116	167.1000061	167.8000031	0.699996482	15	22
117	176.8600006	171.8000031	-5.059997559	16	22
118	194.8999939	194.0000000	-0.899993895	17	22
119	195.7200012	192.1999869	-3.52000427	17	22
120	166.8800049	188.6000031	-21.72000272	18	21
121	197.3899994	198.1000061	0.7100067139	5	22
122	199.2399902	199.6999969	0.4600067139	6	23
123	199.2399902	199.6999969	0.4600067139	6	23
124	199.4949951	199.6999969	0.2050018311	7	23
125	199.4949951	199.6999969	0.2050018311	7	23
126	198.4799957	197.1999869	-1.279988779	8	23
127	195.7850037	191.8999939	-3.885009166	9	24
128	195.7850037	191.8999939	-3.885009166	9	24
129	194.2500049	184.0000000	-10.25500488	10	24
130	194.2500049	184.0000000	-10.25500488	10	24
131	180.0050049	174.6000061	-5.404998779	11	23
132	180.0050049	174.6000061	-5.404998779	11	23
133	177.0500031	172.8000031	-4.250000000	12	23
134	178.8099976	174.8999939	-3.910003662	12	24
135	189.6900024	186.3000031	-3.389999390	9	22
136	175.7999878	169.6000061	-6.199981689	13	22
137	173.2050018	171.0000000	-2.205001831	13	23
138	173.2050018	171.0000000	-2.205001831	13	23
139	171.5899963	167.6999969	-3.889999390	14	24
140	177.7799988	172.0000000	-5.779998779	13	24
141	172.4900055	168.1999869	-4.290008545	15	23
142	191.6300049	189.6999969	-1.930007935	16	23
143	191.6300049	189.6999969	-1.930007935	16	23
144	197.4700012	199.1000061	1.630004883	17	24
145	197.7000043	199.1000061	1.330001831	17	24
146	198.0299988	199.6999969	1.669998169	18	23
147	198.0299988	199.6999969	1.669998169	18	23
148	203.6999969	204.6999969	1.000000000	19	23
149	182.2899933	193.3000000	11.210006714	4	24
150	195.8950043	195.5000000	-0.3950042725	5	25
151	195.8950043	195.5000000	-0.3950042725	5	25
152	194.8600006	192.3999939	-2.460006714	5	26
153	194.7100067	195.0000000	0.2899932861	8	25
154	193.1250000	193.3999939	0.2749938965	7	26
155	194.3999939	192.0000000	-2.399993896	9	25
156	171.5899963	167.6999969	-3.889999390	14	24
157	182.0549927	182.0000000	-0.5499267578E-01	15	26
158	182.0549927	182.0000000	-0.5499267578E-01	15	26
159	185.3399963	188.6000061	3.260009766	16	25
160	193.3899994	193.6999969	0.3099975586	16	24
161	195.3399963	188.6000061	-6.739999390	16	25
162	193.2400055	199.8999939	6.659988403	18	24
163	196.0700073	199.6999969	3.629988624	18	24
164	198.4499969	203.1000061	4.650009155	19	25
165	205.5299988	207.5000000	1.970001221	21	26
166	205.8999939	209.6999969	3.800003052	22	26

167	205.2299957	207.5000000	2.270004272	21	27
168	199.2899963	199.1999969	-0.89996337899-01	18	28
169	190.4900055	193.0000000	2.509994507	16	27
170	193.2200012	194.3000031	1.080001831	16	28
171	189.9900055	188.8999939	-1.090011597	15	27
172	191.4700012	191.8999939	0.4299926758	15	28
173	187.2400055	186.5000000	-0.7400054932	14	27
174	192.2200012	191.5000000	-0.7200012027	9	26
175	189.9700012	189.1000061	-0.8699951172	9	27
176	188.7400055	187.8999939	-0.8400115967	7	28
177	193.1250000	193.3999939	0.2749938965	7	26
178	187.2599945	186.8000031	-0.4599914551	5	27
179	186.0000000	186.5000000	0.5000000000	9	29
180	184.3699951	185.1000061	0.7300109863	9	30
181	187.1199951	188.3999939	1.279998779	10	29
182	185.8033447	187.8000031	1.996658325	10	30
183	185.8033447	187.8000031	1.996658325	10	30
184	188.8399963	189.5000000	0.6600036621	11	29
185	190.6799927	188.8000031	-1.879998624	12	28
186	191.5299988	190.8000031	-0.7299957275	13	29
187	191.5299988	190.8000031	-0.7299957275	13	29
188	191.2949982	191.5000000	0.2050018311	13	30
189	193.0200043	191.8000031	-1.220001221	14	29
190	191.4700012	191.8999939	0.4299926758	15	28
191	194.2600098	195.0000000	0.7399902344	16	29
192	194.2600098	195.0000000	0.7399902344	16	29
193	194.2600098	195.0000000	0.7399902344	16	29
194	193.9199982	195.8000031	1.880004883	16	30
195	203.4700012	201.3000031	-2.169998169	19	30
196	204.1633301	203.8999939	-0.2633361816	20	29
197	204.1633301	203.8999939	-0.2633361816	20	29
198	204.1633301	203.8999939	-0.2633361816	20	29
199	184.3699951	185.1000061	0.7300109863	9	30
200	185.8033447	187.8000031	1.996658325	10	30
201	186.6699982	187.0000000	0.3300018311	10	31
202	183.6300049	186.1999969	2.569992065	10	32
203	191.2100067	190.6000061	-0.6100006104	12	30
204	191.2949982	191.5000000	0.2050018311	13	30
205	193.7299957	193.6000061	-0.1299986240	15	30
206	190.8950043	196.1999969	5.304992676	16	31
207	190.8950043	196.1999969	5.304992676	16	31
208	200.4900055	198.0000000	-2.490005493	17	31
209	201.1000061	199.8000031	-1.300003052	18	31
210	203.6199951	205.6000061	1.980010986	20	31
211	188.1699982	190.1999969	2.029998779	12	32
212	189.2299957	191.1000061	1.870010376	13	32
213	183.7899933	184.8999939	1.110000610	10	33
214	186.4100037	189.3000031	2.889999390	12	33
215	186.6799927	190.3000031	3.620010376	13	33
216	175.8000031	190.6999969	14.89999390	14	33
217	189.5099945	191.6999969	2.190002441	14	32
218	196.2599945	196.0000000	-0.2599945068	16	32
219	200.8000031	197.8000031	-3.000000000	17	32
220	175.8000031	190.6999969	14.89999390	14	33
221	189.1100006	188.5000000	-0.6100006104	15	33
222	196.8000031	195.6999969	-1.1000006104	15	33
223	202.1499939	200.8000031	-1.349990845	16	33
224	200.0700073	200.8999939	0.8299865723	22	33
225	200.7399902	204.1000061	3.360015869	21	33
226	200.7399902	204.1000061	3.360015869	21	33
227	182.0000000	187.8000031	5.800003052	12	34
228	180.2500000	189.1999969	8.949998948	13	34
229	197.6699982	193.0000000	-4.669998169	16	35
230	201.4900055	199.8999939	-1.590011597	19	34
231	199.7500000	196.6999969	-3.050003052	17	34
232	199.1950073	200.5000000	1.304992676	21	34
233	199.1950073	200.5000000	1.304992676	21	34
234	199.3800049	197.0000000	-2.380004883	21	35
235	196.6900024	199.3999939	2.7099991455	20	35

average of discrepancies = 0.2033738196  
 root mean square discrepancy = 3.835682631

**APPENDIX 6 - output files from MODFLOW, flow to drains, rivers and constant head cells.**

layer	row	col	flow rate	net flow into cell, positive values - net flow out of cell
2	33	15	-0.3189697117E-01	24
2	35	13	-0.2011413500E-01	36
2	35	12	-0.1210021973E-01	
2	34	11	-0.2499389462E-02	
2	34	11	-0.2027282678E-01	
2	34	10	-0.8291625418E-02	
2	34	9	-0.2975463867E-02	
2	35	10	-0.3094482236E-02	
2	33	9	-0.192413301E-01	
1	32	8	-0.1368713286E-01	
2	32	8	0.000000000E+00	
2	31	8	-0.3213500977E-01	
2	30	7	-0.1098937914E-01	
2	29	7	-0.3495177999E-01	
2	29	6	-0.1503601018E-01	
2	29	5	-0.1091003418E-01	
2	28	4	-0.1158447191E-01	
2	27	3	-0.1011657715E-01	
2	26	3	-0.5435180385E-02	
2	25	3	-0.4998778924E-02	
2	24	3	-0.5792235956E-02	
2	24	3	0.000000000E+00	
2	23	3	-0.2150288480E-01	
1	23	3	0.000000000E+00	
2	22	3	-0.1487731840E-01	
1	22	3	0.000000000E+00	
2	21	3	-0.6982421502E-02	
2	21	3	0.000000000E+00	
1	20	3	-0.1701965183E-01	
2	20	3	0.000000000E+00	
1	19	3	-0.4284667969E-01	
2	19	3	0.000000000E+00	
1	16	3	-0.1805114746E-01	
2	16	3	0.000000000E+00	
1	15	2	-0.3717040876E-02	
2	15	2	0.000000000E+00	
1	14	2	-0.3138122335E-01	
2	14	2	0.000000000E+00	
1	13	3	-0.8536376804E-01	
2	13	3	0.000000000E+00	
2	5	11	-0.1996734552E-01	
2	6	11	0.000000000E+00	
2	7	11	-0.2153442241E-01	
2	8	12	-0.3491210809E-03	
2	9	12	0.000000000E+00	
2	6	10	-0.2133209072E-01	
2	7	10	-0.1040618867E-01	
2	7	9	-0.1948333718E-01	
2	25	15	-0.4514016956E-01	
2	24	15	-0.3114596588E-01	
2	11	13	0.000000000E+00	
2	9	17	0.000000000E+00	
1	33	21	0.000000000E+00	
2	33	21	0.000000000E+00	
2	32	21	0.000000000E+00	
2	32	21	0.000000000E+00	
1	33	22	0.000000000E+00	
2	33	22	0.000000000E+00	
1	33	23	0.000000000E+00	
2	33	23	0.000000000E+00	

total sum of flows = -0.9484448433  
 Flow rates for springs in SE = -0.2712432742

Dec 14 1992 14:37:49		river.info		Page 1	
Net cell-by-cell flow terms for river cells					
flow rates in l**3/t					
negative values - net flow into cell, positive values - net flow out of cell					
kstp, kper, icol, irow, ilay	1	1	24	36	2
Number of river cells in layer	27				
row	col	flow rate			
1	14	0.8779907366E-03			
2	17	0.000000000E+00			
1	14	0.000000000E+00			
2	16	-0.1827392541E-01			
1	14	0.000000000E+00			
2	15	-0.1823547333			
1	15	0.000000000E+00			
2	15	0.000000000E+00			
1	14	0.2747344971E-01			
2	14	0.000000000E+00			
1	14	-0.3662109375			
2	14	0.000000000E+00			
1	13	-0.4342010617			
2	13	0.000000000E+00			
1	12	-0.4790771604			
2	12	0.000000000E+00			
1	11	0.2068939209			
2	11	0.000000000E+00			
1	10	0.9620361030E-01			
2	10	0.000000000E+00			
1	9	-0.8222655952E-01			
2	9	0.000000000E+00			
1	8	-0.1075164825			
2	8	0.000000000E+00			
1	7	-0.3441696241E-01			
2	7	0.4127502441E-01			
1	6	-0.1885833591E-01			
2	6	0.7695007604E-02			
1	5	0.000000000E+00			
2	4	-0.3964233398E-01			
1	3	0.1319580059E-01			
2	3	0.000000000E+00			
1	2	-0.2259521559E-01			
2	2	0.000000000E+00			
1	1	-0.3486328293E-02			
2	1	0.000000000E+00			
1	20	0.8804259822E-02			
2	20	0.000000000E+00			
1	21	0.5290664732E-01			
2	21	0.000000000E+00			
1	22	-0.3577056900E-01			
2	22	0.000000000E+00			
1	22	0.000000000E+00			
2	22	0.000000000E+00			
1	21	-0.5350817740E-01			
2	21	0.000000000E+00			
1	13	0.4834808409			
2	13	0.000000000E+00			
1	14	0.2164413333			
2	14	0.000000000E+00			
1	15	0.4561309814			
2	15	0.000000000E+00			
total sum of flows = -0.4420106411					
Flow rates for Rissa river = -1.921705842					
Flow rates Hersjoen to Rissabru = -0.1997506618					
Flow rates for Transjoen-Hersjoen river = -0.2756783925E-01					

```

Net cell-by-cell flow terms for constant head cells
flow rates in l**3/t
negative values - net flow into cell, positive values - net flow out of cell
kstp,kper,icol,irow,ilay
Number of constant head cells is
layer row col
1 1 0.000000000E+00
2 1 0.4324987531E-02
11 1 0.2512730192E-02
12 1 0.8855989203E-02
13 1 0.1239921525E-01
14 1 0.1288261614E-02
15 1 0.1682206406E-02
16 1 0.8524260920E-04
17 1 -0.3599552670E-02
18 1 -0.1942480412E-04
19 1 -0.5583088845E-02
20 1 -0.2489967665E-04
21 1 0.1149423700E-01
22 1 0.5191951277E-04
23 1 0.4847203568E-01
24 1 0.1889392006E-03
25 1 -0.2777301911E-01
26 1 -0.4310255099E-04
27 1 -0.8594832383E-02
28 1 -0.6443018719E-05
29 1 -0.3477390390E-02
30 1 -0.1185233850E-04
31 24 -0.1210805494E-02
32 24 -0.6170213223E-02
33 24 -0.5846171640E-02
34 24 -0.4919835832E-02
35 24 -0.4075833596E-02
36 24 -0.4045531619E-02
37 24 -0.2740506083E-02
38 24 -0.3100136933E-02
39 24 -0.5296288058E-02
40 24 -0.1633769646E-01
41 23 -0.1834069612E-02
42 22 -0.580800925E-02
43 21 -0.6674275268E-02
44 20 -0.3035686444E-02
45 20 -0.9319806122E-03
46 19 -0.5015324336E-02
47 19 -0.3730241733E-03
48 14 -0.1455520932E-01
49 16 -0.9869552217E-02
50 16 -0.2006976400E-02
51 17 0.000000000E+00
52 17 -0.2497273264E-02
53 18 -0.4121921025E-02
54 18 -0.3625699319E-03
55 5 0.000000000E+00
56 5 0.000000000E+00
57 6 0.000000000E+00
58 7 0.000000000E+00
59 7 0.000000000E+00
60 8 0.000000000E+00
61 8 0.000000000E+00
62 5 -0.3651133738E-02
63 6 0.000000000E+00
64 6 0.000000000E+00
65 7 0.000000000E+00
66 7 0.000000000E+00
67 8 0.000000000E+00
68 8 0.000000000E+00
69 6 -0.2034629724E-03
70 6 -0.4104258027E-02

```

```

1 3 0.000000000E+00
2 3 0.000000000E+00
3 4 -0.4531591258E-03
4 6 -0.9382458404E-02
5 7 0.000000000E+00
6 7 0.000000000E+00
7 9 0.000000000E+00
8 9 0.000000000E+00
9 6 -0.4391283542E-01
10 7 -0.1777783968E-01
11 8 -0.6254647393E-02
12 9 -0.6991866976E-02
13 16 -0.1350457128E-01
14 17 0.2879552310E-02
15 17 -0.9807439521E-02
16 17 -0.1468977984E-01
17 18 -0.3901800513E-01
18 21 -0.6850904226E-01
19 22 0.6989737600E-01
20 23 0.1115912944E-01
21 24 0.000000000E+00
22 14 -0.5093380809E-01
23 14 -0.4603963345E-01
24 13 -0.3443370014E-01
25 13 -0.4001548141E-01
26 14 -0.5959716182E-02
27 14 -0.1793069951E-01
28 14 -0.6344031543E-01
29 14 -0.7423953448E-01
30 14 -0.15066618261
31 25 -0.6747183800
32 18 -0.3326489031
33 19 -0.9660165012E-01
34 19 0.1752918065
35 20 0.8908209205
36 25 0.8908209205
total sum of flows = -0.6747183800
Flow rates for Hursjoen = -0.3326489031
Flow rates for Hurdalsjoen = -0.9660165012E-01
sum of positive flows in buff 0.1752918065
sum of negative flows in buff -0.8908209205

```

**APPENDIX 7 - listing of recharge model**

```

C PROGRAM RECHARGE
C
C Calculates aquifer recharge from meteorological data
C using the Penman-Grindley model (Rushion and Redshaw, 1979,
C 'Seepage and Groundwater Flow') with modifications to
C include effects of accumulating snow cover and snow melt.
C
C Written by Noelle Odling (BSC) and David Banks (NGU)
C at IBM Bergen Environmental Sciences and Solution Centre (BSC),
C Bergen Norway.
C
C 9th April 1992
C
C .....
C Variable definitions:
C
C rg = recharge (mm)
C pe = potential evapotranspiration
C ro = runoff (fraction of precipitation)
C rf = precipitation
C rc = root constant
C sm = soil moisture deficit
C ps = potential change in soil moisture
C as = actual # #
C ae = actual evapotranspiration
C .....
C
C PARAMETER (NUM=20000)
C real*4 sm(num), ps(num), as(num), ae(num), pe(num), rg(num)
C real*4 rf(num)
C integer*4 dat(2,num), snod(num), ntyp(num), sdur(6,num), maxs(num)
C character*20 title
C
C data sm(121) / 0.0 /
C data rc / 175.0 /
C
C read rainfall, pot.evap. data set
C
C
C read (77,8) title
C format (a20)
C ndata = 0
C nyear = 0
C do 10 i = 1,num
C read (77,*,end=11) ndum, dat(1,i), dat(2,i), pe(i), rf(i),
C # if (pe(i).lt.0.0) then
C snod(i),ntyp(i)
C rf(i) = rf(i) - pe(i)
C pe(i) = 0.0
C end if
C ndata = ndata + 1
C if (dat(2,i).eq.200) nyear = nyear + 1
C continue
C 10
C 11
C -----
C find periods of significant snow cover and day max snow depth
C
C nper = 0
C do 50 i = 1,ndata
C if (i.eq.1) nprev = 1
C if (i.gt.1) nprev = ntyp(i-1)
C detect snow cover start
C if (nprev.lt.2) then
C nper = nper + 1
C if (nper.gt.num) write (6,*)'array bounds exceeded'
C maxs(nper) = 0
C nflag1 = 1
C sdur(1,nper) = dat(1,i)
C sdur(2,nper) = dat(2,i)
C end if

```

```

C end if
C
C find day with max snow cover depth
C
C if (nflag1.eq.1) then
C if (snod(i).gt.maxs(nper)) sdur(5,nper) = dat(1,i)
C if (snod(i).gt.maxs(nper)) sdur(6,nper) = dat(2,i)
C if (snod(i).gt.maxs(nper)) maxs(nper) = snod(i)
C end if
C
C detect snow cover finish - day after last ntyp=2
C
C if (nflag1.eq.1) then
C if (nprev.ge.2) then
C if (ntyp(i).lt.2) then
C nflag1 = 0
C sdur(3,nper) = dat(1,i)
C sdur(4,nper) = dat(2,i) + 1
C check for end of year and leap years
C if (mod(dat(1,i),4).eq.0) then
C if (dat(2,i).eq.366) then
C sdur(3,nper) = dat(1,i)
C sdur(4,nper) = dat(2,i) + 1
C end if
C else
C if (dat(2,i).eq.365) then
C sdur(3,nper) = dat(1,i) + 1
C sdur(4,nper) = dat(1,i) + 1
C end if
C end if
C
C 50
C continue
C
C -----
C CALCULATE RECHARGE PER DAY
C -----
C
C nflag = 0
C kflag = 0
C nper1 = 0
C nper2 = 0
C nper3 = 0
C DO 100 I = 122,ndata
C
C detect start, finish and time of max snow cover
C nflag=i: snow cover, kflag=1: snow melting period
C start period
C do 101 j = 1,nper
C if (dat(1,i).eq.sdur(1,j)) then
C if (dat(2,i).eq.sdur(2,j)) then
C nflag = 1
C storff = 0.0
C nper1 = nper1 + 1
C end if
C end if
C
C start melting period
C
C if (nflag.eq.1) then
C if (dat(1,i).eq.sdur(5,j)) then
C if (dat(2,i).eq.sdur(6,j)) then
C nper2 = nper2 + 1
C kflag = 1
C
C no days over which melting takes place
C
C if (sdur(3,j).eq.sdur(5,j)) then
C meitd = sdur(4,j) - sdur(6,j)

```



```

else
  meltcd = 365 - sdur(6,j) + sdur(4,j)
  if (mod(dat(1,i),4).eq.0) meltcd = meltcd + 1
end if
end if
end if
end if
end if

c finish period
c
  if (dat(1,i).eq.sdur(3,j)) then
    nflag = 0
    kflag = 0
    nper3 = nper3 + 1
  end if
end if

c 101 continue
c calculate precipitation storage in form of snow during snow buildup
c
  if (nflag.eq.1) then
    if (kflag.eq.0) then
      storrf = storrf + rf(i)
    end if
  end if

c.....potential change in soil moisture.....
c 1) when zero snow cover
  ps(i) = pe(i) - (1-ro)*rf(i)
c 2) when snow is accumulating
  if (nflag.eq.1) then
    if (kflag.eq.0) then
      ps(i) = pe(i)
    else if (kflag.eq.1) then
      ps(i) = pe(i) - (1-ro)*rf(i) - (storrf/float(meltd))
    end if
  end if

c
  if (sm(i-1).lt.rc) then
    as(i) = ps(i)
    ae(i) = pe(i)
  end if

c
  if (ps(i).gt.0.0) then
    if (sm(i-1).ge.rc) then
      as(i) = 0.1*ps(i)
      ae(i) = rf(i)*(1-ro) + as(i)
    end if
  else
    if (sm(i-1).ge.rc) then
      as(i) = ps(i)
      ae(i) = pe(i)
    end if
  end if

c calculate present sm and rg
c
  sm(i) = sm(i-1) + as(i)
  if (sm(i).lt.0.0) then
    rg(i) = -sm(i)
    sm(i) = 0.0
  else
    rg(i) = 0.0
  end if

c 100 continue
c calculate yearly averages

```

```

c
  write (55,*) 'Year
#transpiration,
  sumae = 0.0
  sumrf = 0.0
  sumrg = 0.0
do 150 i = 122,ndata
  if (dat(2,i).eq.1) then
    avae = sumae / dat(2,i-1)
    avrf = sumrf / dat(2,i-1)
    avrg = sumrg / dat(2,i-1)
  write (55,151) dat(i,i-1),sumrg,sumrf,sumae
  format (14,2x,3(1pe12.3))
  sumae = 0.0
  sumrf = 0.0
  sumrg = 0.0
end if
sumae = sumae + ae(i)
sumrf = sumrf + rf(i)
sumrg = sumrg + rg(i)
150 continue
c calculate monthly averages
c call month (dat,rg,rf,ae,122,ndata,nyear)
c write output data
c
  write (66,*) 'year day rf rg pe
  sm
  do 200 i = 122,ndata
    write (66,210) dat(1,i),dat(2,i),rf(i),pe(i),ps(i),sm(i),as(i),
  # ae(i),rg(i)
210 format (2(i4,1x),7(1pe12.3))
200 continue
c
c*****
c subroutine month (dat,rg,rf,ae,nstart,ndata,nyear)
c calculate monthly averages of recharge, rainfall, actual evapo-
c transpiration.
  parameter (NUM=20000)
  real*4 rg(num),rf(num),ae(num)
  integer*4 dat(2,num)
c header for output file
c
  write (88,*) 'Gardemoen meteorological station - monthly values'
  write (88,*) ' actual evapotranspiration'
  # year month recharge rainfall
c
  i = nstart
  jmon = 0
  do 50 iyear = 1,nyear
    do 100 imonth = 1,12
      jmon = jmon + 1
    c for first year, start in May
  c
  nflag = 0
  if (iyear.eq.1) then
    if (imonth.lt.5) nflag = 1
  end if
  if (nflag.eq.1) go to 100
c determine no days in present month
c

```

```

if (mod(dat(1,i),4).eq.1) then
if (dat(2,i).eq.335) nday = 31
if (dat(2,i).eq.305) nday = 30
if (dat(2,i).eq.274) nday = 31
if (dat(2,i).eq.244) nday = 30
if (dat(2,i).eq.213) nday = 31
if (dat(2,i).eq.182) nday = 31
if (dat(2,i).eq.152) nday = 30
if (dat(2,i).eq.121) nday = 31
if (dat(2,i).eq.91) nday = 30
if (dat(2,i).eq.60) nday = 31
if (dat(2,i).eq.32) nday = 28
if (dat(2,i).eq.1) nday = 31
else if (mod(dat(1,i),4).eq.0) then
if (dat(2,i).eq.336) nday = 31
if (dat(2,i).eq.306) nday = 30
if (dat(2,i).eq.275) nday = 31
if (dat(2,i).eq.245) nday = 30
if (dat(2,i).eq.214) nday = 31
if (dat(2,i).eq.183) nday = 31
if (dat(2,i).eq.153) nday = 30
if (dat(2,i).eq.122) nday = 31
if (dat(2,i).eq.92) nday = 30
if (dat(2,i).eq.61) nday = 31
if (dat(2,i).eq.32) nday = 29
if (dat(2,i).eq.1) nday = 31
end if

c averages for month
c
sumrg = 0.0
sumrf = 0.0
sumae = 0.0
c
do 200 j = 1,nday
sumrg = sumrg + rg(j)
sumrf = sumrf + rf(j)
sumae = sumae + ae(j)
i = i + 1
200 continue
c
c write to output file
c
nyear = dat(1,1) + iyear - 1
write (88,201) jmon, nyear, imonth, sumrg, sumrf, sumae
201 format (3(14,2x),2x,3(lp12.3))
c
100 continue
50 continue
c
return
end

```